DOCTOR OF PHILOSOPHY

Exploring the application of remote sensing to the monitoring of continuous cover forestry

Stoddart, Jaz

Award date:
2024

Awarding institution:
Bangor University

DOCTOR OF PHILOSOPHY

EXPLORING THE APPLICATION OF REMOTE SENSING TO THE MONITORING OF CONTINUOUS COVER FORESTRY

Stoddart, Jaz

Award date:
2024

PRIFYSGOL
BANGOR
UNIVERSITY

EXPLORING THE APPLICATION OF REMOTE SENSING TO THE MONITORING OF CONTINUOUS COVER FORESTRY

Jaz Michael Stoddart
MA (Cantab)
FHEA

A DOCTORAL THESIS SUBMITTED IN FULFILMENT OF REQUIREMENTS FOR THE DEGREE OF DOCTOR OF PHILOSOPHY

MMXXIII

“Habitarunt di quoque silvas . . . nobis placeant ante omnia silvae.”

“Even the Gods dwelled in the woods . . . For us, the woods shall be our greatest delight.”

Virgil, Eclogue II.

DECLARATION

I hereby declare that this thesis is the product of my own work, except where explicitly stated in the text; that all other sources are acknowledged by bibliographic references; and that no part of this work has previously been accepted in substance for any degree nor is being concurrently submitted in candidature for any other degree. I confirm that I am submitting this work with the agreement of my supervisors.

Jaz M. Stoddart

ACKNOWLEDGEMENTS

The title page may bear my name alone, but I know better than anyone that this work could not have been completed without the ongoing support of my friends, family, and supervisors. To do justice to everyone who deserves credit would be impossible so if you find yourself omitted here, please know that it is not a reflection of my ingratitude for all that you have done.

I wish first to extend my thanks to my supervisors, Prof. Ruben Valbuena and Dr Juan Suarez, whose friendship and tutelage have guided me through these years. It would have been an insurmountable task without you both. Thank you for who you have helped me to become.

I must thank Knowledge Economy Skills Scholarships for funding my 90% of my doctoral studies and to their administrative team who supported me through my studies. Knowledge Economy Skills Scholarships (KESS 2) is a pan-Wales higher level skills initiative led by Bangor University on behalf of the HE sector in Wales. It is part funded by the Welsh Government's European Social Fund (ESF) convergence programme for West Wales and the Valleys.

I must also thank Forest Research which acted as an industry partner, provided funds for 10% of my doctoral studies, and whose staff welcomed me warmly as a part of the team; greatly aiding and facilitating my fieldwork and data collection campaigns.

To my contemporaries in our shared office of F5 - Ollie, Tontho, Stuart and his dog Scout - thank you all for making the office an inviting and motivating place to be. I would never have done as much work as I have if were not for your company through the hardest times.

Of course, I wish to thank my family - my parents, my siblings, and beyond – profusely for their endless support. You all know better than anyone that my pursuit of a doctorate started years before I arrived at a university; I am beyond grateful for the many years of understanding and encouragement that have led me here and I hope I've made you proud. I

know it hasn't been easy with me missing many family events for my studies, but I hope you will agree that it was worth it.

Finally, Betty, my cat, who saw an isolated and somewhat defeated student and chose to grace me with your enduring adoration. Since they day you moved in with me, and out of the street you, have been an integral part of my life. You gave me back a work-life balance when I needed it most, by being there for me to come home to and by lying across my keyboard when it was time to call it a night. I owe you a lifetime of gratitude and cat treats.

ABSTRACT

This work has focused on the application of remote sensing to continuous cover forestry (CCF), primarily within Britain, with the intent to identify new methods of inventory, monitoring and biomass quantification. CCF is a silvicultural approach with a focus on sustainability through which forest stands, often of varied species composition, are manipulated to create irregular stand structures through practices of partial harvesting in a manner that retains constant forest cover of a site and allows for natural regeneration. Owing to the great differences between CCF and traditional approaches of forestry, in which even-aged monocultures are maintained, the traditional methods of assessment, such as productivity (yield class) calculations, are less applicable. There is a need to identify new methods of inventory, biomass estimation and stand monitoring for use in operational forestry and research environments and remote sensing has been identified as a potential tool to meet this need. The hypotheses of this work relate to the ways in which remote sensing can overcome the challenges posed by the complexity introduced by the adoption of CCF and the aims of this work relate to demonstrating methods for working with remote sensing and CCF. This work addresses multiple different approaches to remote sensing; aerial laser scanning (ALS), ground-based laser scanning (TLS and MLS), and photogrammetry.

The first part of this work reviews the extent of existing research that addresses the application of remote sensing in CCF and considers the transferability of remote sensing methodologies from other complex forest ecosystems to CCF.

Following from this, is a summation of contributions made towards a greater effort within the European Cooperation in Science and Technology to collate information on forestry-specific ground-based point cloud processing solutions and their functions, presented as a brief review of tools. The intent of the work and the greater effort it contributes to is to improve accessibility to and promote democratisation of such tools for forestry researchers and professionals.

This work then moves onto remote sensing in complex forest systems demonstrating how ALS timeseries data can be used for detecting disturbance directly and the importance of remote sensing for modelling the structural traits of a forest ecosystem. This chapter finds that maps of change in LiDAR metric descriptors of forest structure can be used to detect selective logging activities and visualise stand growth over time. An attempt to develop a more accurate model for AGB using three forest structural metrics was made, however the results indicated no improvement over an existing, widely adopted, single variable model.

Following on from the exploration of ground-based point cloud processing tools, an exploration of how well three of these tools can be employed to replicate and expand upon existing traditional inventory methodologies in complex CCF stands and ancient forest. We compare plot level distributions of stem diameters extracted from point clouds against those from field data. This work demonstrates that it is currently possible to use TLS as an alternative means of inventory data collection to traditional, manual measurements, though this is subject to the correct processing methods and data quality.

Finally, this work closes with a discussion of how this work is justified in light of the ongoing climate crisis, how this work addresses the needs for remote sensing research in CCF, shortcomings, and future directions for work.

PUBLISHED WORKS

1. **Continuous cover forestry and remote sensing: A review of knowledge gaps, challenges, and potential directions**
   Stoddart, J.; Suarez, J.; Mason, W.; Valbuena, R.
   Current Forestry Reports, **2023,** 9, 490-501

2. **A Conceptual Model for Detecting Small-Scale Forest Disturbances Based on Ecosystem Morphological Traits.**
   Stoddart, J.; de Almeida, D.R.A.; Silva, C.A.; Görgens, E.B.; Keller, M.; Valbuena, R.
   Remote Sensing. **2022**, 14, 933.

3. Predicting leaf traits of temperate broadleaf deciduous trees from hyperspectral reflectance: can a general model be applied across a growing season?
   Chen, L.; Zhang, Y.; Nunes, M.H.; **Stoddart, J.**; Khoury S.; Chan, A.H.Y.; Coomes, D.A
   Remote Sensing of Environment. **2022,** 269.

4. Beyond Trees: Mapping Total Aboveground Biomass Density in the Brazilian Savanna Using High-Density UAV-Lidar Data.
   Costa, M.A.T.; Silva, C.A.; Broadbent, E.N.; Leite, R.V.; Mohan, M.; Liesenberg, V.; **Stoddart, J**.; Amaral, C.H.; Almeida, D.R.A.; da Silva, A.L.; et al.
   Forest Ecology and Management. **2021**, 491, 119155.

5. Comparison of Statistical Modelling Approaches for Estimating Tropical Forest Aboveground Biomass Stock and Reporting Their Changes in Low-Intensity Logging Areas Using Multi-Temporal LiDAR Data.
   Rex, F.E.; Silva, C.A.; Dalla Corte, A.P.; Klauberg, C.; Mohan, M.; Cardil, A.; Silva, V.S.; Almeida, D.R.A.; Garcia, M.; Broadbent, E.N.; Valbuena, R.; **Stoddart, J.**; Merrick, T.; Hudak, A.T.
   Remote. Sensing. **2020**, 12, 1498.

N.B. Only the works listed with their titles in **bold** have contributed to the body of work presented in this document. The others are included to illustrate additional contributions to the field.

CONTRIBUTION STATEMENT

This thesis includes work which was generated through collaborative efforts which extend beyond my immediate supervisory team, and which were contributions to larger projects beyond the scope of my own doctoral studies. I wish to briefly address the work presented in this thesis, chapter by chapter, outlining the extent of external contributions to any work presented herein.

Chapter 2: A sanity check of the text regarding the nature and history of CCF was provided by William Mason of Forest Research during the writing process with suggestions made for further points of discussion.

Chapter 3: This work was instigated and conceived as part of a larger COST action and as such the concept and goals were not of my design. I acted within the guidelines provided, making use of some questionnaire data that had been collected previously to deliver this work but had no part in the design nor the follow up in which the data I provided was used to form a public repository of information.

Chapter 5: External assistance was provided first in the provision of the dataset, which was generated from a study that had been conceptualised and funded by an outside party. Conceptualisation of the analyses and work presented in the chapter was undertaken by my supervisors and me, Modelling approaches were discussed with a post-doc member of the lab group.

Chapter 6: Due to a limited license for the initial processing of MLS data, from the proprietary format of the scanner into a standardised .las format, Forest Research were responsible for the initial processing of raw scanner data. The subsequent analyses were then conceptualised and conducted independently.

TABLE OF CONTENTS

LIST OF FIGURES

LIST OF TABLES

LIST OF CODE SNIPPETS

GLOSSARY OF ABBREVIATIONS

AGB	Aboveground Biomass
ALS	Aerial Laser Scanning
ANOVA	Analysis of Variance
BC	Bhattacharyya Coefficient
CCF	Continuous Cover Forestry
CHM	Canopy Height Model
CI	Confidence Interval
DBH	Diameter at Breast Height (measured at 1.3 m)
EMT	Ecosystem Morphological Trait
eCOST	European Cooperation in Science and Technology
FHD	Foliage Height Diversity
GC	Gini Coefficient (of the Distribution of Heights)
LiDAR	Light Detection and Ranging
LOOCV	Leave-One-Out Cross Validation
MD	Mean Difference (Bias)
MLS	Mobile Laser Scanning
RMSE	Root Mean Square Error
SD	Standard Deviation
SE	Standard Error
SLAM	Simultaneous Localisation and Mapping
TCH	Top of Canopy Height
TLS	Terrestrial Laser Scanning
UAV	Unmanned Aerial Vehicle

CHAPTER 1

Introduction and Objectives

1.1 Introduction

1.1.1 Context

The phrase ‘production forests’, forests grown and managed for timber production, conjures images of even-aged stands of a single tree species planted into evenly spaced rows; far from the image imagined by most considering a natural forest. Natural forests hosting a range of species of different sizes and ages, growing in a random arrangement, are largely considered to be more aesthetically appealing than the plantations of production forests. Intuitively to most, a more diverse and more varied forest structure provides greater environmental benefits than even-aged monocultures. The ecosystem services provided by more diverse forest structures and species compositions have been shown to include improved diversity of habitat provision, and greater resistance to pathogens and changes in environmental and climatic conditions [1-3].

Harvesting approaches to production forests, such as clear-felling, are traditionally also considered less aesthetically pleasing than partial or selective harvesting systems which leave some trees in situ to continue to provide ecosystem services and grow. As with the comparison between production and natural forests, the more aesthetically pleasing partial harvesting approach provides a greater number of ecosystem services, and in this case reduces the impact of timber production on the environment through reduced soil erosion, loss of habitats, and windthrow in surrounding stands, relative to clear felled sites [4-7].

Given the strongly negative aesthetic appearance associated with traditional forestry, rendering the forestry sector an easy target for environmental campaigning and activism, governments and their forestry bodies are eager to promote silvicultural approaches which give forests more natural appearances. Since 2004, in the UK, there have been standards in place from the government and certifications under the UK Woodland Assurance Standard, which certifies all nationally owned forests and much private forest, to promote sustainable management activities. These national standards for sustainable forest management are reassessed approximately 5 years with the latest editions published in 2017 [8,9] and are intended to ensure forests are managed to provide improved community and ecosystem services without significantly sacrificing timber production. The standards broadly outline silvicultural practices which all fall within the definition of continuous cover forestry, CCF; a management approach in which forest stands, often of varied species composition, are manipulated to create irregular stand structures through practices of partial harvesting in a manner that retains constant forest cover of a site and allows for natural regeneration [10] (see 2.2.1).

CCF is not without its drawbacks; pre-existing means of estimating the standing stock, and the harvestable yield or forecasting future stocks are all inapplicable to continuous cover systems due to the heterogeneity of the size, age, and potentially also species of the trees in a stand. At present there are no comprehensive and fully established methods for estimating, monitoring, or forecasting stocks in CCF in the UK and thus is a need to develop new methods of monitoring for CCF and, thus, addressing this through use of remotes sensing tools is the focus of this work.

1.1.2 Remote Sensing

Point clouds are a three-dimensional (3D) representation of space that consists of a collection of individual points comprising the surfaces of objects. Each point in the cloud is defined by its position coordinates in the x, y, and z axes; often they also include additional information such as the colour or return intensity. Point clouds are typically produced through use of laser scanning however they can also be generated through photogrammetry.

The data contained within a point cloud provides valuable spatial information about the scanned environment and when used in conjunction with other techniques, such as surface reconstruction algorithms. Surfaces or meshes, formed by connecting proximal points with such algorithms, can allow for visualization and analysis of complex structures.

The increasing availability of high-resolution sensors and advancements in computational power have led to the widespread use of point clouds in various applications. They serve as a foundational data format for 3D modelling, visualization, simulation, and analysis, enabling interaction with and manipulation of real-world spatial information in a digital environment.

1.1.2.1 Laser scanning

Laser scanning, also known as LiDAR, is a remote sensing technology that uses laser pulses to measure distances and generate point clouds. It is a non-contact method of data collection that provides highly accurate and precise measurements, making it widely used in a range of fields including forestry.

Laser scanners emit laser pulses in a sweeping pattern, covering a large area or field of view, and then detects reflected laser light as it returns to the sensor and records the time-of-flight

or change in phase. From this, laser scanners can calculate the distance between the scanner and the incident surface. This information, combined with the scanner's position and orientation, allows the creation of a detailed 3D representation of the scanned area. Laser scanners can capture millions of distance measurements per second, resulting in a dense point cloud.

Laser scanners can be mounted to a range of platforms; airborne platforms such as UAVs [11,12] and planes [13,14] for ALS, stationary ground-based platforms such as tripods for TLS [15], and mobile ground-based platforms which are often handheld, or backpack mounted, for MLS [16,17]. A selection of the variables that can be measured and derived from different laser scanning platforms can be found in Table 2-1.

As laser scanning tools allow for the generation of comprehensive and high-resolution 3-D models of complex structures they have naturally been applied to below-canopy forestry applications. In recent years, terrestrial laser scanning (TLS) has become an established method of monitoring forests and plants, owing to their capacity for sub-centimetre accuracy and precision. Occlusion by understory growth, branches, and the trunks of trees significantly limits the range and extent that a TLS scan can reliably model and although this can be overcome by taking a multi-scan approach this can be rather time consuming and require additional features such as highly reflective targets to serve as tie-points for co-registration and alignment of scans [18,19]. To cover larger areas and to overcome issues with occlusion MLS solutions can be used. MLS use in forestry can take multiple forms, and there are examples of vehicle-mounted laser scanners [20] for use from tracks and roads, and backpack-mounted [21,22] or handheld scanners [17,23] for use in the forest stands.

MLS systems often consist of one or more laser scanners in combination with a positioning (GNSS) and/or orientation system (inertial navigation system). The density of the produced point cloud is strongly dependent on the movement speed and scan rate of the scanning platform and can produce homogeneous point clouds of similar density to TLS single scans when used correctly, where TLS multi-scans tend to have variable point cloud densities resulting in non-homogeneous point clouds when used over larger areas. [24].

1.2 Statement of intent and hypotheses

This thesis examines the use of remote sensing - here referring to photogrammetry, ground-based and aerial laser scanning – for describing and quantifying the biomass, volume, and structural change in CCF stands. This study is based on data from complex tropical forest in the Brazilian Amazon and data from three sites in the UK consisting of mixed species CCF, and ancient natural and semi-natural forest across Southern England. The key aims of the research are to investigate how remote sensing can capture and monitor disturbances in forest structure in continuous cover systems and monitor growth over time, and how remote sensing can be used to capture inventory data in CCF stands.

1.2.1 Aims and hypotheses

There were three key aims to this thesis and they were:

1. To assess and review the state of remote sensing in continuous cover forestry - addressed in Chapters 2 and 3.
2. To investigate how remote sensing can capture and monitor disturbances in forest structure in continuous cover systems and monitor growth over time - addressed in Chapter 5.

3. To investigate how remote sensing can be used to capture inventory data in CCF stands - addressed in Chapter 6.

The hypotheses of the analysis chapters, Chapters 5 and 6, were linked to aims 2 and 3 respectively, and are as follows:

Chapter 5 Hypothesis: Remote sensing can detect disturbances and changes in forest structure associated with selective logging and the subsequent recovery. The most disturbance sensitive remote sensing metrics of horizontal structural complexity, vertical structural complexity, and forest stand height will more accurately calculate stand biomass than a single variable model.

Chapter 6 Hypothesis: Remote sensing can be used to replicate traditional field inventory methods at the plot level through use of appropriate data collection methods and processing tools.

1.3 Thesis structure

Chapter 1 has provided context to the drivers behind the transformation to CCF and the need for methods of monitoring CCF. The aims and hypotheses of the thesis have been introduced.

Chapter 2 introduces CCF in greater detail, including discussion of analogous silvicultural systems and the relative advantages and disadvantages of CCF compared to traditional - 20th century, timber production focused - forestry. A review of the overlap between remote sensing and CCF is presented including the ways that remote sensing could address the challenges and knowledge gaps of CCF. There is also discussion of how interested parties can get started with remote sensing to promote remote sensing use in the field of CCF.

Chapter 3 is a summation of work conducted as part of an action for the European Cooperation in Science and Technology (eCOST) and acts a s a review of publicly available TLS processing solutions. The work is a novel presentation of information regarding publicly available TLS processing solutions and is the first example of a single point of reference for information about such solutions and their functions.

Chapter 4 is a description of the methods used for data collection and processing within this work. This chapter covers traditional field methods of inventory and the methods relating the remote sensing data collections. A summary is provided of the key concepts of remote sensing, the tools and equipment used, the programs for data processing, and an outline of the processing methodology.

Chapter 5 is a published work describing the applications of remote sensing in complex tropical forest. It specifically describes the use of remote sensing for detecting small-scale forest disturbances and developing a model for biomass estimation using disturbance sensitive metrics that correspond to traits of forest morphology.

Chapter 6 examines how remote sensing can be used to replicate traditional forest inventory methods such as recording DBH measurements and heights. This chapter then goes on to explore how remote sensing can be used to directly measure additional inventory relevant values such as stem volume and thus how in concert with species data collected in the field it is possible to estimate merchantable volume by species.

And finally, Chapter 7 provides a summary of the findings and contributions of this work, specifically regarding public sector parties to whom the work provides value. Chapter 8 also

reflects on the challenges that CCF continues to pose for inventory assessment and monitoring going forward.

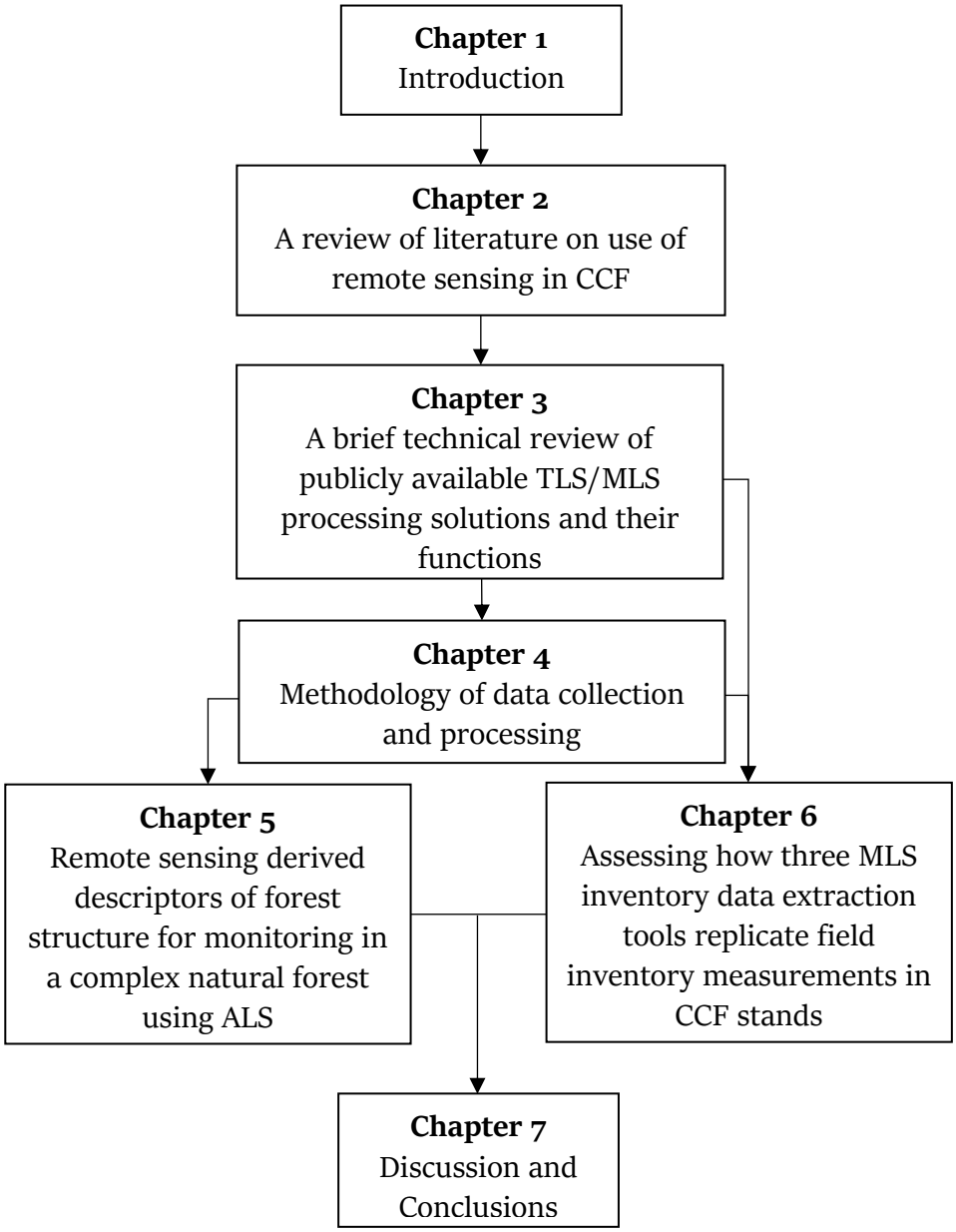

Figure 1-1. A schematic diagram of the thesis structure

CHAPTER 2 Review of Literature: Continuous cover forestry and remote sensing

2.1 Preface

This chapter is comprised of a lightly edited version of the published manuscript for the work:

Continuous Cover Forestry and Remote Sensing: A Review of Knowledge Gaps, Challenges, and Potential Directions.

Stoddart, J., Suarez, J., Mason, W. et al. Current Forestry Reports, 9, 490–501 (**2023**)**.** https://doi.org/10.1007/s40725-023-00206-0

Continuous cover forestry and remote sensing: A review of knowledge gaps, challenges, and potential directions

Jaz Stoddart[1]*, Juan Suarez[2], William Mason[2], Ruben Valbuena[3]

1. School of Natural Sciences, Bangor University, Bangor, LL57 2DG, UK
2. Forest Research, the Agency of the Forestry Commission, Northern Research Station, Roslin, Midlothian EH25 9SY, Scotland, UK
3. Division of Forest Remote Sensing, Department of Forest Resource Management, Swedish University of Agricultural Sciences (SLU), Skogsmarksgränd 17, SE-901 83 Umeå, Sweden

2.2 Abstract

2.2.1 Purpose of review

Continuous cover forestry (CCF) is a sustainable management approach for forestry in which forest stands are manipulated to create irregular stand structures with varied species composition. This approach differs greatly from the traditional approaches of plantation-based forestry, in which uniform monocultures are maintained, and thus traditional methods of assessment, such as productivity (yield class) calculations, are less applicable. This creates a need to identify new methods to succeed the old and be of use in operational forestry and research. By applying remote sensing techniques to CCF it may be possible to identify novel solutions to the challenges introduced through the adoption of CCF.

2.2.2 Recent findings

There has been a limited amount of work published on the applications of remote sensing to CCF in the last decade. Research can primarily be characterised as explorations of different methods to quantify the target state of CCF and monitor indices of stand structural

complexity during transformation to CCF, using terrestrial and aerial data collection techniques.

2.2.3 Summary

We identify a range of challenges associated with CCF and outline the outstanding gaps within the current body of research in need of further investigation, including a need for the development of new inventory methods using remote sensing techniques. We identify methods, such as individual tree models, that could be applied to CCF from other complex, heterogenous forest systems and propose the wider adoption of remote sensing including information for interested parties to get started.

Keywords: Remote sensing; Continuous cover forestry; Biomass estimation; Individual tree growth models, Forest inventory

2.3 Introduction

2.3.1 Continuous cover forestry and its challenges

As concern for the environment has grown in the past decades, the role of forest management in mitigating the impacts of climate change and biodiversity losses has garnered greater importance. The landmark resolutions for a coordinated international move towards sustainable forest management in the 1990s, the Rio Forest principles [1] and the Helsinki Process [2], promoted a resurgence in interest in 'close-to-nature' forestry and continuous cover forestry (CCF), having initially gained popularity in the early years of the 20th century with concepts such as the 'Dauerwald' [3-5]. These sustainable silvicultural practices are based around a set of five defining principles: partial harvesting rather than clear-felling; preferential use of natural regeneration rather than planting; developing

structural diversity and spatial variability within forests; fostering mixed species stands and avoidance of intensive site management practices such as soil cultivation, herbicide application and fertiliser input [6,7]. For the purposes of this paper, we will refer to the sustainable silvicultural practices that adhere to these five principles as CCF, though many terms are used [6,8,9]. There is a level of contention over the use of close-to-nature as a term within these practices as the level of human interference within these silvicultural systems can be considered far from natural [10-12]. The specific silvicultural systems that fall within the definition of CCF include irregular shelterwoods, and group and single stem selection (terminology follows Matthews 1989). [7,13,14].

The driving forces behind the adoption of CCF are the many environmental advantages CCF presents over clear-cutting in traditional uniform even-aged forest monocultures. CCF is recommended by the European Union (EU) Biodiversity Strategy as a beneficial form of forest management for biodiversity [15]. Where transformation to CCF accompanies a transition away from monocultures the increased tree species diversity provides additional habitats; as tree species richness strongly influences the diversity of forest inhabiting species [16]. Increased diversity of tree species and genetics are important contributing factors to increased resilience, resistance, and capacity for adaptation with regards to climate change [17], pathogens, and pests [18].

The persistence of stands between harvests, characteristic of CCF, has been found to improve multifunctionality of production forests in Fennoscandia and specifically to improve diversity of ectomycorrhizal fungi and herbivorous larvae [19]. CCF also has better retention of late successional forest species – particularly with regards to shade-tolerant understory plants, and bird species assemblages - than traditional clear cutting [20-23]. CCF

is thought to be second only to retention forestry with regards to habitat preservation [24]; where retention forestry is itself a form of CCF in which dead wood, habitat trees and trees with larger contributions to diversity are retained during harvesting [24,25]. The risk and impact of soil erosion, particularly on slopes, is also reduced dramatically by the continued presence of vegetation and thus CCF provides greater soil stability and reduces soil losses relative to clear cutting [26]. Additionally, continuous cover reduces the creation of brown edges, which are newly exposed edges in neighbouring stands when a site is clear felled, that are less resilient to windthrow and particularly susceptible to storms [27] CCF shows greater windthrow stability and resistance to storms than clear cut sites [28,29] and the increased structural complexity of the stands also appears to have a positive impact on wind resilience [29].

In addition to the environmental benefits of CCF, there are also economic considerations surrounding CCF uptake. It can be a smaller financial burden to manage and thin naturally regenerating forest than to establish and tend restocking sites after clear cutting [30,31], though the regular respacing of some prolific species such as Sitka spruce can itself incur large costs. Natural regeneration also mitigates much of the impact of pests such as the pine weevil [32] which can devastate restocked sites owing to the vulnerable and attractive nature of the seedlings. The products of CCF can also be larger and more valuable than equivalent volumes of even-aged forest. For example, study by Hanewinkel et al [33] found that CCF stands produced many more high-value large-sized logs which commanded high timber prices and thus increased the profitability of CCF almost 2-fold over even-aged stands. However, it should be noted that to produce more valuable timber yields, CCF stands

require appropriate management, which is specialist knowledge that many foresters lack, and for which there continues to be a significant lack of adequate guidance [7].

2.3.2 Challenges and knowledge gaps in CCF

Whether CCF adoption presents an economic advantage over clear cutting and even-aged forestry is unclear and debated and this is one of many challenges facing the adoption of CCF [7,31,34]. From a management perspective, CCF can be a considerably more complex procedure than traditional clear cutting in even-aged stands and this requires specialist knowledge and training for forest managers and harvest workers [7]. Selective harvesting can limit the use of mechanised felling and extraction machinery which can subsequently drive-up costs for labour to manually fell the desired trees and extract the timber without significantly disturbing the stand. Additionally, yields for each harvest are smaller owing to the very nature of selective harvests, thus it takes a longer time or a greater area to produce yields of equivalent volume to clear felling which can disincentivise investment and adoption.

The timber industries in the majority of the European countries where CCF uptake is increasing are set up to receive near-uniform logs from even-aged monocultures with little variability within their dimensions and properties. However, CCF produces logs of a wider range of diameters and potentially different species with each harvest and thinning [7,35] and this introduces a need for investment into new equipment and tools which is only justifiable if the supply of these forest products is both predictable and reliable.

Estimating standing stocks and future harvest volumes in CCF is considerably more difficult than in clear cutting systems as the forest manager must be able to estimate the whole

volume of the stand in addition to the volume of exclusively either the harvested or retained stems. Forest managers must map which stems are to be harvested, to subsequently estimate harvest yield and retained stock. This challenge is being addressed by the advent of precision forestry - greater volumes of detailed information facilitating targeted interventions aimed at maximising yields of more valuable products - which is inextricably linked to developments in remote sensing.

CCF often requires multiple interventions throughout its growth to maintain the desired forest structures where clear cutting typically requires less active management. Typically, in a clear-cutting system, a monoculture stand of even-age will be planted on a previously cleared site, maintained during its growth, and harvested upon reaching the desired size or age. By contrast, CCF is a multi-stage cycle of harvests, regeneration, and growth with no clear demarcation between the end of one cycle and the start of the next. Due to the selective nature of the harvests and varied approaches to CCF, harvests can vary in scale from large group fellings to individual stems as required. To direct harvesting, forest managers may rely upon target diameters (maximum diameters) for a species in each stand to inform when a harvest is due. Alternatively, there is also the reverse-J distribution (J-curve model) for stem diameters which is considered an easily identifiable and achievable distribution within CCF that could be used as an indicator of when to harvest and where to concentrate harvests in accordance with which diameter classes are found to be in surplus to maintain the desired forest structure [36,37].

The constant regeneration, management, and recruitment of understory trees provide a challenge for mapping inventory as there is a need to record the locations and species of trees as well as their development over time. Currently, inventory protocols for CCF are

based on relatively labour-intensive manual data collection methodologies [36]. Monitoring regeneration is of particular importance as many forest managers overestimate the likelihood of regeneration at their sites or find the success of regeneration to be less predictable than that of planting [37].

Future yield forecasting and growth modelling are currently significantly under-developed areas of research for CCF, and for mixed species stands in general. In the UK there are currently no models for CCF forecasting [7] and approaches used in traditional methods of even-aged forestry are inapplicable to CCF, e.g. yield classes which are an index of the potential productivity of even-aged stands of trees [7].

2.4 Remote sensing and CCF

2.4.1 Existing research

There is currently a dearth of research exploring the application of remote sensing to CCF, despite the general growth of interest in both fields separately in recent years. Searches for literature to include in this review were conducted using Google Scholar and Scopus with search queries comprising keywords used for CCF, the Boolean operator 'AND', and keywords for remote sensing. The keywords used were: 'CCF', 'Shelterwood', 'sustainable forestry', 'Dauerwald', or 'close-to-nature' plus 'remote sensing', 'LiDAR', 'earth observation', 'laser scanning' or 'photogrammetry'. Once completed, the returned titles and abstracts of highlighted papers were assessed for relevance, and the few relevant studies were subsequently reviewed. Relevance here being defined as works exploring the intersection of the two fields, sustainable forestry, and remote sensing, thus eliminating the

significant proportion of the search results returned which only made passing reference to continuous cover systems or remote sensing.

There is an obvious need for more work specific to the overlap of these subjects to further encourage the adoption of CCF [38,39]. The need for accurate information to support CCF also requires a cost-effective method that traditional field data collection cannot solve. Therefore, remote sensing is being applied to forestry at a range of scales from that of a landscape down to the individual saplings, owing to the efficient and scalable nature of remote sensing, and yet there are few examples of remote sensing being applied to CCF. Remote sensing can be used to derive a range of forest metrics or to directly monitor stands and trees which can then be used to inform models or identify observable trends in growth [40-44]. There are a range of remote sensing data sources which could be applied to monitoring CCF, however they do not all describe the specific forest stand traits. As such each data source is best suited to monitoring specific traits; ALS for height and canopy cover, TLS for stem structure, and spectral data to monitor photosynthetic capacity.

A selection of key forest metrics and traits and that can be measured operationally by different remote sensing data sources are explored below, in (Table 1.). The listed traits and remote sensing methods are themselves presented grouped into categories with shared characteristics. The “inventory data” traits - tree location, tree height, and diameter at breast height – are all forest traits which are commonly recorded and measured as part of forest inventory activities. “Structural metrics” describes all measurements of horizontal complexity, such as gap fraction, leaf area index, and percentage cover; as well as vertical complexity, such as foliage height diversity, Gini coefficient of heights and standard deviation of heights. The “other CCF traits” is a catch all category for remaining observable

traits of specific interest in CCF. Stem volume is included owing to its potential for yield measurement and forecasting in uneven-aged stands where traditional models are not applicable. Similarly, regeneration is included as it is a defining characteristic of CCF and the capacity to monitor regeneration also has implications for yield measurement and forecasting. Tree species is of interest as CCF can includes species mixtures and so remote identification of species is necessary for stock mapping and monitoring successional development of the forest.

The remote sensing methods, presented in Table 1, are separated by whether they generate 3-dimensional point cloud or 2-dimensional image data. Within the 3-dimensional point cloud generating methods there are three laser scanning methods and two photogrammetric methods. Photogrammetric data typically also captures optical data owing to the use of optical (camera) sensors for data collection, and it is possible to generate photogrammetric point clouds with images from outside the visible spectrum, however it is uncommon. The "optical" 2-dimensional image based remote sensing method includes a range of methods such as multispectral and hyperspectral imaging in addition to specialist imaging methods such as hemispherical photography used in canopy cover measurement [45].

Table 1 - Remote sensing data sources and the types of information they can be used to observe operationally in CCF

		Inventory Data			Structural Metrics		Other CCF Traits		
		Tree location	Tree height	Diameter at breast height	Vertical structural complexity	Horizontal structural complexity	Stem Volume	Regeneration	Tree Species
3-Dimensional Point Cloud Data	Aerial Laser Scanning (ALS)	✓ [46-48]	✓ [49-53]	X	✓ [44,49,50,54]	✓ [47,54-56]	✓ [51]	✓ [50,57]	# [58]
	Terrestrial Laser Scanning (TLS)	✓ [59-61]	~ [53,61]	✓ [53,59-62]	✓ [61,63-65]	✓ [63,66,67]	✓ [59, 68, 69]	✓ [59,81]	# [70,71]
	Mobile Laser Scanning (MLS)	✓ [53,60, 72-74]	~ [53,73-75]	✓ [53,60, 72-76]	✓ [77]	✓ [77]	✓ [72, 73]	✓ [72]	# [78]
	Aerial Photogrammetry	✓ [47]	✓ [47, 79,80]	X	X	✓ [47,48]	✓ [79,80]	~ [81]	# [82]
	Below-canopy photogrammetry	✓ [83,84]	X	✓ [83-85]	~ [83,84]	X	X	✓ [83,84]	X
2-Dimensional Image Data	Optical (RGB, multispectral, hyperspectral)	✓ [57,86, 87]	X	X	✓ [88]	✓ [48]	X	X	✓ [51,52,57 ,82,86, 87,89]

✓ represents information that can be reliably and directly extracted using this remote sensing data source, ~ represents information which may be extracted using the stated data source but can be subject to complications such as occlusion which may impact or reduce reliability, # represents information which has only been derived from the outputs of the stated data source using machine learning methods, X indicates that we did not find references that showed this information could be directly and reliably extracted with the stated data source

Relevant remote sensing research on CCF, Dauerwald and shelterwood systems has shown that it may be possible to both monitor the transformation of a traditional stand to CCF and monitor the progression of growth and the associated changes in forest structural type that can be applied to describe CCF stands. At the individual tree level, Bennet et al [46] describe a novel method of using aerial data from photogrammetry and ALS to detect individual trees with improved detection rates among smaller diameter trees than previous methods, which makes the model applicable to monitoring transformation to CCF. This model relies upon a Bayesian optimisation approach to the parameterisation of the tree detection algorithm; by utilising external datasets they eliminate the requirement for site specific allometric models derived from field data which can also reduce required fieldwork [46]. At the stand level, Stiers et al. [5] used TLS to measure structural complexity within forest and proposed a novel index of structural complexity. This index quantifies stands by their structural type and serves as an indicator of how close a stand is to the CCF 'target structure'. This work has strong similarities to the work of Valbuena et al. who instead used ALS to classify the forest structural types of a stand [49]. Their classification was based upon two more widely used measures of forest

structure; Lorenz asymmetry, where greater asymmetry is associated with the idealised 'target structure' (characterised by the reverse-j shape), and the Gini coefficient, a measure of inequality in size (DBH). By integrating these classifications into forest structural types as a guideline, forest managers could make informed decisions about when to harvest for large regions of forest without the need for extensive fieldwork. Annually updated maps of structural types could be used to monitor important processes within CCF systems and inform managers of where regeneration and recruitment are occurring.

2.4.2 Remote sensing for CCF inventory measurement and stock mapping

Inventory protocols for CCF currently rely upon labour and time intensive fieldwork for data collection with three variations of commonly used protocols across a handful of plots (radii varying from 8 - 15m depending on protocol) taking one operator a whole working day and complete enumeration of plots taking a day for two operators [90]. By contrast, remote sensing can be used to completely enumerate a plot [91] and collect all protocol relevant data with greater efficiency resulting in faster, more cost-effective data collection [59]. Studies have shown that using TLS and MLS it is possible to detect and segment up to 100% of the trees within a plot [53] and 97% within 20m radius of a TLS scanning position, although this falls to 75% at a 40m radius due to occlusions and decreasing point density [90,92]. Combining data from TLS multi-scans or using MLS from less than 20m can mitigate occlusion-based inaccuracy. Consequently, MLS data from within the plots collected with a handheld or backpack mounted platform would be expected to suffer from less occlusion-based error than data from a vehicle mounted platform on a forest track, such as in Bienert et al. [60]. There is consensus in the literature that both TLS and MLS can be used for the accurate collection of inventory data such as DBH and height. Donager et al. found

that TLS had an RMSE of 7.2% for DBH and 2.7% for height, and in the same study MLS was found to have an RMSE of8.1% for DBH and 1.6% for height [53]. Hartley et al similarly found that for MLS derived DBH and height measurements they achieved RMSE values of 5.4% and 3.0%, with R^2 values of 0.99 and 0.94 respectively [74]. The accuracies achieved in these studies are very high and for the height measurements are more accurate than can be expected to measure from the ground with traditional field methods [93]. It can thus be argued that even if there is a potential decrease in accuracy relative to fieldwork it is likely to be extremely small and can be offset against the speed and efficiency with which data can be collected. It is worth noting that ground-based LiDAR systems can cost tens of thousands of dollars and, while this can be offset against the reduced costs for the labour brought about by greater data collection efficiency, it may not always be financially beneficial.

In addition to improving the efficiency of data collections in existing inventory protocols, there is the potential for the development of novel remote sensing specific protocols. With remote sensing it is possible to calculate volumetric measurements of stands or individual trees directly from point clouds [68,69]. Direct measurement of volumes may allow for estimates with higher accuracies and lower uncertainties. Lowering uncertainty in volume estimates can directly improve sales prices, and profits, where the law of conservativeness is used in pricing, as is particularly common in forest products sold for pulp or fuel and the sale of logging rights.

Tree identification and diameter measurement can be approached with remote sensing from either above or below the canopy. Aerial datasets can be used to map trees quite accurately within the overstory as there are many publicly available solutions with tools for tree identification and crown delineation that make use of optical and LiDAR data [46-48]. Tree

identification within the understory is also possible from high point density aerial LiDAR datasets however due to occlusion the precision drops off with smaller trees such as those from regeneration [50]. Below-canopy remote sensing techniques - such as TLS, MLS, and photogrammetry - are better suited to the accurate mapping of regeneration [59,72,82-84] and it has been shown in irregular tropical forests that MLS can identify small diameter understory trees with far greater geospatial positioning accuracy, 6cm, than methods using aerial data, which had 6m positioning error [91]. The field of tree detection algorithms from below-canopy point clouds is rapidly developing and there are several solutions available which can accurately locate, identify, and measure trees and saplings from point cloud data [95-98]. In addition to tree identification, it is also possible to measure metrics such as the straightness of trees and even the calculation of lengths and sizes of logs that can be harvested from below-canopy point clouds [98-100]. Trunk straightness and merchantable log estimation from the integration of remote sensing technology into CCF inventory protocols could potentially allow forest managers to tailor harvests to meet market demands or to list their stocks for sale in advance more accurately.

There continue to be challenges in remotely identifying tree species, as LiDAR data alone appears to be insufficient for species delineation. Current literature suggests that it is possible with the use of deep learning and tree species classification systems and optical remote sensing techniques, and there is evidence that channels in these algorithms can be substituted with LiDAR metrics [101]. These methods could be applied to CCF stands for stock mapping, mapping of inventory with species distributions and abundance, [57,86,87,89,94] however for aerial data occlusion below dense canopy would limit reliability and for terrestrial data the extent would be limited. Modern ALS methods with

laser scanning at angles close to NADIR can improve canopy penetration though dense canopy continues to obscure the understory and the close to NADIR angled pulses are less likely to reflect off the vertical stem surfaces.

2.4.3 Remote sensing for CCF yield modelling and forecasting

Beyond improving data collection for existing inventory protocols, remote sensing could be used for the development of new models estimating current biomass yields. Biomass estimation is typically performed with single variable models, such as the model by Asner and Mascaro [102] which uses top of canopy height to predict biomass in each area. However, the variables used in these models cannot describe the irregular horizontal and vertical structure of CCF, as such there is a need for models with variables that better describe the structure of CCF. Remote sensing-informed multivariate models are already being applied to similarly complex irregular forest systems, such as selectively logged tropical forests, and thus it may be prudent to apply similar approaches to CCF. Various approaches have been proposed to involve other non-height morphological traits of forest ecosystems [43] - often one of either cover or vertical structural complexity - to make a biomass prediction that would be better applicable to CCF systems [44,103-106]. One example of note is the 'ecosystem morphological trait' (EMT) framework proposed by Valbuena et al. which is intended to be applicable across a range of diverse and complex ecosystems and across multiple sources of 3D data [43]. The proposed EMT framework posits that all forest can be effectively characterised through use of measures for all three morphological traits of height, horizontal structural complexity, and vertical structural complexity. The EMT model lacks a trait to describe species diversity and distribution, and this could be considered an essential trait of forest structure however the EMT model was

intended to provide a sensor, scale, and ecosystem agnostic means of describing three-dimensional ecosystem structure.

In addition to estimating current biomass there is also the need to predict future biomass yields which requires that biomass estimations be combined with growth models to provide estimates of future biomass. Observed trends of growth are an effective way to create estimates of future growth by simply projecting past patterns of growth forward. The location specificity of observed trends makes them particularly appealing tools for growth forecasting however such trends are limited by their specificity to current and historical climatic conditions. Multi-temporal data for tree heights and diameters can be modelled to find trends and these can be projected forward using individual tree growth models, at both the tree and stand level. Such multi-temporal data can be used to train individual tree growth models which can be used to simulate growth of individual trees within a stand. Individual tree growth models have historically been successfully applied to traditional uniform age monocultures to model and identify dominant and subdominant trees and responses to management activities such as thinning [107,108]. The most recent form of the Canadian tree and stand simulator (TASSIII) can model complex systems with multiple species (a limited number for now but including several key timber species) and spatial heterogeneity and thus could be suitable for use in CCF [108]. An earlier iteration of TASS was applied to CCF in the UK by Suarez and found to be useful for modelling the growth of trees in CCF stands [109] and thus with the improvements made in the newer TASSIII could render it a valuable tool for CCF forecasting.

There are other individual tree models that could also be applied to CCF using data from remote sensing sources, such as CAPSIS which is already used to assess the sustainability of

harvests by predicting the impacts of harvests on the future growth of trees in the stands [110]. Such insights within CCF could allow forest managers to predict the impacts of management and harvests on a CCF stand. Further development of these predictive tools could inform harvesting approaches and potentially allow managers to influence the future forest products as desired, prioritising the retention of slow growing, high density timber or alternatively prioritising harvests which create conditions which favour faster growing, high volume wood for fuel or pulp.

2.4.4 Practicalities of remote sensing

To further develop remote sensing tools for CCF there is a need for a wider remote sensing culture among foresters with greater adoption and development of remote sensing techniques for inventory assessment and monitoring. Promoting adoption of remote sensing will require opening communication between existing remote sensing practitioners and interested parties, particularly forest managers, and thus the intent of this section is to introduce the practicalities of remote sensing.

Getting started with remote sensing can seem technically daunting however it does not need to be a challenge; there are multiple ways to approach data collection and processing, varying in their required investment of time and money, and from relatively accessible to requiring programming skills.

To illustrate this point, below is a list of point cloud data acquisition approaches in an order indicative of typical associated costs per unit area, informed by the combined experience of the authors, and descending from most to least expensive.

1. Inventory fieldwork requires operators to travel to the plots and collect data manually which is a relatively slow and inefficient method with low spatial coverage.
2. MLS and TLS require relatively expensive, specialist equipment and an operator to attend each of the plots and collect the data. However this method is considerably faster than conventional inventory fieldwork allowing for greater spatial coverage in a day [58,90,91].
3. Unmanned aerial vehicle (UAV) mounted ALS requires an unmanned craft to be flown over a forest at a relatively low altitude collecting high point density data. UAV mountable laser scanners vary in price but tend to be relatively expensive, however they are often commercially available. Additional costs are the UAV, which are becoming relatively affordable for the required payload capacities, and an operator. Spatial coverage and data collection speed is generally greater than that of ground-based techniques and can vary greatly between quadcopters and fixed-wing UAVs; the latter being capable of larger scale data collections owing to longer flight times.
4. UAV mounted photogrammetry has many of the same requirements as UAV mounted ALS however the costs for the UAV and sensors are typically lower. Photogrammetry coverage can be similar to ALS however canopy penetration is often greatly reduced.
5. Manned aerial vehicle mounted ALS requires a plane to be flown over a forest and tends to be performed by third parties that survey areas of interest with contractually stipulated minimum point densities. These companies either perform

surveys of their own and sell access to data they have already collected or may also be commissioned to survey specific areas. This method can be used to collect data over a whole forest in a single survey and thus can be extremely cost effective when a large spatial coverage is required.

6. Publicly available ALS datasets are provided by some government agencies or bodies at no or low cost. A significant disadvantage of using public datasets is that there is no control of spatial and temporal coverage, there may be limited data for some areas and the period between surveys may be several years These datasets also tend to have low point densities due to the high altitudes these ALS datasets are collected from which can be particularly limiting for CCF due to the vertical complexity below the canopy.

   Examples include the UK (data.gov.uk), Finland (maanmittauslaitos.fi), Denmark (download.kortforsyningen.dk), Spain (centrodedescargas.cnig.es), and the Netherlands (lists.osgeo.org).

Most of the discussed methods of remote sensing data acquisition produce point clouds which can be processed directly to extract inventory information; photogrammetry first requires conversion of photographs into a point cloud. Point clouds yielded from photogrammetry are not directly equivalent to point clouds yielded from laser scanning primarily due to lower vegetation penetration and this can restrict their utility, as outlined in Table 1. Solutions for photogrammetry point cloud generation are available within suites of commercially available tools for data acquisition, such as the Pix4D suite, as standalone commercial packages for point cloud generation, like Agisoft Metashape, and even as open-source solutions which are freely available to install, such as WebODM.

Processing point clouds to extract inventory information can be performed in multiple programming languages. However, some of the most comprehensive packages appear in R where lidR [111] is the first choice of many for processing aerial data. For terrestrial data there are a range of packages with different utilities, such as TreeLS (available at https://github.com/tiagodc/TreeLS)[97] rTLS[112], and FORTLS[113], some such as ITSMme[98] and aRchi[114] even include tools to produce quantitative structure models of trees. Additionally, there is soon to be a public database of publicly available terrestrial point cloud processing solutions for forestry including information on their function and guidance on their use. It is to be an output of the 3DForEcoTech COST action and was publicised at the Silvilaser conference in 2023 [115,116]. For those not wishing to use programming there are standalone software solutions available such as: LiDAR360, a commercial solution produced by GreenValley International, which has aerial and terrestrial point cloud specific forestry packages available; LASTools, a licensable library of executables specific to various processing functions; Cloudcompare, an open-source solution with forestry specific tools available and for which public users and researchers often develop add-ons and; FUSION/LDV, a freely available software for point cloud data analysis and visualisation produced by the United States Department of Agriculture (USDA) Forest Service.

2.5 Conclusion

As we have explored it is evident there are a host of ways in which remote sensing could be used to address the challenges CCF faces for monitoring and management. It is our belief that there needs to be a concerted effort to further research the ways remote sensing can be applied to CCF. Remote sensing can monitor several parameters relevant to CCF, as shown in Table 1, and thus it is simply the identifying how monitoring these parameters can inform

our management and understanding of CCF that is the required. As forests are increasingly being transformed from even-aged stands to irregular CCF systems, there is increasing opportunity to make use of remote sensing in the monitoring and management of the changes in stand structure that characterise the transformation to CCF. Methods such as those already presented by Bennet et al, Stiers et al and Valbuena et al. [5,46,49] will be important contributors to the success of these efforts. Models, such as TASIII and CAPSIS, will similarly become more important over time with the increased availability of multi-temporal CCF datasets allowing the impacts of management and environmental conditions to be seen; providing the data required to inform more accurate yield forecasting models.

The accuracy and precision of remote sensing methods have dramatically improved in the years since CCF began to gain widespread traction and adoption; thus, where CCF historically represented a challenging and complex system to study, it is now well within the capabilities of the technology and the limitation has now become the lack of research into applications of remote sensing for CCF. We invite further research into the topics listed below exploring how the application of remote sensing can improve the management of CCF so that it might become a more easily adopted and managed silvicultural approach.

Topics for further research:

- Development of remote sensing supplemented inventory protocols for improved CCF management
- Stem volume estimation from below-canopy point clouds to improve estimates of standing stocks
- Stem segmentation and marketable timber estimation from below-canopy point clouds

- Application of individual tree growth modelling approaches to CCF yield estimation and forecasting
- Use of multi-temporal remote sensing datasets to develop methods to produce spatially localised growth trends and yield forecasts for CCF
- Improving regeneration prescriptions from localised information about canopy gaps and competition

2.6 Funding

Mr Stoddart received funding from the Knowledge Economy Skills Scholarships. Knowledge Economy Skills Scholarships (KESS 2) is a pan-Wales higher level skills initiative led by Bangor University on behalf of the HE sector in Wales. It is part funded by the Welsh Government's European Social Fund (ESF) convergence programme for West Wales and the Valley

CHAPTER 3

Reviewing Publicly Available TLS Processing Solutions and Their Functions

3.1 Preface

The work presented in this chapter is a brief review of publicly available TLS processing solutions and was completed as part of a short-term scientific mission (STSM) organised by the European Cooperation in Science and Technology (COST) as part of COST action CA20118, “Three-dimensional Forest Ecosystem Monitoring and Better Understanding by Terrestrial-based Technologies”.

Further materials and outputs of this work will be produced and shared by those involved in the COST action and thus the materials presented represent an early milestone in understanding and assessing the current state of processing solutions for three-dimensional TLS data in forestry. One such output of this work was the conference presentation, Cabo et al. (2023) [1], which presented this work and the conference presentation that presented the platform in which it is now publicly available, Mokros et al. (2023) [2].

3.2 Purpose of review

The purpose of this work was to create a single point of reference for information about publicly available TLS processing solutions for forest inventory applications to improve accessibility to information and lower the bar to entry for forestry researchers and practitioners. Specifically, the focus was on TLS processing solutions that could yield tree or stand level metric of forest structure rather than for more general processing such as

classification or normalisation of point clouds. The output was to a database of processing solutions and their functions in addition to details regarding applicability, ownership, availability, licensing, and documentation, found at https://3dforecotech.eu/database/. This review contributed to work presented in the Cabo et al. (2023) and Mokros et al. (2023) conference presentations [1,2] and can be seen included in an edited format in the upcoming publication "A review of point cloud processing software solutions in forest applications" Murtiyoso, et al. (2024)[3].

3.3 Methodology

Efforts to identify publicly available TLS processing solutions started with a survey distributed both to the working group of the COST action and the public, with a call for responses from practitioners and researchers that currently use TLS, to crowdsource a list of TLS processing solutions for forest inventory. This crowdsourced list was then expanded upon through systematic searches of Google, GitHub, and the R CRAN directory of packages; the search terms used for the search were permutations of "Forest" and "Forestry" and then one of "TLS," "Terrestrial LiDAR", "MLS", "Mobile LiDAR" and either the terms "processing" or "inventory". A total of 40 solutions were identified by name from the survey and searches. Results were assessed for relevance; discounting all ALS exclusive solutions, solutions without forestry applications, and any solutions for which a version could not be found publicly. After discounting there were 16 TLS processing solutions remaining and these were individually investigated populate a spreadsheet consisting of general information about each solution.

The investigation process for each solution involved testing to confirm function but no comparative assessments nor benchmarking as the solutions served a range of purposes and at this early stage of the larger COST action it was not within the scope of the work. Two test files of TLS point clouds were used, a circular plot and an individual tree extracted from the plot point cloud, as not all solutions operated at plot or stand level. The point clouds were selected for ease of testing with low noise, and collected in a low density, thinned Black Pine (*Pinus nigra*) forest in Southern Spain, where the trees have few low branches obscuring the stems. The point cloud was generated from multiple scans made using a RIEGL VZ-400i laser scanner (RIEGL Laser Measurement Systems GmbH; Horn, Austria).

3.4 Publicly available TLS processing solutions

The primary output of this work is a table to be used as a reference tool for parties interested in TLS processing in forestry (Table 3-1), the table is entirely novel with there being no comparable collection of this information or similar information. It holds great potential for facilitating easier access to information and marks the beginning of the larger work of the COST action into 3D forest monitoring and terrestrial-based technology.

The outputs of this work, Table 3-1, are correct as of their writing in November 2022 however as this field continues to develop with new solutions being developed and newer versions being released for existing solutions it is likely that list remains incorrect or contains some out-of-date information.

In time it is hoped that this table will become the foundation of a maintained database that will contain accurate, and up-to-date information for all the solutions and their functions in addition to standardised documentation of how to get started with each solution. By

providing a user-friendly and accessible repository of information the hope is that we can remove the barrier to entry to working with TLS in forestry and can promote the democratisation of information.

Table 3-1 – A novel collation of information regarding TLS processing solutions

Solution Name	Point cloud technology			Input format			Applicability	
	TLS single scan	TLS multiscan (single file)	MLS	.Las / .Laz	Other	Batch processing (multiple files)	Plot level	Tree level
FSCT [4]	✓	✓	✓	✓	X	✓	✓	✓
Dendrocloud [5]	✓	✓	✓	✓	✓	X	✓	✓
3D Forest [6]	✓	✓	✓	✓[1]	✓	✓	✓	✓
Crossing3dforest [7]	✓	✓	✓	✓	✓	X	✓	X
Point-Cloud-Tools [8]	X	✓	✓	✓	X	X	✓	✓
LIDAR 360 [9]	✓	✓	✓	✓	✓	✓	✓	✓
ITSMe (Individual Tree Structural Metrics) [10]	✓	✓	✓	✓	✓	X	X	✓
SimpleForest [11]	✓	✓	✓	✓	X	X	✓	✓
Computree [12]	✓	✓	✓	✓	X	X[2]	✓	✓
treetool [13]	?	✓	✓	✓	X	X	✓	✓
TreeQSM [14]	✓[3]	✓[3]	X	✓	X	X	X	✓
TreeLS [15]	?	✓	✓	✓	✓	X	✓	✓
LeWoS [16]	?	✓	✓	✓	✓	X	✓	✓
FORTLS [17,18]	✓	✓	✓	✓	X	✓	✓	✓
rTLS [19]	?	✓	?	X	✓	X	X	✓
TLSeparation [20]	✓	✓	X	X	✓	X	X	✓

✓ represents information that has been confirmed from documentation or testing, and was found to be reliably and repeatably extracted, through using this remote sensing data source; ? represents information which we could not find documentation to confirm or deny and which was not able to be tested for in during this work; X indicates a confirmed lack of function from documentation or testing.

1 - This solution is only compatible with las files saved in las version 1.2; **2** - This solution has a new version releasing soon with batch processing functionality; **3** – This solution requires scans in leaf off conditions. **4** – This functionality requires the use of outputs from TreeQSM.

Solution Name	Output parameters											
	Individual tree detection	DBH	Diameters along stem	Tree Height	Stem Volume	Leaf-wood classification	LAI	QSM	Crown Parameters	Total leaf area	Stem segmentation	Percolation
FSCT	✓	✓	✓	✓	✓	✓	✓	✓	✓	?	✓	X
Dendrocloud	✓	✓	✓	✓	✓	X	X	?	✓	X	✓	X
3D Forest	✓	✓	✓	✓	✓	✓	?	✓	✓	?	✓	X
crossing3dforest	✓	X	X	X	X	X	X	X	X	X	X	✓
Point-Cloud-Tools	X	✓	✓	✓	✓	✓	X	?	?	X	X	X
LIDAR 360	✓	✓	✓	✓	✓	?	✓	?	?	X	X	X
ITSMe (Individual Tree Structural Metrics)	✓	✓	✓	✓	✓	✓	X	X[4]	✓	X	X	X
SimpleForest	✓	✓	?	✓	✓	?	?	✓	X	X	✓	X
Computree	✓	✓	✓	✓	✓	?	?	X	?	?	✓	X
treetool	✓	✓	X	X	X	X	X	X	X	X	X	X
TreeQSM	✓	✓	✓	✓	✓	✓	X	✓	✓	X	X	X
TreeLS	✓	✓	✓	✓	✓	✓	X	X	?	X	✓	X
LeWoS	✓	X	X	X	X	✓	X	X	X	X	X	X
FORTLS	X	✓	?	✓	✓	X	X	X	X	X	X	X
rTLS	✓	✓	?	✓	✓	X	X	X	✓	X	X	X
TLSeparation	✓	X	X	X	X	✓	X	X	X	X	X	X

Solution Name	Information and availability					
	Availability	Licence	Implementation	Download	Documentation / Instructions	Owner/Author contact
FSCT	Free software	GPL3	Python	https://github.com/SKrisanski/FSCT	https://github.com/SKrisanski/FSCT	Sean.Krisanski@utas.edu.au
Dendrocloud	Non-commercial	Own	Standalone	http://gis.tuzvo.sk/dendrocloud/default.aspx	http://gis.tuzvo.sk/dendrocloud_tutorial/	milan.koren@tuzvo.sk
3D Forest	Free software	GPL3	Standalone	https://www.3dforest.eu/#download	https://github.com/VUKOZ-OEL/3d-forest-classic/wiki	martin.krucek@vukoz.cz
crossing3dforest	Free software	GPL3	R package	https://gitlab.com/Puletti/crossing3dforest/	https://gitlab.com/Puletti/crossing3dforest/	nicola.puletti@gmail.com
Point-Cloud-Tools	Free software	CC BY 4.0	Matlab	https://github.com/tuomasyr/Point-Cloud-Tools	https://github.com/tuomasyr/Point-Cloud-Tools	tuomas.yrttimaa@uef.fi
LIDAR 360	Commercial	Own	Standalone	https://greenvalleyintl.com/LiDAR360/	https://greenvalleyintl.com/static/upload/file/20220124/1642998782719933.pdf	info@greenvalleyintl.com
ITSMe (Individual Tree Structural Metrics)	Free software	MIT	R package	https://github.com/lmterryn/ITSMe	https://github.com/lmterryn/ITSMe	Louise.Terryn@UGent.be
SimpleForest	Free software	GPL3	Computree Plugin	https://www.simpleforest.org/pages/download.html	https://www.simpleforest.org/pages/tutorials.html	jan.hackenberg@posteo.de
Computree	Free software	GPL3	Standalone	http://computree.onf.fr/?page_id=64	http://rdinnovation.onf.fr/projects/computree/wiki/En_wiki_v5	alexandre.piboule@onf.fr
treetool	Free software	MIT	Python	https://github.com/porteratzo/TreeTool	https://github.com/porteratzo/TreeTool	omar.alfonso.montoya@hotmail.com
TreeQSM	Free software	GPL3	Matlab	https://github.com/InverseTampere/TreeQSM	https://github.com/InverseTampere/TreeQSM/blob/master/Manual/TreeQSM_documentation.pdf	pasi.raumonen@tuni.fi
TreeLS	Free software	GPL3	R package	https://github.com/tiagodc/TreeLS	Documentation available in R	tiagodc@usp.br

LeWoS	Free software	MIT	Matlab	https://github.com/dwang520/LeWoS	https://github.com/dwang520/LeWoS	di-wang@foxmail.com
FORTLS	Free software	GPL3	R package	Available in CRAN	https://cran.r-project.org/web/packages/FORTLS/FORTLS.pdf	juanalberto.molina.valero@usc.es
rTLS	Free software	GPL3	R package	Available in CRAN	https://cran.r-project.org/web/packages/rTLS/rTLS.pdf	antguz06@gmail.com
TLSeparation	Free software	GPL3	Python	https://github.com/TLSeparation	https://tlseparation.github.io/documentation/index.html	matheus.boni.vicari@gmail.com

Free software here means it has a free software license, can be downloaded, and distributed freely, and may be modified for personal use. Commercial means that users must pay for access to the full version of the software. Non-commercial means that the software is available free of charge however it is not “Free software” and may not be modified by the user.

3.5 Discussion

While this work is simply a review of the publicly available processing solutions for ground-based remote sensing and their functions, there is still room for discussion regarding the impact of this work and the state of the field and further work regarding benchmarking performance and other means of intercomparison.

This work identified and characterised the functions of 16 processing solutions, many with significant overlaps in their functions and scope. This highlights a common issue in academic fields where individuals are not aware of pre-existing work and tools, duplication, and repetition of tools. While a selection of tools can be beneficial, opening the possibility of comparisons between different algorithms and the opportunity for tool specialisation, it can also result in confusion of which solutions to use, what is 'best', and the developers committing significant time to the creation and upkeep of tools which they may otherwise have spent on other work. These concerns were raised in Cabo et al. (2023) and Mokros et al. (2023) and were the driving force behind this work. This is not however a call for the cessation of the development of new tools. Since this work was completed there have been at least three new solutions made public and this is likely to continue however it hoped that with the advent of a centralised database, outlined in Mokros et al. (2023), fewer new tools will be developed and the community can instead rally behind the current solutions, aiding in their development and innovation through use, and feedback.

Going forward there will be a need for the development and implementation of robust benchmarking to assess the performance of these tools both in terms of speed and processing demand but also accuracy and precision against a known high-quality dataset

with field validated measurements. This may be most easily achieved through use of virtual machines that can be initiated with the same allocated resources and thus be functionally comparable. Much of the complication regarding benchmarking for accuracy and precision comes from the differences between the processing solutions, it may not be possible to run each solution with the same parameters, and it also may not be reasonable to attempt to standardise parameters owing to any optimisation the authors may have performed. The 3DForEcoTech working group have already begun efforts to benchmark and further compare solutions as part of a workshop however the results of this benchmarking are still being collated and verified and thus there are publicly available results at this time.

CHAPTER 4

Methods of Data Collection and Pre-Processing

4.1 Introduction

In this chapter the sites are briefly introduced, their locations provided, and detailed descriptions of conditions given. Explanations of the methods of data collection and the collection protocols are also provided. Most of this data was collected specifically for use in this work or was from previous data collections at the sites, as is the case of the earlier data in the temporal datasets and is used with the express permission of those that initially collected it.

4.2 Study areas

4.2.1 Amazon – Fazenda Cauaxi

The Fazenda Cauaxi study area is a site of tropical rainforest arranged into 12 blocks of 100 hectares and served as the field site for Chapter 5. The area is subject to selective logging activities and different blocks have been logged at different times between 2006 and 2013. The site is in the Paragominas region of the northern state of Pará in Brazil at 3°43' S, 48°17' W. The study area has a tropical climate and the soils in the region are described as low fertility due to limited availability of key minerals such as potassium, phosphorus and magnesium and saturating concentrations of aluminium. A full characterisation of the site's soil information and vegetation structure is available in Rex et al. (2020) [1].

The region is humid and tropical with the average total precipitation annually being 2,200 mm and predominantly flat topology and an elevation ranging between 74 and 150 m above sea level [2]. The primary form of vegetation in the region is Ombrophilous Dense Forest with the upper canopy having a mean height between 30-40 m and emergent trees reaching above the canopy up to 50 m tall [2,3]. The site consisted of a region split into 12 blocks of 100 ha which were either left unlogged or subject to selective logging of similar methods at different times in the years 2006-2013 [4]. Previous works in this same area have carried out assessments of forest types at different stages of degradation [5], the impact of LiDAR pulse density on the accuracy of AGB estimations [6], an identification of logging damage impacts and recovery [5], and the development of an improved framework for reduced impact logging [7]. Previous AGB models from LiDAR in this study area were 'statistical models' using either machine learning or statistical approaches for variable selection [1,4,5,6,8,9].

4.2.1.1 Field data

The Amazon field dataset was collected in 2014 and comprised of 85 plots located at 100 m intervals along transects through logged regions of the study area. Plots were square with an area of 0.25 hectares (50 x 50 m) and their corners were registered using differential GNSS (GeoXH6000, Trimble Navigation, Ltd.; Dayton, OH, USA). Each plot contained a sub-plot of 5 × 50 m (250 m^2) along one side. Trees with a diameter at 1.3 m breast height (DBH; cm) greater than or equal to 35 cm were measured within the entire of the larger plot, whereas trees with DBH 35-10 cm were measured exclusively within the 250 m^2 subplot. DBH was measured using DBH tapes (scaled in π·mm) at a height of 1.3m from the ground or from the top of a buttress if present. AGB estimates for each field data plot were

aggregated from the AGB estimated for each tree using the Chave et al. (2014) [10] allometric model. The value for the environmental stress parameter (E) used in the model for all calculations was E = -0.104.

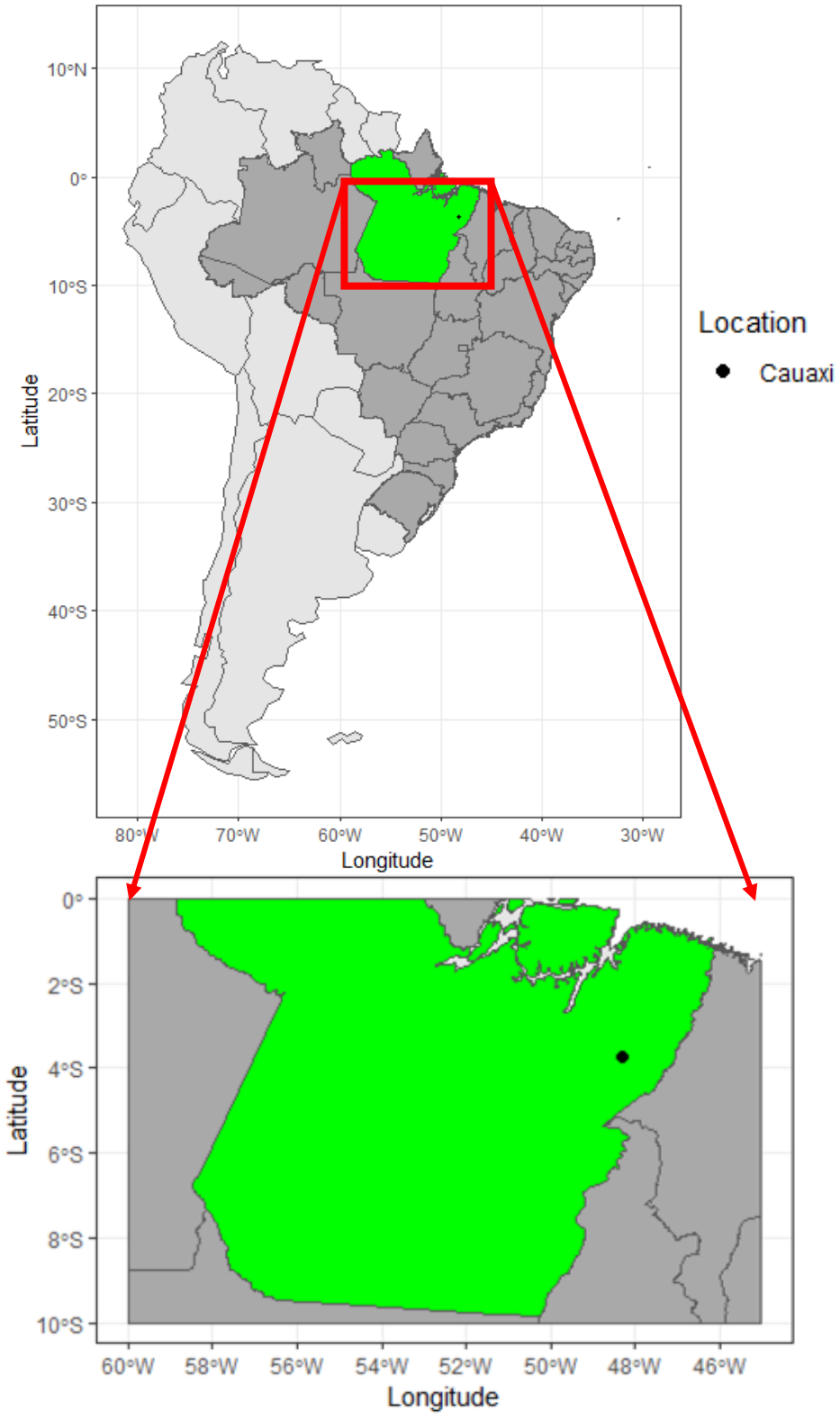

Figure 4-1. A map depicting the location of the study area in Brazil (dark grey), South America (grey), and its location within the state of Pará (green).

4.2.2 British Mixed Forest – Alice Holt, Penwood, and Eartham

Chapter 6 focuses primarily on British mixed forest across Southern England. All three forests are natural or semi-natural, managed continuous cover systems with a mixture of typical British woodland tree species, the species distributions in the areas chosen are heavily skewed towards broadleaves with however some coniferous species interspersed. All three sites share the same climatic conditions given their geographic proximity. The climate is characteristic of southern England, displaying a yearly temperature span and precipitation levels akin to the inner regions of south-central Britain. The data from the weather station at Alice Holt Lodge from 1971 to 2000 indicates an average annual precipitation during of 782 mm and an annual temperature range of -0.5 °C to 22.5°C with a mean of 10.5 °C [11].

The selected areas of forest in which plots were placed were chosen for their highly complex vegetation structures consisting of species and height mixtures as well as significant understory vegetation. The justification for selecting such complex sites is to assess the methods used in chapter 6 against the most complex structures that might be anticipated from CCF.

All data in the British mixed forest dataset was collected from 7 plots of 30 x 30 m (0.09 ha), plots of this size were selected to reduce the processing demand of the corresponding MLS data being collected at each site. Each tree of DBH greater than 70mm was recorded using digital callipers along with their species.

Plots were marked out using 50mm wide red and white barrier tape. Starting from the southwest corner, a compass was used to identify a bearing to the next corner and a measuring tape was used to mark 30m. The barrier tape was placed at approximately 1.3 m above the ground and care was taken not to twist the tape so that the flat surface would be visible in TLS scans to denote the edges of the plot. The barrier tape also serves as a clear indication of the edge of the plot when manually measuring trees.

Figure 4-2. Images depicting the range of vegetation structures found across the British mixed forest sites. Top: Two panels depicting species and height mixtures within plots. Middle: An example of dense understory vegetation on the site which can make MLS data processing more challenging. Bottom: An example of a sparser understory with regeneration including younger trees.

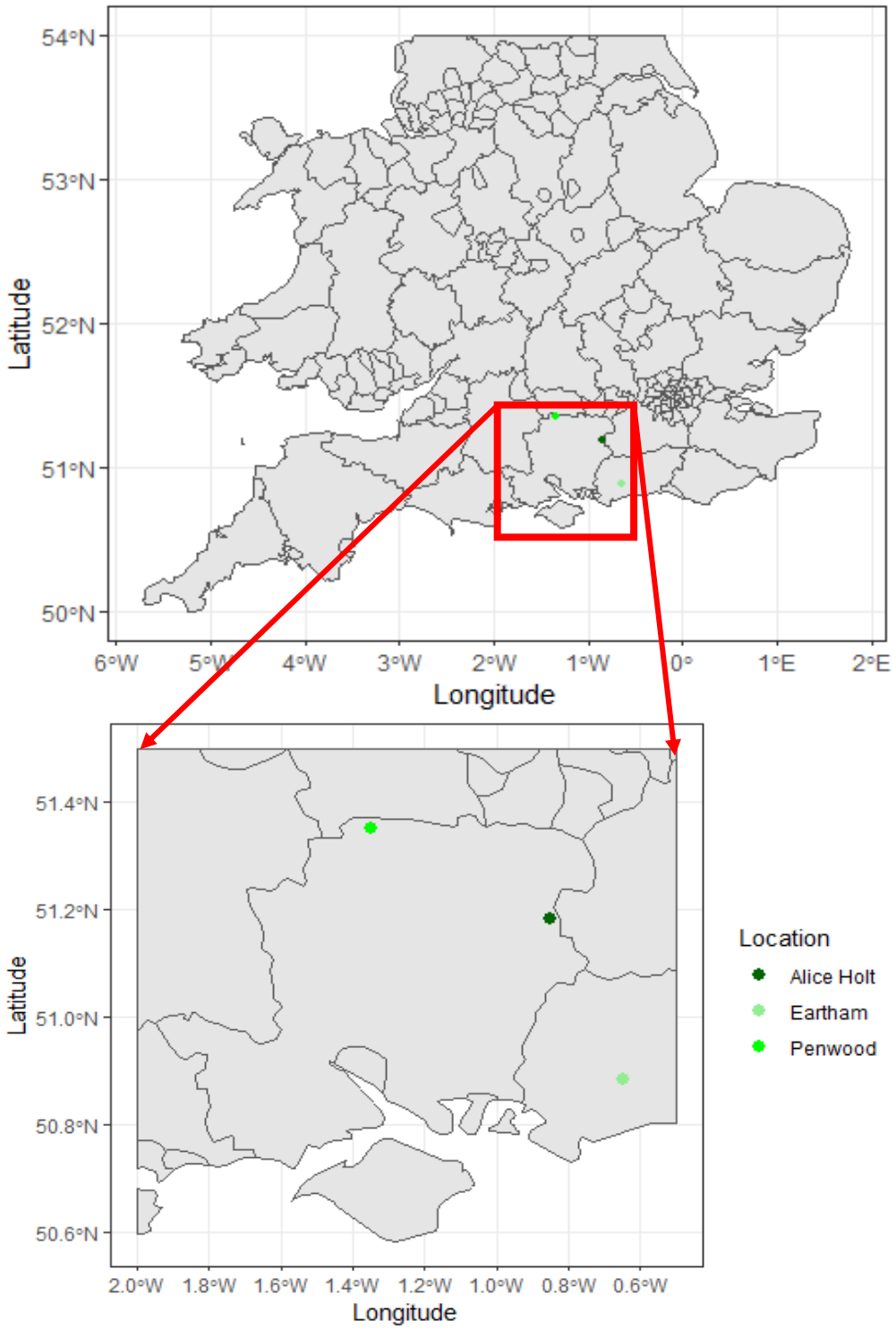

Figure 4-3. A map depicting study area locations in the south of England with colour-coded legend.

4.2.2.1 Alice Holt

The Alice Holt plots were located just outside the grounds of Alice Holt Lodge, Farnham, the headquarters of Forest Research at 51°11' N, 0°51' W. Geologically Alice Holt is situated in the north-western part of the Weald region, where the encircling perimeter of chalk transitions from an orientation running from south to north to the east-west arrangement of the Hog's Back anticline. Much of the forest lies primarily on Gault Clay but is also underlain by gravel deposits and greensands. These are topped by a range of soils from widespread brown earths and podzols to Gley soils in the wetter areas towards streams and rivers [11].

The species composition for chosen areas at Alice Holt were predominantly broadleaved dominated by Fagus sylvatica and Betula pendula with further mixtures of *Quercus robur, Fraxinus excelsior, Castanea sativa,* and *Salix alba.* Where coniferous species were present, they were predominantly *Pinus nigra* and *Tsuga heterophylla*.

4.2.2.2 Penwood

The plots in Penwood are in Great Pen Wood, found at 51°21'N, 1°21'W. The ground in the area is heavily waterlogged owing to the 4 rivers that flow through the woodland and as such the soils are characterised as Gleys. Approximately 10% of the forest area of Great Pen Wood is classed as semi-natural ancient woodland. The sample plots at this site were located within this area where the species composition is primarily Betula pendula mixed with other broadleaves such as *Quercus robur, Alnus glutinosa, Fagus sylvatica, Populus tremula,* and *Fraxinus excelsior* [12].

4.2.2.3 Eartham

Eartham Wood is located on the south downs, at 50°53'N, 0°39'W, and thus predominantly overlies chalk geology. The soils vary from brown earths to rendzinas with better soil towards the bottom of the south facing slop on which the wood sits. Eartham is predominantly replanted ancient woodland, dominated by *Fagus sylvatica* with some conifer plantations [13]. Additional species found distributed across the site include *Betula pendula, Fraxinus excelsior, Salix alba,* and *Corylus avellana.*

4.3 Fieldwork

4.3.1 Measuring DBH

Measuring DBH is a core practice of field-based inventory within forestry and thus a standardised approach is taken. Below is an illustration of the correct practices of how to locate the DBH point when measuring from ground level on a tree under a range of circumstances (Figure 4-4) as outlined in Forest Mensuration: A handbook for practitioners [14] which serves as the Forestry Commission handbook for mensuration guidelines.

In the case of buttressed trees, the 1.3 metres to the DBH point is measured from the top of the buttress and not from the ground but guidance regarding forking, swelling, and leaning is still applicable.

Once the appropriate point on the tree has been identified, DBH is measured using either callipers (scaled in cm or mm) or diameter tapes (scaled in π·mm) and recorded. Where callipers are used, two diameters are measured with the callipers rotated around the tree 90° between measurements. The average of these measurements is then recorded in an effort eliminate error from non-circular trees.

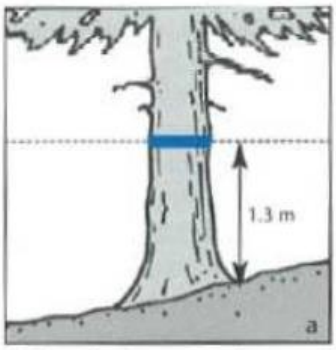

a) On sloping ground, measure the diameter at 1.3 m from ground level on the upper side of the tree.

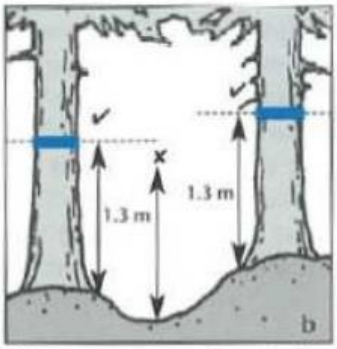

b) On uneven or ploughed ground, measure the diameter at 1.3 m from the ground level at the base of the tree.

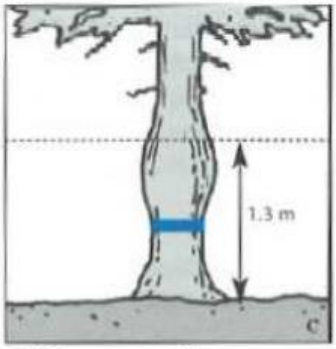

c) Where a swelling occurs at 1.3 m above ground level, measure the diameter below the swelling at the point where the diameter is smallest.

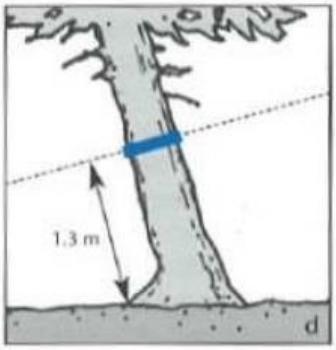

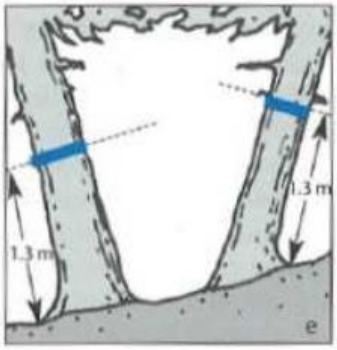

d) and e) On leaning trees, measure the diameter at 1.3 m from ground level on the underside of the tree, at right angles to the axis of the stem.

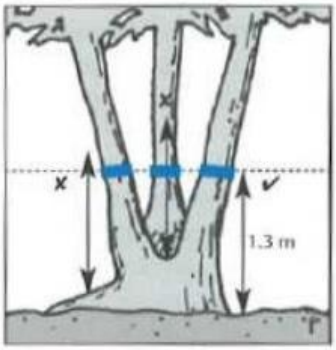

f) On coppiced trees, measure the diameter at 1.3 m from ground level and not stool level.

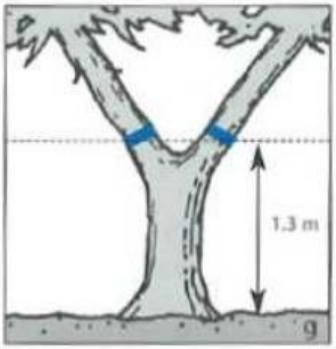

On trees that fork below 1.3 m, treat each limb as a separate tree and measure the diameter of both trees.

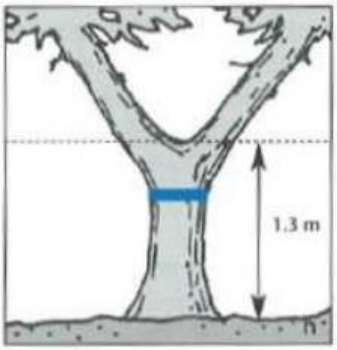

On trees that fork at 1.3 m, treat as one tree and measure the diameter below the fork at the point where it is smallest.

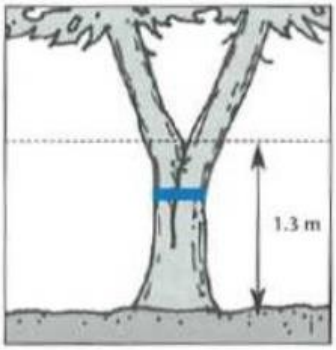

On trees where the forks have fused up to and above 1.3 m, measure the diameter below 1.3 m where it is the smallest.

Figure 4-4. An illustrated guide to locating the correct DBH point. Reproduced with author permission from Matthews and Mackie, 2006.

4.4 Remote sensing

4.4.1 Aerial laser scanning

4.4.1.1 Amazon

The LiDAR datasets for the Amazon were collected as part of a joint venture between the Brazilian Corporation of Agricultural Research (EMBRAPA) and the United States Forest Service (USFS), called 'Sustainable Landscapes Brazil.' The data was collected from manned flights in 2012, 2014, and 2017, with a survey path altitude of 850m and a horizontal overlap of the scan path of the laser scanner of 65-70%. Further details regarding LiDAR data collection such as sensor attributes and flight details are available in Table 4-1 which is reproduced from Table 2 of Rex et al. (2020) [1].

Table 4-1 Details of LiDAR data acquisitions - reproduced from Table 2 of Rex et al. (2020)

Specifications	**2012**	**2014**	**2017**
LiDAR system	ALTM 3100	ALTM 300	ALTM 3100
Acquisition date	27–29 July	26–27 December	12 December
Datum	Sirgas 2000	Sirgas 2000	Sirgas 2000
Pulse density (pulses/m^2)	13.89	37.50	22.61
Flying height (m)	850 m	850 m	850 m
Field of view (°)	11	12	15
Scanning Frequency (Hz)	59.8	83.0	40.0
Overlap Percentage (%)	65	65	70

4.4.2 Mobile laser scanning

4.4.2.1 MLS data acquisition

For MLS data acquisition in this work a GeoSLAM ZEB Horizon (GeoSLAM Ltd., Nottingham, U.K.) handheld laser scanner platform was used. The ZEB Horizon has 300,000 scanner points per second and can achieve relative accuracies of 6mm [15]. The field of view for the scanner is 360°x270° and the scanning range is 100m however due to divergence increasing with distance from scanner, and thus point density decreasing in accordance with the inverse square law, scans can be cropped during processing to only include returns within a set distance of the scanner's path, as desired. MLS data collection occurred concurrently with field data collection at the British mixed forest sites, in the spring, from mid-March until the start of April when broadleaves were still mostly in leaf off conditions.

At each site, the data capture happened in one continuous path. The laser scanner was carried by an operator at approximately 1.5m from the ground and held in front, with the operator outside the field of view to avoid artefacts. Starting from the southwest corner, the operator first walked around the outer perimeter of the plot, following the barrier tape, to capture a clear boundary and to ensure edge trees were captured from the outside. Then a path was taken from each corner to its diagonal opposite and from the centre of each side to the opposite side, with deviation from direct paths permitted owing to understory vegetation and tree stems. The scanner must then return to the starting point to complete a scan and prepare data for copying from the datalogger, such loop closure is necessary to minimise drift error [16]. An approximation of the basic path for MLS coverage is illustrated in Figure 4-5.

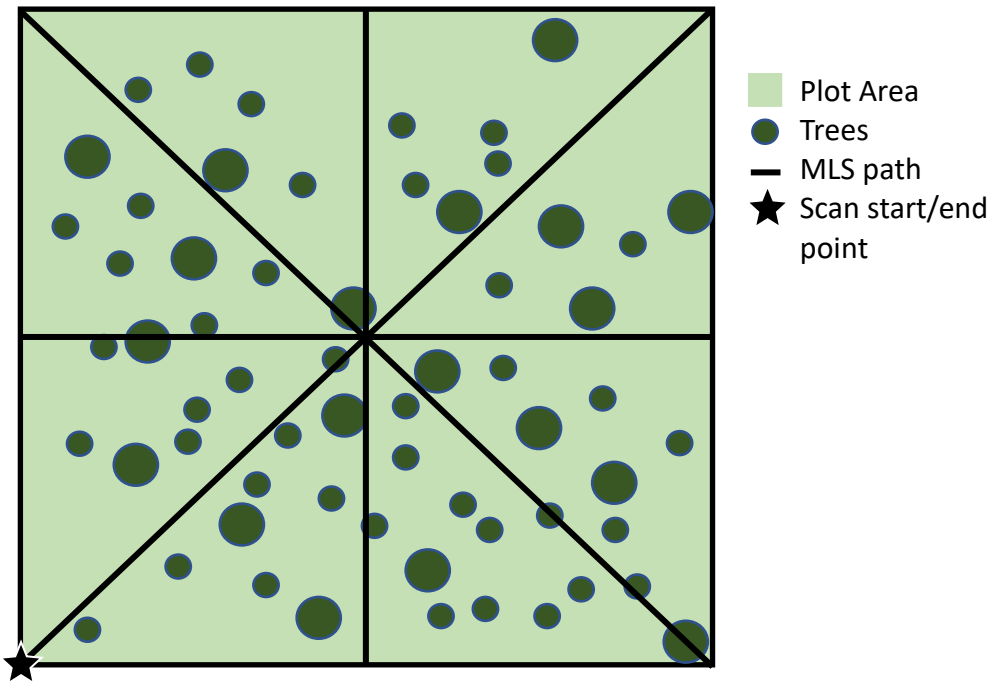

Figure 4-5. An illustration of the basic path for MLS coverage. The plot area is depicted in light green with trees shown in dark green. The path starts and ends at the southwest corner, marked with a star, and follows the black lines in a continuous path.

After each scan, data is offloaded from the datalogger and must be processed to produce the final point clouds. The processing of collected data into point clouds is performed through GeoSLAM's Hub software (https://geoslam.com/solutions/hub/) which processes the laser scanner returns with a SLAM (simultaneous localisation and mapping) algorithm. The specific mechanisms of GeoSLAM's SLAM algorithms are not disclosed. During this stage it is possible to restrict the laser scan returns used in point cloud generation to those within a set distance from the scanner platform and to specify specific algorithms for different use cases. We set this distance, the returns limit, to 15m from the scanner and used a closed loop algorithm to minimise drift [16] Once generated, point clouds are finally exported in the .LAS format ready for pre-processing.

4.4.2.2 Point cloud pre-processing

Point clouds must undergo pre-processing before they can be used for calculations of LiDAR metrics or used for inventory measurements. The extent of a point cloud is typically larger than the study plots and thus point clouds must be clipped to size. Additionally, point clouds capture information that is not relevant to the work, such as topographical information, and this must be removed to prevent errors – called point cloud normalisation.

There are multiple ways point clouds can be processed, clipping and normalisation can be performed in standalone software solutions such as LiDAR360 or through use of LiDAR specific packages in R and python.

All pre-processing of point clouds used in this work was performed through use of the lidR package in R [17,18].

The locations of the corners of the plots were recorded either using GNSS locations for ALS or through visualisation in a point cloud viewing software, CloudCompare [19], for MLS point clouds which use a local coordinate system. An example of a plot corner, as visualised in CloudCompare is displayed in Figure 4-6.

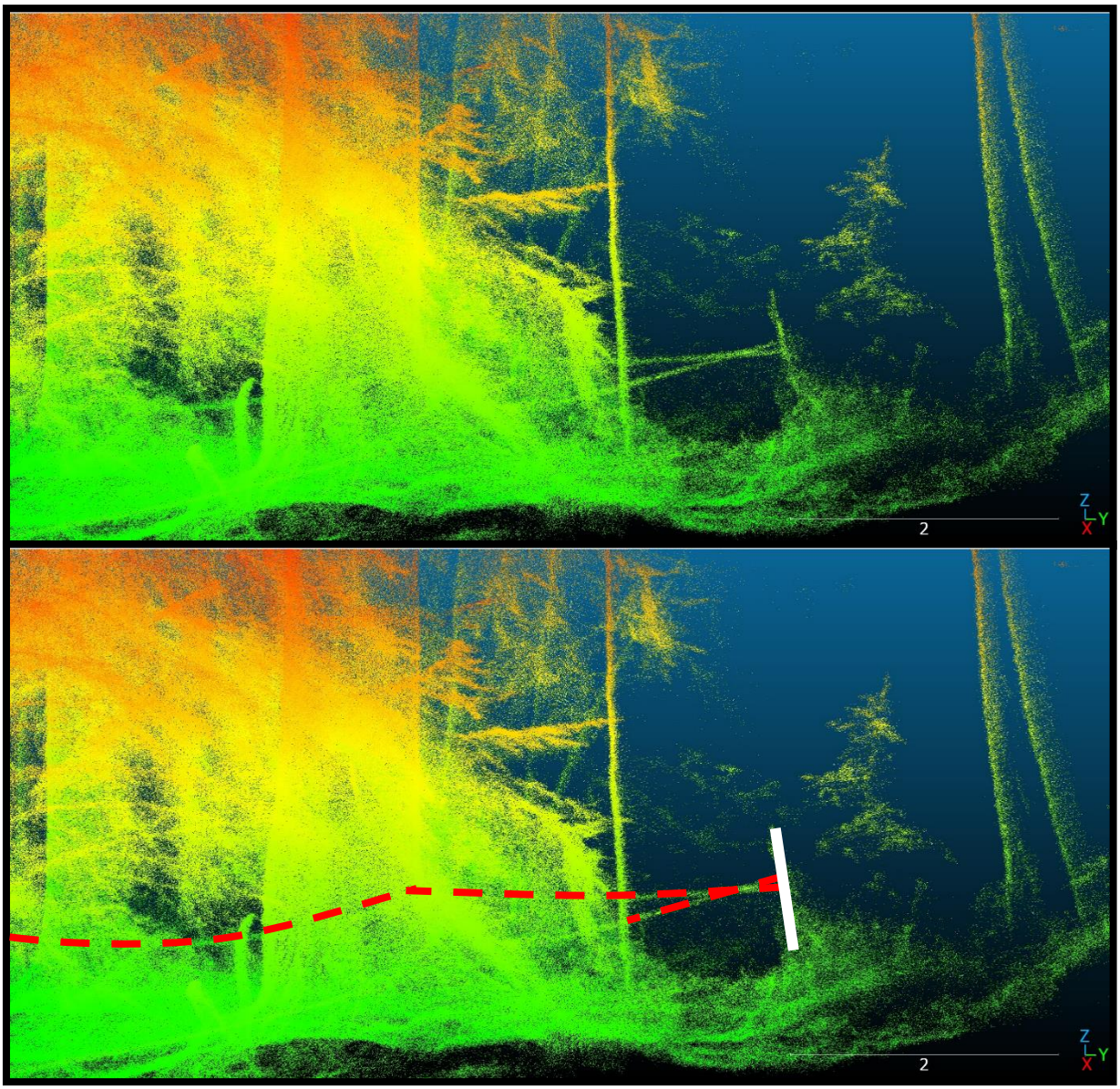

Figure 4-6. A depiction of an MLS- derived forest point cloud at a plot corner. Top: The point cloud as seen in CloudCompare. Bottom: The point cloud as seen in cloud compare with overlayed illustration to highlight the post marking the plot corner, white line, and the boundary tape, dashed red line.

Point clouds were first clipped to the area of the plot, this was done using the clip_polygon function. clip_polygon requires vectors of x and y coordinates for each of the corner locations of a plot.

The clipped point clouds were then classified through use of the classify_ground function. This uses a cloth simulation function [20] to identify ground points and classify them as class 2 – ground – in the point cloud.

The classified point clouds were normalised using the normalize_height function. The elevation of the ground is removed through use of a spatial interpolation algorithm, based upon a Delaunay triangulation, which performs a linear interpolation within each triangle and generates a convex hull - the smallest convex polyhedron, that encloses all the points in a set – for the classified ground points. The values of the z coordinates at each point on the surface of this convex hull are then subtracted from those of all points which share the same x and y coordinates. The resultant z coordinates have had the topography of the ground removed, leaving a normalised point cloud, the difference between non-normalised and normalised point clouds is depicted in Figure 4-6.

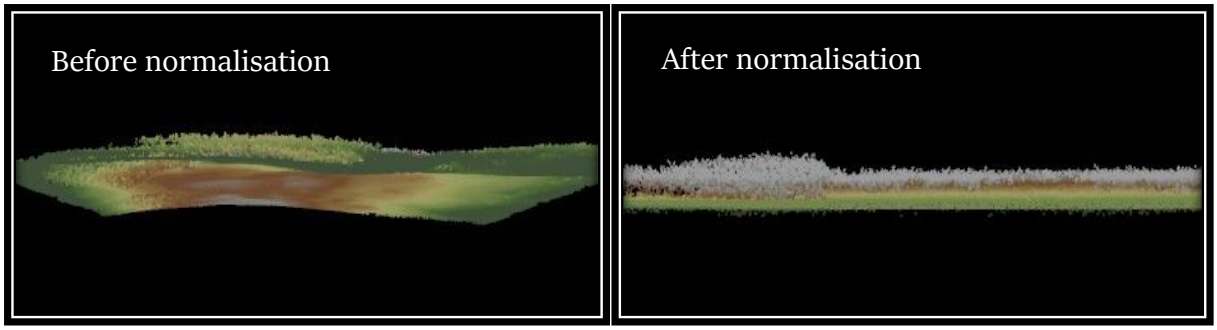

Figure 4-7. A 3D depiction of a forest point cloud before and after normalisation. The point cloud is viewed from the side and is first depicted non-normalised, with topography, and normalised, without topography.

CHAPTER 5

Applications of Remote Sensing in Complex Tropical Forest

5.1 Preface

Owing to the SARS-CoV-2 (Covid-19) pandemic and the associated restrictions imposed by the UK government it became impossible to travel and collect field data for analysis in the early stages of this work and so the decision was made to work with an available dataset from the Brazilian Amazon. The work conducted was based upon the 2020 publication by Valbuena et al. [10] which proposed the use of a system of ecosystem agnostic descriptors of morphological traits which can describe a wide range of ecosystems and thus the principles of the modelling are applicable to UK forestry despite the dataset used being from Amazonian Forest.

This chapter is adapted from the published work:

A Conceptual Model for Detecting Small-Scale Forest Disturbances Based on Ecosystem Morphological Traits

Stoddart, J.; de Almeida, D.R.A.; Silva, C.A.; Görgens, E.B.; Keller, M.; Valbuena, R. Remote Sens. 2022, 14, 933. doi:10.3390/rs14040933

The version of the work presented herein has been amended with the benefit of hindsight and experience gained over the course of my studies. The most significant deviations from the published text can be found in the discussion section.

A conceptual model for detecting small-scale forest disturbances based on ecosystem morphological traits

5.2 Abstract

Current LiDAR based methods for detecting forest change use a host of statistically selected variables which typically lack a biological link with the characteristics of the ecosystem. Consensus of literature indicates many authors use LiDAR to derive ecosystem morphological traits (EMTs) – namely vegetation height, vegetation cover, and vertical structural complexity – to identify small scale changes in forest ecosystems. Here we provide a conceptual, biological model for predicting forest above ground biomass (AGB) change based on EMTs. We showed that through use of a multitemporal dataset it is possible to not only significantly identify losses caused by logging in the period between data collections but also identify regions of regrowth from prior logging. This sensitivity to the change in forest dynamics was the criterion by which LiDAR metrics were selected as proxies for each EMT.

For vegetation height, results showed that the top-of-canopy height derived from a canopy height model was more sensitive to logging than the average or high percentile of raw LiDAR height distributions. For vegetation cover metrics, lower height thresholds for fractional cover calculations were more sensitive to selective logging and the regeneration of understory. For describing the structural complexity in the vertical profile, the Gini coefficient was found superior to foliage height diversity for detecting the dynamics occurring over the years after logging.

The subsequent conceptual model for AGB estimation obtained a level of accuracy which was comparable to a model that was statistically optimized for that same area. We argue a widespread adoption of an EMT-based conceptual model would improve the transferability and comparability of LiDAR models for AGB worldwide.

Keywords: Vegetation structure, Carbon stock, LiDAR, Modelling

5.3 Introduction

Tropical forests are complex ecosystems which importantly provide ecosystem services, especially relating to global carbon and water cycles [1,2]. Tropical forests suffer from deforestation and illegal logging which has significant environmental, ecological, and economic impacts locally and globally [3,4]. Remote sensing technologies are becoming increasingly efficient at detecting large-scale deforestation [5], however small-scale clearance activities in the Amazon rainforest account for half of Brazil's deforestation rate [6]. This small-scale deforestation includes natural windfall, legal, and illegal selective logging and is difficult to detect. There is therefore a need to further develop remote sensing technologies into methods that are more sensitive to such selective logging which would then be capable of detecting and monitoring the deforestation.

Ecosystem morphological traits (EMTs) – namely vegetation height, vegetation cover, and vertical structural complexity – are a proposed framework of 'ecosystem-agnostic' variables, which can be derived from a suite of three-dimensional (3D) remote sensing methods, to comprehensively describe the structural properties of a range of diverse ecosystems environments [7-10]. Ecosystem disturbance, such as small-scale selective logging in tropical forests, can cause changes in any of these EMTs [11], and therefore each of these

EMTs may be independently relevant to monitor to effectively fight tropical forest deforestation. Efforts to fight deforestation have been typically based on the detection of changes in either forest cover only [5] or forest height only [12]. These approaches can potentially miss selective logging activities concentrating on small trees underneath the upper canopy. There is thus a need to develop methods that can identify deforestation from changes in any of these EMTs, and not simply based on the loss of either forest cover or vegetation height.

Since remote sensing methods are best suited to tackle large-scale logging [5], the monitoring and mapping of small-scale selective logging in tropical forests still relies on expensive and time-consuming field survey techniques [13]. Among the multiple techniques that can be used to combat deforestation, airborne LiDAR – one type of 3D remote sensing [10] – has become of widespread use due to its capacity to reliably measure detailed characteristics of forest ecosystems at very high spatial resolutions [14-18]. In addition to reliable and accurate data collection, the use of airborne LiDAR benefits from fast and affordable large-scale estimation, which allows to detect logging activities and subsequent biomass changes over large and inaccessible landscapes [19, 20].

Models using data from airborne LiDAR can be used to generate maps of above ground biomass (AGB) estimates over large areas [16-18, 21-32]. Multi-temporal LiDAR can be used to evaluate small-scale changes [33, 34] but the capacity of these maps to quantify small scale changes in forest biomass is contingent upon AGB estimation models being accurate enough to detect forest disturbance [35]. The selection of predictor variables for AGB estimation models from LiDAR follow two fundamentally distinctive approaches: data-driven methods employing a statistical criterion that delivers an ad hoc selection of variables

(referred to as ‘statistical models’ hereafter), or conceptual approaches driven by knowledge of biological relationships and aim to obtain generalisable models of global validity (referred to as ‘conceptual models’ hereafter). Statistical models are based on the selecting predictors under a given criterion tested over a given sample: such as statistical significance [15,33,35], information criteria [36], penalized likelihood [37], maximization of accuracy [21, 30], or algorithms combining several criteria [38]. These models only work ad hoc, and potential issues have been identified, such as tendencies to overfit to their sample and lack of transferability [39-41]. By contrast, conceptual models employ variables that are decided beforehand because they are known to have biological and physical relationship with forest AGB and thus allow for a generalisation of the approach to AGB estimation [22, 41,]. We argue that modelling forest AGB should be based on EMTs, and thus an investigation on LiDAR proxies identified for each of them can help identify forest AGB changes from small-scale logging. The approach to conceptual modelling taken in this work fundamentally builds upon the previous work of Rex et al., 2020 [33] which used the same data set for a statistical modelling approach.

The current paradigm shift around LiDAR remote sensing is that EMTs may be better measured directly using LiDAR than by other methods, including ground assessments [42]. Thus, LiDAR could ultimately ‘ground truth’ other data sources and serve as reference to combine different data sources [27]. However, there is still a lack of consensus as to which exact LiDAR proxies (a.k.a. LiDAR metrics, sensu. Naesset, 2002) that would most suitably correspond to each of the EMTs: height, cover, and complexity [10]. For this reason, in this study we focus on identifying the LiDAR proxies for each EMT on the basis of their sensitivity to small-scale disturbances (e.g. Nunes et al., 2021 rather than on the estimated AGB change

itself (e.g. Rex et al., 2020). The expected behaviours of each of the EMTs in response to small-scale disturbance are outlined below (Figure 5-1). For each EMT there is a range of proxies that are commonly employed by authors in AGB

modelling (Table 5-1).

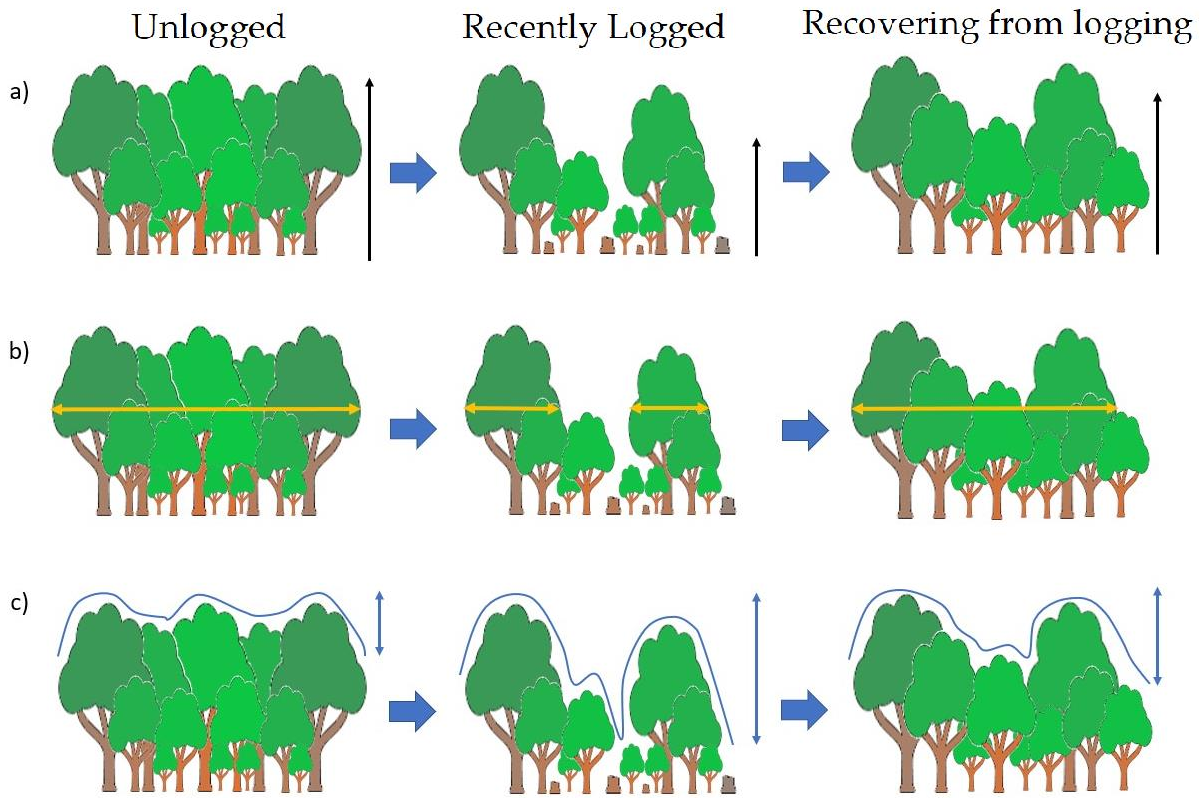

Figure 5-1. An illustration depicting the changes in each of the three ecosystem morphological traits over time in a forest stand which is subject to both selective logging and then a period of stand recovery. (a) Vegetation height – there is expected to initially be a decrease in the vegetation height EMT immediately after logging and this will then increase over time as the stand recovers and the trees continue to grow. (b) Vegetation cover – there is expected to be an initial reduction is the vegetation cover EMT immediately after logging due to gaps in the canopy. This then increases over time as the stand recovers and the canopy infills. (c) Structural complexity of vegetation – The measurable structural

complexity is expected to increase after logging due to the heterogeneity of the stand increasing and the opening of the canopy to permit greater detection of the understory. This is expected to decrease as the canopy infills and the understory grows over time.

EMT	Metrics		References
Vegetation height	Top of Canopy Height (TCH)		Lefsky et al., 1999 [43]; Asner and Mascaro, 2014; Fahey et al., 2019; Silva et al., 2019; Almeida et al., 2019.
	Mean Height (MEANH)		Næsset et al., 2002, Hinsley et al., 2009 [44], Kane et al., 2010 [45]; Fahey et al., 2019; Rex et al., 2020; Zellweger et al., 2016 [46]
	Modal Height (MODEH)		Næsset et al., 2002, Rex et al., 2020, Fahey et al., 2019
	Median Height (MEDIANH)		Næsset et al., 2002, Rex et al., 2020
	Percentiles of height (H95, H75 etc.)		Næsset et al., 2002; Kane et al., 2010; Bater et al., 2011 [47]; Zellweger et al., 2016
Vegetation cover	Leaf area index/plant area index	Percentage First Returns above threshold COVER2 COVER5 COVER10 COVER20	Nelson et al., 1988 [48]; Næsset et al., 2002 Morsdorf et al., 2006 [49]; Solberg, 2010 [50]; Korhonen et al., 2011 [51]; Görgens et al. 2017; Schneider et al., 2017;
	Gap Fraction		Wedeux & Coomes, 2015 [52]; Jucker et al., 2018; Silva et al., 2019
Structural complexity of vegetation	Entropy	Foliage Height Diversity (FHD)	Clawges et al., 2008 [53]; Bergen et al., 2009 [54]; Valbuena et al. 2012 [55]; Zellweger et al., 2016; Schneider et al., 2017

	Variability	Standard Deviation of Heights (SD)	Kane et al., 2010; Bouvier et al., 2015; Coops et al., 2016; Zellweger et al., 2016
		Gini Coefficient of Heights (GC)	Kane et al., 2010; Valbuena et al., 2013; 2017b; 2020; Adnan et al., 2021

Table 5-1 – Ecosystem morphological traits. their associated metrics, and examples of their use

In this study, we set out to identify which LiDAR-derived metrics best detect small scale disturbances and then to see if the same metrics could be applied as proxies for EMTs – namely vegetation height, cover, and structural complexity – to model AGB more accurately in selectively logged forests. Specifically, we evaluated the temporal dynamics of LiDAR-derived metrics after selective logging activities, assessing which of these metrics were more sensitive to logging. Additionally, we assessed the capacity of the metrics to identify historical logging which preceded LiDAR survey through detection of additional growth in multitemporal data sets. These analyses identified candidate LiDAR proxies for each of the three EMTs – those most sensitive to small-scale selective logging. In turn, this allowed us to develop a conceptual model for AGB estimation using EMTs to produce the most suitable LiDAR model both in terms of its accuracy and its capacity to describe the overall variability in AGB. The advantage of our EMT-based conceptual model is that the traits have a mechanistic link with the characteristics of the ecosystem rather than being selected via machine learning and statistical analyses.

5.4 Materials and methods

5.4.1 Study area

See Chapter 4 section 4.2.1.

5.4.2 Field data

See Chapter 4 section 4.2.1.

5.4.3 LiDAR data acquisition and processing

5.4.3.1 LiDAR data acquisition

See Chapter 4, section 4.4.2.1

5.4.3.2 LiDAR data processing

Processing of LiDAR data was conducted using the software FUSION/LDV version 3.8 [62], LAStools [63] and the LidR package in R [64].

Initially the data was classified to identify ground returns and then the elevation values for returns were normalised to heights-above-ground. The pulse densities were not standardised across the LiDAR data collections, as it was shown in Silva et al. (2017) that for plot level AGB predictions there is no significant impact to the accuracy of mean height measurements when the pulse density is above the range of 2.0 pulses·m^{-2}. As the pulse densities of the scans are all sufficiently above this threshold it is unlikely there will be any meaningful impact on accuracy or resolution for height measurements. We therefore do not anticipate any meaningful impact on other LiDAR-derived structural metrics, such as vertical and horizontal complexity as these are calculated from measurements of point heights.

Of the metrics listed in Table 5-1, not all were selected in this study as candidates for EMT proxies. MEANH, P75 and P95 were calculated directly from the pointcloud. A canopy height model (CHM) was generated at 1-m spatial resolution using the grid_canopy function available in LidR. TCH, was subsequently calculated as the mean of the CHM values aggregated at the grid resolution of 50m; differences in pulse density are again believed to

be negligible during this aggregation. The cover was calculated at a range of height thresholds: 2, 5, 10 and 20 m above the ground (COVER2, COVER5, COVER10 and COVER20 respectively). FHD was calculated based upon Shannon's diversity [65] abundances being the proportion of LiDAR returns within six contiguous strata along the vertical profile: <2, 2-5, 5-10, 10-20, 20-30, >30 m above the ground. GC was calculated as half of the relative mean absolute difference [39]. Unless otherwise specified the LiDAR-derived metrics were available from the outputs of functions in FUSION, and they were calculated for the LiDAR returns at the position of the field plots, and throughout the entire study area using a grid of 50-m spatial resolution, resulting in one complete grid for each of the collection years.

The maps of percentage change between 2012 and 2014 in LiDAR-derived metrics were generated using the raster package in R [66] and the software QGIS [67]. To produce graphs of temporal dynamics for each metric, we calculated the number of complete years since logging which was then subsequently used as the variable expressing the temporal dimension. Since metrics were expressed in different units and had disparate variances, we used normalised z-scores to fairly compare the changes observed at different metrics. The normalised z-scores of each metric were plotted against the years since logging - calculated from all three collection years - using the R package ggplot2 [68], showing the mean of all the corresponding 50 × 50 m cells of the grid along with ribbons showing their 95% confidence intervals.

5.4.4 AGB modelling

The dataset used for the development of models consisted of the plot aggregate AGB estimations from the field data and the 2014 LiDAR metrics calculated at the location of

those same plots. The power-law equation for the Asner et al. (2012) model (hereafter referred to as the 'TCH model') was:

$$AGB = a \times TCH^{b} \quad (1)$$

where AGB was the aboveground biomass in Mg/ha and TCH the top-of-canopy height in meters derived from LiDAR. The model parameters a and b were determined through the linearized log-log version of the model [12], including the correction for the intercept value when back-transforming the parameter a from the linear model [69].

Further from TCH model which accounted for a vegetation height EMT only, we considered a conceptual model under the postulate that all the EMTs considered in Valbuena et al. (2020) – vegetation height, vegetation cover and vertical structural complexity – explain an independent proportion of variability in AGB. The theory behind this is that there is a power to which height, as a measure of distance in physical space, can describe the volume of a forest stand as a cuboid. This value could be multiplied by a constant, e.g. a density, to give AGB – this is what the TCH model does. In our conceptual model there is no constant thus this is equivalent to attempting to describe a volume equal to AGB thus by using powers of height, cover, and complexity multiplied together we describe a larger volume in which each variable essentially alters the scale of the dimensions of the cuboid. Given that each EMT has low collinearity (addendum 1) and thus describes unique variation in forest structure the AGB described by three EMTs should be more accurate and capture more of the variation than AGB calculated from a monovariate model, This conceptual model

of three EMTs hereafter referred to as the 'EMT model,' has a power-law form as is typical in these relationships [70, 71, 72] and in LiDAR modelling [15]:

$$AGB = height^{b1} \times cover^{b2} \times complexity^{b3} \quad (2)$$

were height was the value of the LiDAR metric chosen for vegetation height ETM (TCH being one of the candidates) in meters above the ground, cover was the value of the LiDAR metric chosen for vegetation cover in units between 0-1 expressing the proportion of area covered by vegetation above a chosen height threshold, and complexity is the value of the LiDAR metric chosen for the structural complexity trait. The units for expressing complexity are dependent upon the metric chosen, with the SD being expressed in meters, the GC ranging 0-1 with GC = 0 denoting no height variability and GC = 1 denoting maximally variable, and FHD being a dimensionless measure ranging between FHD = 0 for an area with no vegetation and the logarithm of the number of strata used in its calculation which provides a value for maximum entropy (FHD = ln(6) = 1.79 in this case). Again, the model parameters a, b1, b2, and b3 were determined in the linearized log-log from of the model, including Baskerville's (1972) correction for bias in the estimation of a.

To identify the metrics that would serve as the LiDAR proxies for the EMTs in the EMT model (equation 2) several means of variable selection were employed:

1. Maps of percentage change in metrics (denoted as Δ in front of each metric). From the maps of change in the metrics it was possible identify the metrics which showed the greatest percentage change in areas of recent and historical selective logging, and thus sensitivity to small-scale disturbance and this was one factor that was used to select

LiDAR proxies. One-tailed Wilcoxon rank tests, for data grouped by the logging year, was used to assess the significance of the increase or decrease in a given metric compared to the baseline defined by the unlogged areas.

2. Graphs of temporal dynamics of metrics in the years following logging. The graphs of normalised Z-scores (in which the mean is equal to 0) were used to identify which metrics showed the greatest change in the years after selective logging and the graphs also highlighted how long it took metrics to stabilise and thus for how long after logging metrics were sensitive to the impacts of small-scale disturbance.
3. Correlation plots and Pearson correlation coefficients. Plots of the correlation of change in metrics, with trendlines and inset correlation values. These identified relationships between metrics that allowed for informed decisions to be made with regards to the use of metrics which may be explaining the same variance.

Final selection of the metrics which were used as variables in the EMT model was achieved through comparison of the information derived from the above methods of variable selection and information from accuracy assessments of predictive models using the different metrics to identify the metrics which are most sensitive to small-scale disturbance.

5.4.5 Accuracy assessment

Leave-one-out cross-validation (LOOCV) was carried out to assess the predictions of the two models. This is performed through the iterative removal of one case (i) from the total n, with the remaining used to calculate a new *AGB* prediction for the absence of that case ($pred_i^{cv}$). For the purposes of notation superscript '*cv*' identifies calculations after the cross-validation procedure, as opposed to superscript '*fit*' which denotes non-cross-validated

measures. We employed five analytical measures and two graphical methods for accuracy diagnosis. The analytical measures were employed to evaluate:

1) The precision of predictions given as the absolute and relative root mean squared error (RMSE) of predictions against the observed:

$$RMSE = SS^{cv}/n \quad (3)$$

where SS^{cv} was the predicted sum of squares through LOOCV:

$$SS^{cv} = \sum_{i=1}^{n}(pred_i^{cv} - obs_i)^2 \quad (4)$$

The error in RMSE was given in AGB units, and also the relative error *RMSE%* as the coefficient of variation of *RMSE*, i.e. calculated by dividing it by the mean observed AGB ($\overline{obs}$).

2) The degree of under- or over-prediction as the mean difference (MD) of the predictions minus the observed:

$$MD = \sum_{i=1}^{n}\frac{(pred_i^{cv} - obs_i)}{n} \quad (5)$$

Likewise, *MD* was presented both in *AGB* units and relative mean difference (*MD%*) calculated by dividing *it* by $\overline{obs}$.

3) The agreement between observed and predicted, evaluated by the coefficient of determination R^2 [83]:

$$R^2 = 1 - SS^{cv}/SS_{obs}^{tot} \quad (6)$$

where SS_{obs}^{tot} was the sum of squared differences of each observation from $\overline{obs}$:

$$SS_{obs}^{tot} = \sum_{i=1}^{n}\left(obs_i - \overline{obs}\right)^2 \quad (7)$$

Another measure of agreement depicted in Taylor diagrams (see below) was Pearson's correlation (r) but discarded in favour of adjusted R^2 its analytical use since Valbuena et al.

(2019) [83] showed R^2 to more faithfullty represent the agreement between observed and predicted.

4) The degree of overfitting, comparing the sums of squares obtained with ('cv') and without ('fit') cross-validation [18], calculated as the sum of squares ratio (SSR):

$$SSR = \sqrt{SS^{cv}}/\sqrt{SS^{fit}} \quad (8)$$

where SS^{fit} was the predicted sum of squares without LOOCV:

$$SS^{fit} = \sum_{i=1}^{n}\left(pre_i^{fit} - obs_i\right)^2 \quad (9)$$

SSR provides a suitable measure of increase in the unexplained variance when carrying out the LOOCV. It has been suggested that the difference between model fit and cross-validation exceeding 10% (i.e. SSR = 0.90-1.10) signals a model that is overfitted to the sample [39, 73].

5) The model's capacity to match the AGB variability originally observed. As the standard deviation ratio (SDR):

$$SDR = \sqrt{SS_{pre}^{tot}}/\sqrt{SS_{obs}^{tot}} \quad (10)$$

where SS_{pre}^{tot} was the sum of squared differences of each observation from the mean predicted AGB ($\overline{pre}$):

$$SS_{pre}^{tot} = \sum_{i=1}^{n}(pre_i - \overline{pre})^2 \quad (11)$$

Moreover, the graphical methods employed for accuracy assessment were:

Observed versus predicted plots depicting the LOOCV predictions. The plots include both the 1:1 line and their regression, which can be tested against the null hypothesis of

alpha = 0 and beta = 1 [18], on the basis that predicted be x and observed y in that regression analysis [74].

Taylor diagrams. A prerequisite for AGB models to produce reliable maps (especially to detect small-scale changes) is to ensure that they not just predict the average AGB but the observed variability in AGB too. To that end, we produced Taylor diagrams [75] for each of the LOOCV models using the taylor.diagram function of the package plotrix [76] which was then modified to normalise standard deviation without normalising RMSE and for additional clarity of interpretation through colour coding. Overfitting makes models less transferable by being too specific to a single site and or dataset, whereas the intent with the conceptual EMT model is to have a widely usable alternative to statistically driven, site specific models. Taylor diagrams are a method of summarising multiple aspects of model performance in a single diagram. Three statistics are plotted on Taylor diagrams:

a) Correlation, denoted by the azimuthal angle (blue radial dashed lines and arc) and which represents the Pearson correlation coefficient, evaluating similarity in patterns of distribution of the predicted and observed, which is also a measure of the similarity of the means. The Pearson correlation coefficient a normalised measure of the linear correlation between two datasets, in this case the predictions of a leave-one-out model and the observed dataset [77]. Only the squared correlation gives values comparable to the coefficient of determination in Eq. (3), but correlation is added here as implemented in the R package stats.
b) RMSE, proportional to the distance of a point from the reference for observed data, on the x-axis (which is shown by green arcs).

c) The standard deviation ratio of the cross-validation predictions to the observed is proportional to the radial distance from the origin (black arcs). The standard deviation ratio reflects how well the predictions reflect the variance of observed data.

5.5 Results

5.5.1 Vegetation height

The maps of the percentage change in LiDAR-derived height metrics (Figure 5-2 - *ΔTCH*, *ΔMEANH*, *ΔH75* and *ΔH95*), show that all the height metrics highlight areas of logging in the years between the 2012 and 2014 data collections. The areas of highest decrease in height metrics were the areas which were selectively logged in 2012 and 2013 (significant decrease in all metrics, $P < 0.01$). For *TCH* and *H75* it was even possible to detect logging activities occurring before 2012 from anomalously greater increases compared to the baseline growth in unlogged areas (significant increases, $P < 0.01$). Other common metrics like *HMEAN* or *H95* could not detect this anomalous growth (non-significant increase, $P > 0.05$).

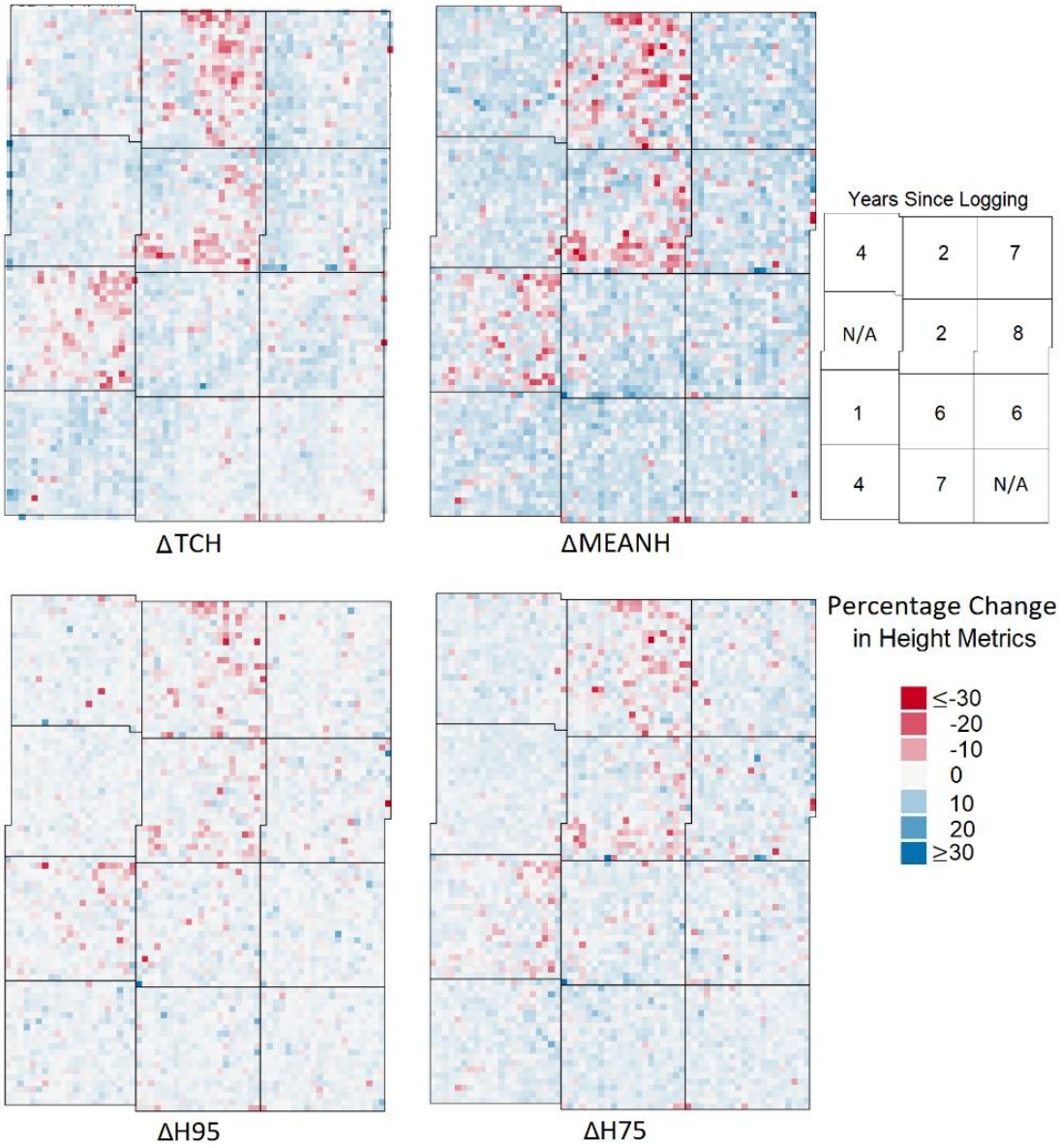

Figure 5-2. Maps of the percentage change in height metrics across the study area between 2012 and 2014 (resolution 50m). Change depicted by colour gradient with red representing the greatest negative change and blue the greatest positive change. ΔTCH – Top of Canopy Height, ΔMEANH – Mean height, ΔP75 and ΔP95 – 75th and 95th percentiles of height.

The graph of the temporal dynamics of height metrics (Fig. 5-3a) shows that *H95* had the greatest decrease in the years immediately following logging. However, it also showed an erratic upward trend after four years since logging, which may be an indication of lack of robustness in this metric. Considering this in addition to the lower sensitivity shown in

the maps of change *H95,* may be an indication that H95 is not a the most suitable LiDAR proxy for vegetation height. Of the other three metrics *H75* also showed low sensitivity in the maps and thus given the dynamics in the years after selective logging are quite similar, indicated by their overlapping confidence ribbons. *MEANH* and *TCH* appeared to be the most sensitive to logging, which can make them the most suitable metrics to select as LiDAR proxy for vegetation height.

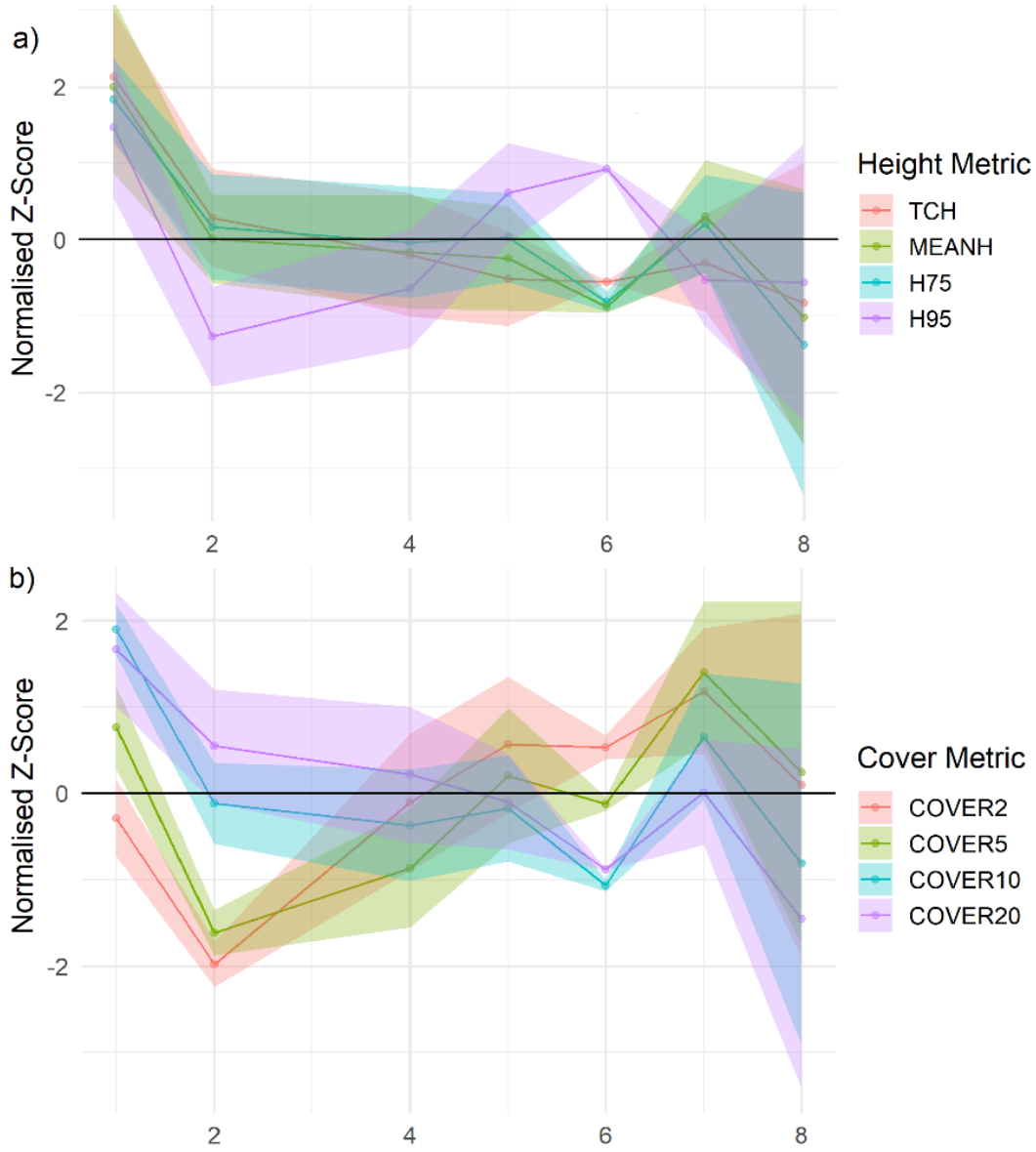

Figure 5-3 Graphs of the temporal dynamics of LiDAR metrics in the years after selective logging for each of the EMTs, normalised using Z-score for comparison between metrics. **a)** EMT – Height, TCH – Top of Canopy Height, MEANH – Mean height, P75 and P95 – 75th and 95th percentiles of height.

b) EMT – Cover, COVER2, 5, 10, and 20 are the percentage cover at height thresholds of 2, 5, 10 and 20m respectively.

c) EMT – Structural complexity, GC – Gini coefficient, SD – standard deviation of height, FHD – Foliage height diversity.

Single variable models of AGB estimation were produced for each of the height metrics to assess their relationship to AGB. Their respective RMSEs (Table 5-2) showed that the model accuracy was greatest for *TCH*. The SDRs also demonstrated that TCH can best model the range of variability in the area, with the *TCH*-based model predicting 88% of total standard deviation in AGB. SSR results show that none of the models were overfitted to the sample, with cross-validated values deviating less than 10% from model residuals. Although the MD of *H95* showed a tendency for higher biasness than other metrics. Based on these

model results, the results of the graph of temporal dynamics, and the maps it is unclear which of *TCH* or *MEANH* would be the most suitable LiDAR proxy for vegetation height. We will use *TCH* as the LiDAR proxy as it allows for a more direct comparison against the mono-variate TCH model.

Table 5-2 Statistics reflecting accuracy and goodness of fit for AGB models

		Adj. R^2	**RMSE (Mg/ha)**	**RMSE (%)**	**MD (Mg/ha)**	**MD (%)**	**SSR**	**SDR**
Height	a* × TCH*	0.82	49.93	20.97	1.64	0.69	1.03	0.88
	MEANH*	0.82	50.66	21.28	-7.89	3.31	1.01	0.69
	H95*	0.60	69.54	29.20	-11.24	-4.72	1.01	0.58
	a* × H75*	0.56	56.73	23.83	1.02	0.43	0.91	0.76
Cover	COVER2*	0.01	87.77	36.86	-15.84	-6.65	1.03	0.10
	COVER5*	0.21	85.67	35.98	-15.53	-6.52	1.04	0.15
	a*×COVER10*	0.50	74.72	31.38	1.41	0.59	1.02	0.52
	COVER20*	0.75	57.54	24.16	-5.85	-2.46	1.01	0.75
Structural Complexity	a* × GC*	0.13	80.79	33.93	1.92	0.81	1.02	0.46
	a* × FHD*	0.37	70.31	29.53	2.64	1.11	1.05	0.80
	a* × SD*	0.07	83.06	34.88	1.62	0.68	1.03	0.32
Bi-variate models								
TCH*×COVER2*		0.82	50.07	21.03	-5.47	-2.30	1.03	0.83
TCH*×COVER5*		0.81	50.96	21.40	-6.15	-2.58	1.03	0.80
TCH*×COVER10*		0.80	52.95	22.24	-7.79	-3.27	1.03	0.72
TCH*×COVER20*		0.80	54.73	22.98	-8.66	-3.64	1.03	0.62
Tri-variate models								
TCH*×COVER2*×GC*		0.81	50.46	21.19	-4.52	-1.90	1.05	0.87
TCH*×COVER2*×SD*		0.81	51.17	21.49	-4.71	-1.98	1.05	0.86

** denotes variable is significant (P<0.05), a=1 if not shown, only significant models shown.*

5.5.2 Vegetation cover

The maps of percentage change in LiDAR-derived cover metrics (Figure 5-4 - *ΔCOVER2*, *ΔCOVER5*, *ΔCOVER10* and *ΔCOVER20*) clearly identify the regions that were logged in 2012 and 2013 (significant decreases, $P < 0.01$). *ΔCOVER2*, *ΔCOVER5*, and *ΔCOVER10* highlight the different stages of regrowth in blocks from earlier logging activities in 2006-2010 (significant increases, $P < 0.01$). On the other hand, this regrowth cannot be identified from *ΔCOVER20* (non-significant increase, $P > 0.05$).

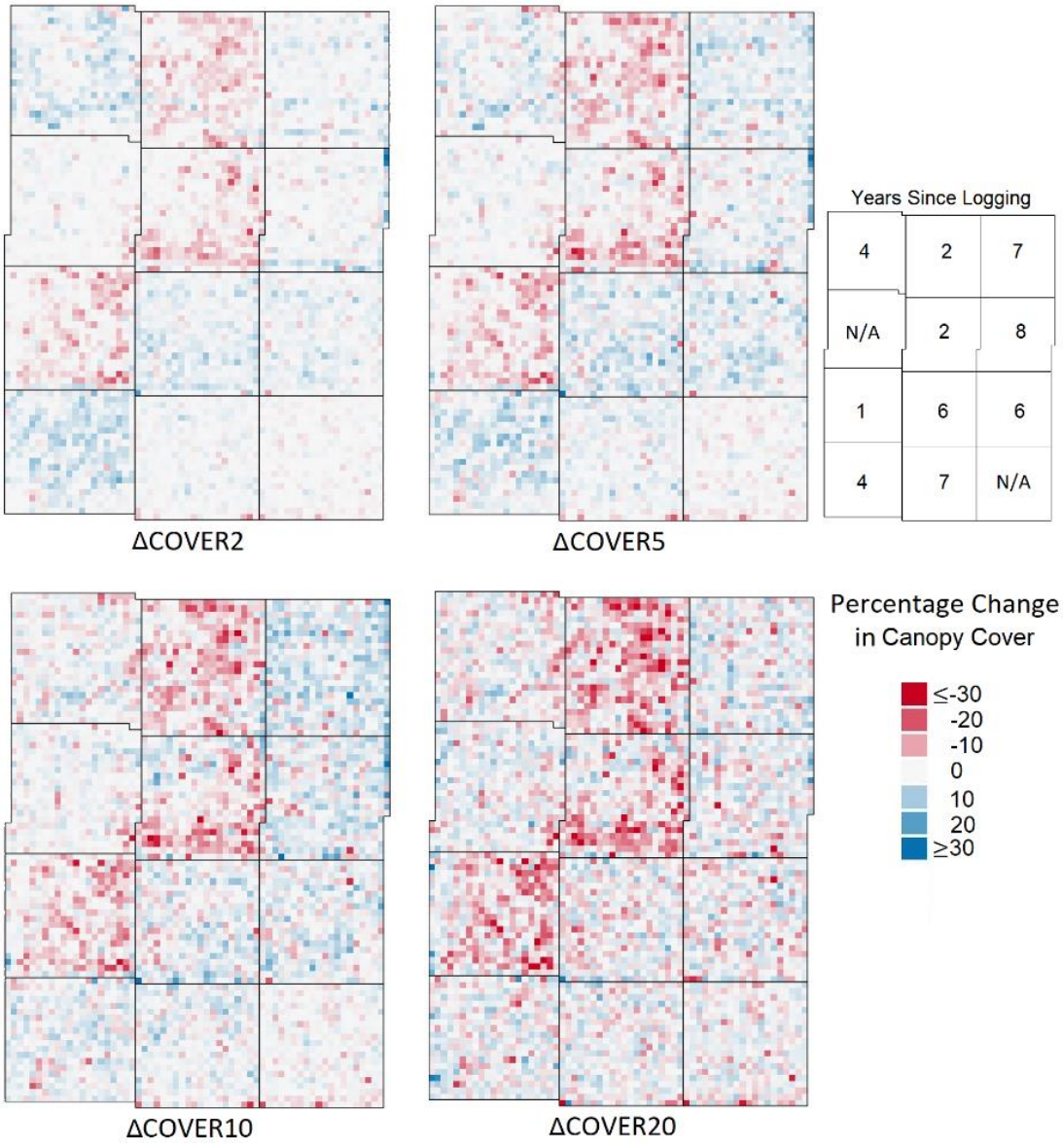

Figure 5-4. Maps of the percentage change in cover metrics of different height threshold across the study area between 2012 and 2014 (resolution 50m). Change depicted by colour gradient with red representing the greatest negative change and blue the greatest positive change. ΔCOVER2, 5, 10, and 20 are the change in percentage cover at height thresholds of 2, 5, 10 and 20m respectively.

The temporal dynamics of the cover metrics (Fig. 5-3) show that the most significant decrease in the years following logging can be detected using *COVER2*. In the short term *COVER2* will be most sensitive to recovery post logging but will provide less useful information after this period as it will return to a pre-logging value range. Metrics with greater height thresholds likely have greater potential to detect changes in cover for more years after logging. These results suggest that lower height thresholds are more sensitive to reduced impact logging in the short term and subsequently may therefore contribute to more accurate estimation of AGB if used as one of the morphological traits in calculations in the years immediately following logging events but may have their reliability and suitability drop off over greater time scales, particularly as larger and older trees are known to be the greater AGB sinks.

Univariate models of cover (Table 5-2) to predict AGB shows a trend of RMSE falling and SDR increasing as the cover threshold height increases, thus accuracy increases with the cover. By contrast when cover is modelled together with *TCH* (Table 5-2, bi-variate models) the trends in the values of RMSE and SDR reverse, and the lower height thresholds performed better. Based on the maps, the graph of temporal dynamics and the accuracy

results of the bi-variate models, *COVER2* is the clear choice of LiDAR proxy for the vegetation cover EMT.

5.5.3 Structural complexity

The maps of percentage change in the structural metrics (Figure 5-5 – *ΔGC, ΔFHD, and ΔSD*) between 2012 and 2014 in the 12 blocks of the study area and an inset map of the years each block was logged. All the metrics show (significant increases, $P<0.01$). *ΔGC* and *ΔFHD* highlight decreases in structural complexity in the regions that were logged prior to LiDAR data collections as the regions regrow (significant decreases, $P<0.01$), by contrast *SD* does not describe regions of regrowth from previous logging (non-significant decrease, $P>0.05$).

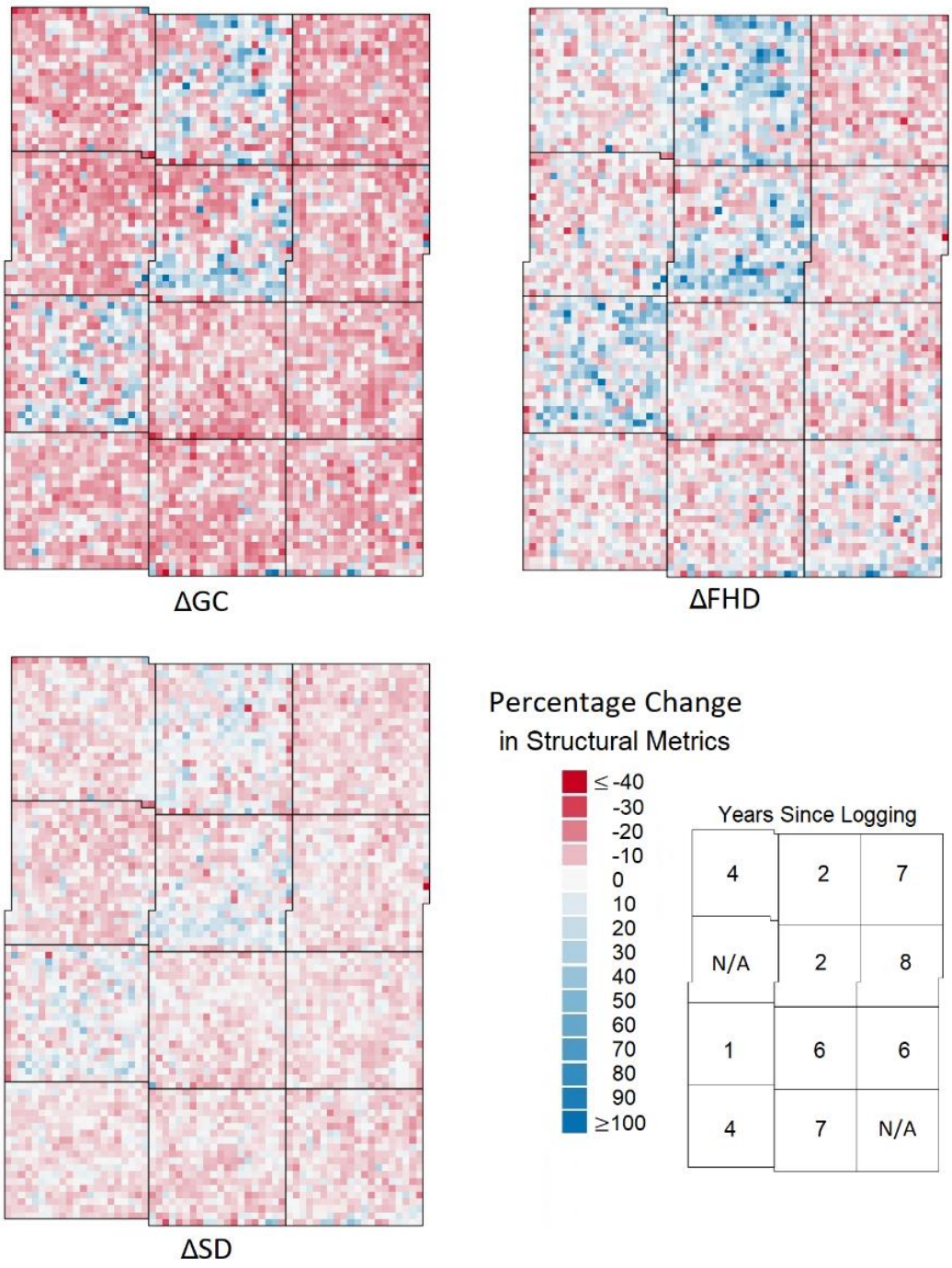

Figure 5-5. Maps of the percentage change in structural complexity metrics across the study area between 2012 and 2014 (resolution 50m). Change depicted by colour gradient with red representing the greatest negative change and blue the greatest positive change. ΔGC – Change in Gini coefficient, ΔFHD – Change in foliage height diversity, ΔSD – Change in standard deviation of heights

The graph of temporal dynamics of structural complexity metrics after selective logging (Fig. 5-3c) showed that all the structural complexity metrics are sensitive to selective logging. The temporal dynamics of all three metrics are quite similar, with sharp increases in the years after logging before beginning to stabilise and the confidence ribbons of all metrics overlap substantially.

Accuracy assessment of the single-variable models of AGB estimation for each of the structural complexity metrics (Table 5-2) shows that *FHD* performs best with the highest explained variance (SDR) and lowest RMSE. Accuracy assessment of three-variable models of the same structure as that proposed for the final EMT model (Table 5-2) found that *FHD* yielded an insignificant model and in further contrast to the univariate models, the tri-variate models with *GC* and *SD* perform similarly to each other. *GC* will be selected as the LiDAR proxy for structural complexity, given the similar performance of *GC* to *SD* in the tri-variate models and that *GC* could significantly detect the changes in structural complexity from the logging 2006-2010.

5.5.4 TCH model versus EMT model

The chosen LiDAR proxies for the EMT model were *TCH*, *COVER2*, and *GC*. The EMT model was compared to the TCH model and the results of the accuracy assessment show that the TCH model and the EMT model were able to predict AGB with very similar levels of accuracy. From the observed vs leave-one-out prediction plots (Fig. 5-6) there appears to be a very high level of correlation between the AGB values derived from field plot observations and the leave-one-out predictions of the two models. The plots for the two models show that both models fail to quite capture the variance of the observed data, as they overpredict low

values and under predict high values but they do have relatively small values for RMSE and mean difference, with the TCH model performing slightly better.

The inset Taylor diagrams show the RMSE values of the two models as well as show that the variance of the predictions of both models are not quite as great as the observed data, with both models showing a SDR of 0.88, thus only 88% of the variance of the observed data is explained. The Taylor diagram also gives a measure of the correlation that is seen between the predictions and the observations, the Pearson Correlation Coefficient, which for both models appears to be approximately 0.8.

The plotted predictions of the LOOCV analyses show very similar relationships to the predictions of the full models which suggests that neither model suffered from significant overfitting. This is corroborated by the SSR values, which show that neither model shows significant overfitting, though the EMT model may be more overfitted than the TCH model. Given the very similar performance of the two models, Occam's razor (lex parsimoniae) suggests that the simpler, monovariate, TCH model is the better choice in this scenario.

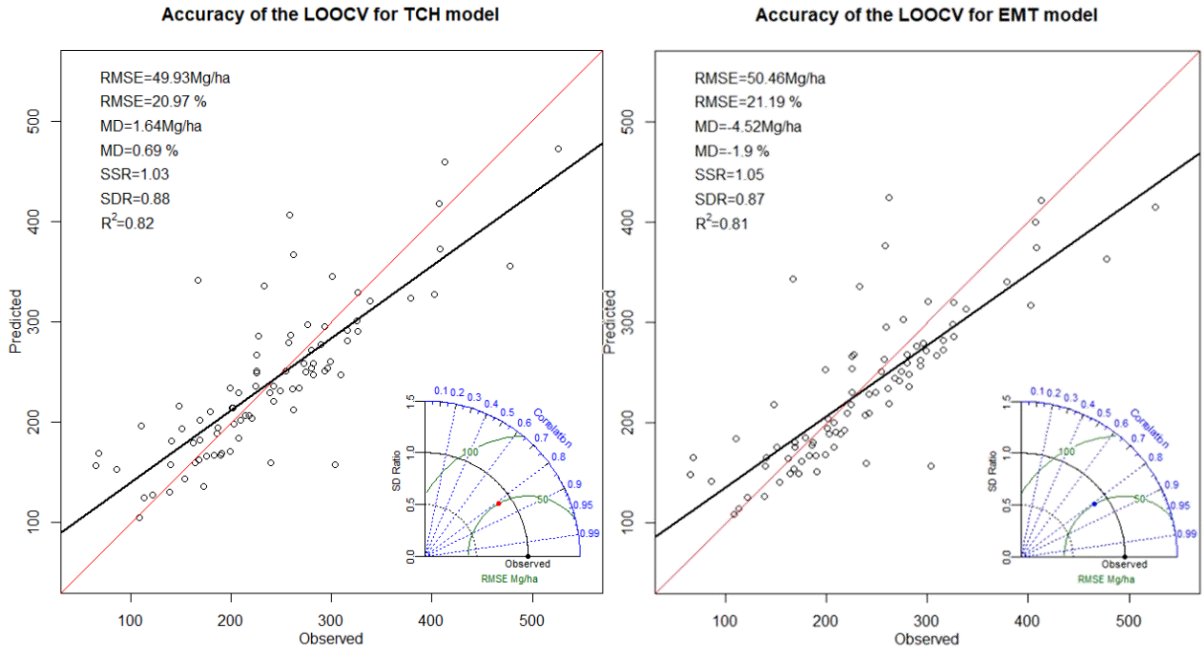

Figure 5-6 - Graphs of predicted vs observed AGB in Mg/ha for the LOOCV of the TCH and EMT models with inset statistical analysis results and a Taylor diagram representing how well the models' predictions reflect the observed data.

5.6 Discussion

Detection of logging continues to be a challenge and the development of new methods and models which can identify small-scale forest disturbance, particularly in the understory, is of great importance. Selective logging is even harder to detect than equivalent amounts of clear-felling as the disturbances are spread out and thus the localised impacts are significantly reduced. As a result, methods of AGB calculation and detection of large-scale deforestation are stretched to the limits of their sensitivity. More sensitive methods which could identify such selective logging practices are still in an early stage of development [79] hence in this study we have identified and proposed a conceptual modelling approach which could be adopted to detect small-scale forest disturbances more accurately.

A standardised framework of essential biodiversity variables could be used to model ecosystems from a range of 3D-imaging remote sensing data sources [10]. This framework is the basis of the conceptual model in this study with terms for the ecosystem morphological traits of vegetation height, vegetation cover and vertical structural complexity. The model developed using this method, the 'EMT model', was compared to a traditional method of AGB modelling presented in Asner and Mascaro (2014) and Coomes et al. (2017), the 'TCH model', a single variable model based upon *TCH*, which is a descriptor of ecosystem height. The TCH model does not account for variation in density of cover nor for a non-uniform ecosystem structure which is not thought to be a limitation of the model in undisturbed

ecosystems replete with old growth and consistently high cover but could be in regions of small-scale disturbance.

Trait selection for the EMT model was based on maps of percentage change of metrics, normalised graphs of temporal dynamics of metrics and the results of accuracy assessments of models using those metrics. The chosen LiDAR proxies to represent the traits in the EMT model were *TCH*, *COVER2*, and *GC*. Developing models for AGB estimation can sometimes be very intensive computationally, relying heavily upon statistics and even machine learning [33, 60, 80] for metric selection. In this study, we made use of visualisations of the change in metrics to determine the suitability of a metric to be included in a model. We believe that the change in metrics is a far better criterion upon which to base metric selection than raw metrics.

The visualisations of the temporal dynamics of metrics (Fig. 5-3) support the conceptual theory of how EMTs were expected to behave over time in a forest stand subject to selective logging and a period of recovery (Fig. 5-1). However as the temporal dynamics only show data for the first 8 years after logging the conclusions that can be drawn from them are somewhat limited. It is likely over longer periods that the higher threshold cover metrics become more meaningful as trees will take far more than 8 years to recover to 10 or even 20 metres height. The initial behaviour of the height metrics over time (Fig. 5-3a) reflects the expected initial decline and there also is evidence of the expected subsequent recovery over time, these changes would be expected to be reflected by the TCH and EMT models which include height as a parameter. However, the EMT model additionally includes parameters for cover and structural complexity, which the graphs of their behaviour show to behave differently to one another and to height metrics. It should however be noted that

there is an expected degree of collinearity between the metrics and height which is observed in correlation plots and that for TCH the collinearity is quite high suggesting that it may be capturing more of the structural variance than initially anticipated. Structural complexity rapidly changes in the first years after logging before rapidly stabilising whereas the cover metrics take longer to stabilise especially at the lower height thresholds where the early regenerative growth is detected. EMTs are sensitive to changes in the stand structure in the years after selective logging and can even detect historical logging that predates the survey through changes in the stand structure as illustrated by the clear delineation of the 12 plots logged at different times in the maps of percentage change in cover metrics (Fig. 5-4).

The choice of *TCH* is notable as, from the visualisations of the change in metrics, the selection of the height metric was not clear. The results of accuracy analysis of univariate models of height metrics, and the graphs of the temporal dynamics of metrics, show that both TCH and MEANH perform similarly to one another and are more sensitive than H75 and H95. The maps of percentage change in the height metrics (Fig. 5-1) were supplemented by additional one-tailed Wilcoxon rank tests to assess how the significance of the change in metrics for each logging year compared to the baseline of the unlogged areas. From the maps it was again clear that the *TCH* and *MEANH* performed similarly and were more sensitive to selective logging than the other height metrics however the Wilcoxon rank tests showed that TCH had sensitivity to historical logging that was not seen in MEANH. Given the similarity in results and the results of the Wilcoxon tests it could be argued that either metric could have made a suitable LiDAR proxy for height EMT. It was decided that TCH would be selected as LiDAR proxy despite it being generated from a CHM rather than directly from the point cloud. Asner and Mascaro (2014) suggested that the top of canopy height (TCH;

[43]) could be a simple proxy for vegetation height universally linked to forest AGB and, although the derivation of CHMs involves additional processing, the use of CHMs provides a common processing milestone across sensors and platforms of 3D remote sensing [81], which enables their robust inter-comparability and combination [10]. It is worth noting that TCH, as derived from the mean of a CHM, will reflect not just the height of the canopy trees, but also cover and vertical complexity to some degree (as the CHM height will decrease in gaps given the high 1m resolution). This may explain why the models were found to perform so similarly as there does appear to be evidence for some degree of collinearity between TCH and the LiDAR-derived metrics selected for the other EMTs (addendum 1).

COVER2 was the standout metric for the cover EMT which was an interesting outcome as in other works that have made use of cover metrics in their predictive models, higher height thresholds were often the norm for cover metrics. Jucker et al. (2018) used a cover metric, which they called gap fraction, which they calculated at 20m above ground level. *COVER20* was included in this study, and it was found to be significantly less sensitive to selective logging than lower height thresholds and the sensitivity to selective logging appears to vary inversely with the height of the height threshold for the cover calculation. The result was not entirely unexpected as Kent et al. (2015) [82] showed that it was possible to identify regions of selectively logged forest in the advanced stages of recovery due to an elevated number of gaps which penetrated to the forest floor, as determined by gaps in vegetation at a height of 2m using LiDAR data.

The chosen structural complexity term was *GC* which describes skewness of the forest structure, with low values representing uniformity of the heights of trees and high values representing an approach to bimodality. The relationship of *GC* and forest structural types

is explored in greater depth by Valbuena et al. (2014) [82]. It should be noted that only the structural metrics describing variability yielded significant tri-variate models, since FHD is a metric which describes entropy and was found to produce an insignificant tri-variate model. SD was not chosen due to relative insensitivity to selective logging. In AGB models from LiDAR, the role of the structural complexity of vegetation is typically neglected, with few exceptions [31,41]. It may be however that vertical structural complexity is not as suitable in certain ecosystems, the amazon included, where the variability in the canopy is dominated by a few large individuals, emergent trees, which reduces the impact of the structural complexity of the smaller trees that make up the canopy and understory.

Direct comparison of the two models, the conceptually derived EMT model and the TCH model, shows that they performed similarly at estimating AGB, however the differences between the models may be understated due to the fraction of plots in areas subject to selective logging being small. Consequently, most plots were not subject to disturbance thus the benefits of the logging sensitive metrics of the EMT model may have been impacted reducing the overall improvement to modelling accuracy. Other factors to consider here are that TCH was found to describe a greater degree of the cover and structural complexity EMTs than initially expected which may have also further reduced the impact that the addition of terms for these EMTs to the model may have had. The field data used was calculated using the Chave model, which like many allometric models, is limited in its capactiy to accurately describe the forest with the training data skewed towards smaller trees [84]. Such field data may therefore better match the predictions of the TCH model which tends towards an average for the heights of trees in a stand. .

Accuracy assessment of the two models found the TCH and EMT models to have very similar levels of accuracy; the explained variance, MD, and RMSE for the two models are extremely similar. An argument could be made for this being a failure of the EMT model and the method of its development as it has been shown in literature that with more variables, models are able to replicate the mean more accurately at the expense of variance [18], and thus by only being marginally more accurate than the TCH model it indicates the model is flawed due to the less significant parameters. A rebuttal to this argument is that the overfitting analyses showed that both models being slightly overfitted, to a very similar degree, and that both underpredict variance by 12-13%. This similar degree of overfitting suggests that the additional terms of the EMT model have therefore fallen victim to the MD-variance trade-off. The method of overfitting analysis used was LOOCV, which is known to yield lower MD, higher variance results than k-fold cross validation. LOOCV was chosen however due to the sample size, and the results of the LOOCV were very similar to the fully fitted models for values of RMSE, MD and variance which suggests the effects of overfitting are small. If one is confident to use the existing TCH model, then similar confidence should extend to the use of our proposed conceptual model outlined in this study, however TCH model remains the default option in accordance with the law of parsimony (lex parsimoniae). One could argue that the proposed form of the EMT model, as found in this study, reflects a development of the TCH model in which the intercept, a, in Equation 1 is replaced by the terms for cover and structural complexity in Equation 2 – and thus the model becomes more informed by biological relationships.

Comparison of both models to the results of the statistically derived multivariate models of Rex et al [33], finds that they perform similarly to the best performing model of that

paper. Their Ordinary least squares (OLS) model had an RMSE of 19.71%, a MD of -0.24%, and a R^2 of 0.70. Thus, the OLS model was capturing a similar amount of variance as both the TCH and EMT models and better captured the mean value however it was markedly less well fitted thus both models presented here arguably performed better than those derived by Rex et al.

5.7 Conclusion

The sensitivity of EMTs to the changes that happen in a selectively logged forest stands over time is evident, and this underlines the potential for a more biologically informed AGB estimation which makes use of EMTs. In addition to being suitable for the detection and quantification of illegal logging practices there are many managed regions of forest that make use of selective logging and so the use of EMTs for detecting changes in forest stands and using those same EMTs for accurate AGB estimation could aid in monitoring these regions. Landscape scale methods of AGB estimation that are sensitive to selective logging will help prevent the over prediction of AGB stocks in regions where illegal logging takes place and may support monitoring of forests in selectively logged regions, particularly below the top of the canopy in the period immediately following logging activities.

More work is needed to assess whether the EMT model structure could prove to be more accurate than the TCH model, ideally using datasets derived from destructive sampling and a greater proportion of plots in selectively logged areas as discussed above.

Author Contributions

R.V., E.B.G., C.A.S. and M.K. conceptualized the study and raised funding and resources. J.S. and R.V. designed the analyses and structured the initial drafts. J.S., D.R.A.d.A. and R.V. carried out the modelling. All authors contributed substantially to the interpretation of the results and in writing the final manuscript.

Funding: This research was funded by the *Knowledge Economy Skills Scholarships (KESS 2) in part funded by the Welsh Government's European Social Fund (ESF)*.

Data Availability Statement: LiDAR data was acquired by the Sustainable Landscapes Brazil project supported by the Brazilian Agricultural Research Corporation (EMBRAPA), the US Forest Service, USAID, and the US Department of State.

Acknowledgments:

J.S. and R.V. acknowledge the funding from the *Knowledge Economy Skills Scholarships (KESS 2) in part funded by the Welsh Government's European Social Fund (ESF)*. D.R.A.A., C.A.S., E.B.G., M.K., and R.V. extend their thanks to project AMAZECO funded by Microsoft Artificial Intelligence for Earth programme, EBVs (Essential Biodiversity Variables) on the cloud join call with GEO BON (Group of Earth Observations – Biodiversity Observation Network). D.R.A.A. also thanks São Paulo Research Foundation (#2018/21338-3). E.B.G. thanks CNPq (301661/2019-7), FAPEMIG (APQ-00943-21), CAPES and UFVJM. LiDAR data was acquired by the Sustainable Landscapes Brazil project supported by the Brazilian Agricultural Research Corporation (EMBRAPA), the US Forest Service, USAID, and the US Department of State.

CHAPTER 6

Assessing the Capacity of Three Inventory Data Extraction Tools and MLS Data for Replicating Field Inventory Measurements in Continuous Cover Forest Stands

6.1 Abstract

Inventory assessments of forests typically make use of labour-intensive field work methods to collect inventory metrics such as tree diameter (DBH), height and location and rely upon allometric modelling with large margins of error. Continuous cover forestry (CCF) stands have a greater diversity of diameters and species than traditional monoculture planta-tions, often requiring multiple allometric models to calculate standing stocks, further increasing potential errors. By contrast, mobile laser scan-ning (MLS) can rapidly measure several forest metrics however it must be processed to extract the inventory measurements of interest, which leads to a dependence upon the processing solution chosen.

This work sets out to identify the capacity of three MLS forest point cloud processing solutions to replicate traditional inventory data collection distributions and values at the plot level. The three solutions tested were FORTLS, TreeLS, and 3DFin. The comparisons were performed using data collected with traditional methods and MLS from seven squared 30 × 30 m field plots in CCF forests across the south of England. The analyses were achieved through comparisons of DBH distributions using Bhattacharyya distances and population level comparisons with Welch's t-test.

Of the three solutions tested, only 3DFin was found to replicate observed diameter distributions in a statistically significant manner ($P<0.05$,) and was found to produce values for individual DBHs with non-meaningful differences from those collected using traditional inventory methods when assessed with Cohen's d.

This work shows that MLS can be used effectively in place of more la-bour-intensive manual methods for inventory data collection, even in complex CCF stands. However, this is only possible when the point clouds are processed with processing solutions which have been demon-strated to be effective in complex forest environments as outwardly sim-ilar processing tools can provide significantly different outputs. Our re-sults showed 3DFin to be superior to other alternatives.

6.2 Introduction

6.2.1 Traditional forest inventory

Traditionally, forest inventories have consisted of systematic or random sampling of large areas with small, fixed area plots. The data collected from these plots consists of measurements of DBH for each tree; tree height, position and species may also be recorded although they may not be required or there may obstacles to their inclusion, such as difficulty collecting the data. Tree height can be difficult to accurately measure from the ground, through use of clinometers or height poles - owing to sources of error such as tree-top occlusion, ground slope and parallax [1-3] - and the accuracy and precision of positioning data from GNSS tools can be impacted by forest canopy [4]. Given the relative ease with which DBH can be collected, DBH measurements are often collected and used in allometric

models to estimate other more difficult to measure parameters such as tree height, volume, and biomass [5].

Allometric models rely upon the principles of allometric theory, outlined as follows: in all organisms, greater linear dimensions imply greater volume and thus greater mass. At its most basic, this is the fundamental relationship called an allometry [6-8]. For trees, this translates to the height being allometrically related to tree dimensions. Theories exist to explain and predict the ways trees are expected to scale, such as the pipe model theory [9]; which suggests that trees can be modelled as a bundle of independent vessels running from the root hairs to the leaves. Given that the vessels are less densely arranged in the crown and roots and constrained in a tight bundle at the trunk, a tree could be theoretically considered a cylindrical object and its volume would then scale as the product of total tree height and trunk cross-sectional area. Alternatively, the West-Brown-Enquist theory of power law scaling suggests that a plant's mass is constrained by its capacity to harvest light, which goes on to predict that tree biomass should scale as the 8/3 power of trunk diameter [10].

In practice, most allometric models are not theoretically derived but instead generated as empirical functions, inferentially derived from reference datasets [5,11,12]. Consequently, allometric models are limited in their applicability as they are dependent upon the reference dataset from which they were inferred and thus are typically species or genus specific, location and climate specific, and only accurate within the range of diameters of the reference data [5]. These local models are often preferred as they are perceived as more accurate than general models however, they can create a need to use multiple models where there is a range of species and diameters, as is common in naturally regenerating forest and

CCF. Therefore, with the widespread transformation of forest to CCF the use of traditional inventory methods to monitor progressively more complex and varied forest becomes impractical. Stands with large intra-specific diameter ranges and species mixtures may require several allometric models to be applied and require the recording of the species for every tree which increases the time taken for inventory in the field.

6.2.2 Remote sensing for forest inventory

In contrast to traditional forest inventory, in which typically only DBH is directly measured, remote sensing tools allow for the direct measurement of a range of inventory metrics, including DBH, height and even volume. Ground-based LiDAR methods, such as MLS and TLS, can produce highly detailed below-canopy point clouds of forests such that it is possible to extract inventory measurements from the point clouds and even reconstruct stem profiles [13-18]. The previous works in which inventory measurements have been taken using MLS datasets have been conducted primarily in well managed or plantation forest with relatively simple forest structures compared to CCF stands. Consequently, there are already several publicly avaible solutions capable of processing MLS and TLS data [19-37] (see chapter 3), to facilitate the extraction of inventory measurements. It has been demonstrated that automatic extraction and measurement of individual trees from MLS point clouds is possible [13-37], however given issues with reliability are often cited for areas with dense understory or complex structures the applicability of this technology to British CCF stands remains to be demonstrated. Furthermore, as many forest products are sold and quantified by volume, it may be possible to increase the accuracy and efficiency of volume estimation through direct measurement from point cloud data [5].

6.2.3 Objectives

This chapter aims to evaluate whether MLS can reliably capture DBH values in complex, heterogenous forest equivalent to a traditional inventory method. Additionally, this chapter will evaluate and compares the performance of three different MLS processing solutions at replicating traditional inventory methods. MLS data from 7 semi-natural, complex forest sites across the south of England will be processed with 3 different TLS/MLS processing solutions and the outputs compared to field data collected at each site.

The DBH measurements from the field data and the remotely sensed data will be compared to indicate whether they could be from the same population and the different MLS processing solution will be compared against one another to test if any solution outperforms the others. Following the results of these tests there will be discussion of the advantages and disadvantages of the remotely sensed approach to forest inventory including potential applications to volume estimation and wood quality assessment and directions for future work on the topic.

6.3 Methodology

6.3.1 Study area and data acquisition

The locations of the field plots for this work, introduced in 4.2.3, are all located in the south of England, and all in mixed, primarily broadleaved forest that is classed as ancient woodland, or replanted ancient woodland. The three forests - Alice Holt Forest, Great Pen Wood, and Eartham Wood – represent some of the most complex mixed forest stands in Britain in terms of structure and were selected on this basis to provide the greatest challenge to the remote sensing inventory approach.

Field data at these plots was acquired in line with the methods laid out in section 4.3, and MLS data was collected and pre-processed in accordance with methods described in section 4.4.

6.3.2 Extraction of inventory data from point clouds

Extraction of inventory data from the pre-processed MLS point clouds was achieved using three separate ground-based forest point cloud processing solutions. The three solutions, TreeLS [32], FORTLS [34,35], and 3DFin [19], were selected for their capacity to measure DBH as well as to perform individual tree detection and segmentation for stand-level processing of point clouds.. This selection contrasts with previous studies which reported high levels of accuracy for inventory data extraction from TLS and MLS point clouds; previous studies used individual tree point clouds for inventory data extraction with the individual tree clouds being generated using separate tree segmentation algorithms such as treeseg [38]. TreeLS and FORTLS are both R packages and thus were selected for added familiarity with the programming language and environment, 3DFin is available as a standalone program and was also selected for the ease of set up prior to testing.

All three solutions were tested with minimal optimisation, keeping to default parameters for ‘out-of-the-box’ testing. This approach as taken as it is likely that the creators or an experienced user could fine tune any solution to work in highly complex forest environments. In contrast, the average user is likely to rely on the default parameters of the creators, who through testing and benchmarking will have, hopefully, identified a default set of parameters sufficiently robust to provide usable outputs in a range of different forest structures.

6.3.2.1 TreeLS

TreeLS is an R package for the manipulation of terrestrial and ground-based point clouds. It is built upon the lidR package's point cloud processing tools and libraries and has many customisable parameters, such as circle fitting algorithms and tree segmentation methodologies.

The following code snippet, Snippet 6-1, illustrates the workflow for a single plot, annotated with comments to explain each step.

```
#Load package and set working directory
library(TreeLS)
setwd("C:\\Users\\jzs19xhz\\OneDrive - Bangor University\\Documents\\TreeLS")
# 1. Open a TLS pointcloud file
mls<-readTLS("..\\Plots\\Plot2_clip_jaz.las")
# 2. Thin the point cloud for mapping
thin <- tlsSample(mls, smp.voxelize(0.02))
# 3. Extract a tree map
map <- treeMap(thin, map.eigen.voxel(), 0)
# 4. Identify points to identify points that make up individual trees
tree <- treePoints(mls, map, trp.voronoi())
# 5. Identify points that make up the stem/trunk of trees
tree_stem <- stemPoints(tree, stm.hough())
# 6. Isolate only stem/trunk points
tree_stem<-filter_poi(ntree_stem, Stem == TRUE)
# 7. Calculate an inventory for all identified trees
inv <- tlsInventory(tree_stem, d_method=shapeFit
                    (shape='circle', algorithm = 'irls'))
# 8. Write inventory data to csv file
inv<-write.csv(inv,".\\Outputs\\Plot2_inventory.csv")

```

Snippet 6-1. Example TreeLS R code depicting the functions used to extract inventory data with comments describing each line.

The process for inventory data extraction using TreeLS first requires that the plot point cloud be loaded as an environmental variable. The point cloud is then subsampled to a resolution of one point per voxel, side length 2cm. The thinned point cloud is then used to produce a tree map – in which trees are identified and the locations of their stem centres recorded to allow tree segmentation. Tree segmentation is performed using an algorithm that sorts points in the un-thinned point cloud based on their nearest tree map coordinate.

Stem points are then identified for each set of tree points, the stem points are identified through use of an adapted Hough Transform circle search algorithm. This applies a constrained circle search on discretised layers of the point cloud and then performs a recursive circle search on each tree with the search area constrained to the area occupied by stem sections below. The initial estimates of the stem's feature space are performed on a baseline stem segment, where the tree's stem is expected to be clearly visible and relatively unobstructed by branches, in this case the slice from 1m to 2.5m above ground was used [39].

The point cloud is then filtered to only include points identified as stem points to reduce point cloud size and increase speed of processing for inventory extraction. Finally, inventory data is extracted and written to a .csv file. To calculate DBH, circles are fitted to the tree at 1.3m using an Iterative Reweighted Least Squares (IRLS) algorithm. This algorithm determines the best circle to fit the cloud at that location by performing automatic outlier assigning iterative reweighting with M-estimators, followed by a Nelder-Mead optimization of squared distance sums; based upon a method by Liang et al. (2012) [32, 40].

6.3.2.2 FORTLS

FORTLS is an R package that among other functions has the capacity to detect trees and estimate DBH and other attributes. It can be used with single-scan TLS data in addition to multi-scan and SLAM MLS, as was used in this work, and is designed to be easy to use. As such, the code required to extract forest inventory is relatively short and simple, see Snippet 6-2. The algorithms and design of FORTLS ae explored in detail in Molina-Valero et al. (2022) [34].

```r
# Load package and set working directory
library("FORTLS")
wd<-"C:\\Users\\jzs19xhz\\OneDrive - Bangor University\\Documents"
setwd(wd)
# 1. Create a for loop to repeat for all plots
for(x in 1:7){
  #Load the input file.
  Cloud <- normalize(las = paste0(".\\Plots\\Clip_",x,".las"),
                     scan.approach = "multi",
                     dir.data = wd,
                     normalized = TRUE)
  # 2. Identify the trees and measure DBH
  tree.list<- tree.detection.multi.scan(data = Cloud,
                                        dbh.min = 7,
                                        dbh.max = 200,
                                        stem.section = c(0.5,5),
                                        understory=TRUE)
  # 3. Write inventory to .csv file
  write.csv(tree.list, paste0(".\\FORTLS\\Outputs\\Plot",x,"_Inventory.csv"))
}
```

Snippet 6-2. Example FORTLS R code depicting the functions used to extract inventory data with comments describing the purpose of each function.

FORTLS does not have a separate point cloud importing function and instead imports as part of the first step in processing, normalisation. Given the data was pre-processed and thus already normalised, the “normalize=TRUE” argument is included to simply import the point cloud without further manipulation.

The next step is tree detection, FORTLS has separate tree detection functions for single scan and multi-scan data, MLS data from SLAM is treated as a form of multi-scan data when choosing between functions in FORTLS. The tree detection algorithm in FORTLS identifies trees, calculates DBH and gives a measure of occlusion through how many sectors around the circle fitted to the tree have points in. The parameters for FORTLS allow systematic exclusion of trees outside the DBH range of interest, as in traditional inventory. The minimum dbh was set to 7cm (70mm) and the maximum at 200cm. The region of interest to identify tree stems was set to 0.5m to 5m elevation, this range is greater than the default used by FORTLS due to significant occlusion but understory in some places. The

"understory" argument was set to "TRUE" to indicate the presence of dense understory vegetation.

Once trees were detected, the recorded data for each tree was stored to a data frame and the data frame was written to a .csv file.

6.3.2.3 3DFin: 3D Forest inventory

3DFin is a free software that is available four ways; as a CloudCompare plugin, a QGIS plugin, a Python package, and as a standalone program. In this work, the CloudCompare plugin was used as it is the recommended way to use 3DFin given the availability of CloudCompare tools to visualise and export outputs, however there should be no difference in functions relative to other implementations [19].

3DFin has 3 tiers of editable parameters – basic, advanced, and expert – which allow for a large range of customisation from basic parameters such as whether or not the point cloud is normalised and the height range in which to search for unobstructed stems, to expert parameters such as allowed deviation of stem profile from verticality and the minimum number of voxels required to determine if a tree is present.

Most parameters were left as default to perform the inventory data extraction as initial tests found they performed well. Pruning intensity, the number of iterations an algorithm is run to eliminate branches and clean up stem surfaces, was set to 3 owing to the number of branches present in height range, the stripe, in which 3DFin searched for stems.

6.3.3 Statistical testing and comparisons

As the field data does not have tree-level location information, in the form of GNSS, the comparisons of the traditional inventory dataset to each remote sensing inventory dataset must be at the plot-level rather than the tree-level. Comparison of the plot-level inventory datasets is achieved through comparison of the distributions of DBH measurements to indicate whether the two datasets could be from the same population, and thus whether the remote sensing approach is performing equivalently to traditional inventory methods. If two compared datasets were found to have different distributions of diameters this would be indicative of the two methods capturing different data and thus, where the traditional inventory represents a benchmark for accuracy, the remote sensing approach would be underperforming.

The process of comparing the datasets derived from the two approaches was conducted entirely in R and first required that for each combination of seven plots and four methods – traditional inventory and the three solutions for point cloud processing – a Weibull distribution was fitted to the distribution of DBH measurements.

6.3.3.1 Weibull distributions

A Weibull distribution is a probability distribution characterized by two parameters: shape, which affects the curve's steepness, and scale, which affects the distribution's overall range. Weibull distributions are flexible and can therefore be fitted to several types of distributions including normal (Gaussian), exponential and skewed (heavy tailed) distributions. The Weibull distributions were fitted using maximum likelihood estimation (MLE).

The R packages dplyr [41], and fitdistrplus [42] were used, in addition to core R packages [43], to fit the Weibull distributions to each dataset, using the code below (Snippet 6-3). The DBH data from all the plots and for each method was aggregated into a single file. Weibull distributions were fitted using the fitdist() function from fitdistrplus with the distribution type set to “weibull” and the method used was maximum likelihood estimation. Upon fitting the Weibull parameters, scale and shape, were written to a data frame for each plot and method. The parameters for traditional field inventory distributions were written to a separate data frame to for ease of comparison to LiDAR inventory parameters at a later stage in the script.

```r
# 1. Load necessary packages
library(dplyr)
library(fitdistrplus)

# 2. Import combined data frame of all DBH data
#    Data frame columns: Diameter, Plot, Method
all_diameters <- read.csv("E:\\Inventory_Chapter\\All_diameters.csv")

# 3. Weibull Calculations for Field Parameters
field_parameters <- all_diameters %>%
  filter(Method == "Field") %>%
  group_by(Plot) %>%
  summarise(scale_field = fitdist(Diameter, distr = "weibull", method = "mle",
                                  lower = c(0, 0))$estimate["scale"],
            shape_field = fitdist(Diameter, distr = "weibull", method = "mle",
                                  lower = c(0, 0))$estimate["shape"])

# 4. Weibull Calculations for Lidar Data
lidar_parameters <- all_diameters %>%
  filter(Method == "TREELS") %>%
  group_by(Plot) %>%
  summarise(scale_lidar = fitdist(Diameter, distr = "weibull", method = "mle",
                                  lower = c(0, 0))$estimate["scale"],
            shape_lidar = fitdist(Diameter, distr = "weibull", method = "mle",
                                  lower = c(0, 0))$estimate["shape"],
            Method="TREELS")

lidar_parameters <- rbind(lidar_parameters,all_diameters %>%
  filter(Method == "FORTLS") %>%
  group_by(Plot) %>%
  summarise(scale_lidar = fitdist(Diameter, distr = "weibull", method = "mle",
                                  lower = c(0, 0))$estimate["scale"],
            shape_lidar = fitdist(Diameter, distr = "weibull", method = "mle",
                                  lower = c(0, 0))$estimate["shape"],
            Method="FORTLS"))

lidar_parameters <- rbind(lidar_parameters,all_diameters %>%
  filter(Method == "3dFin") %>%
  group_by(Plot) %>%
  summarise(scale_lidar = fitdist(Diameter, distr = "weibull", method = "mle",
                                  lower = c(0, 0))$estimate["scale"],
            shape_lidar = fitdist(Diameter, distr = "weibull", method = "mle",
                                  lower = c(0, 0))$estimate["shape"],
            Method="3dFin"))


```

Snippet 6-3. Example R code depicting the process of fitting Weibull distributions to inventory data.

6.3.3.2 Bhattacharyya distances – Analysis of variance and Tukey's HSD

To compare the similarity of distributions, the Bhattacharyya distance was used. The Bhattacharyya distance is a statistical measure quantifying the dissimilarity between two probability distributions. It is based upon the Bhattacharyya coefficient (BC), which gauges the overlap between the two distributions through the overlap of their square root-transformed probabilities; calculated as:

$$BC = \sum \sqrt{p(x) \times q(x)} \quad (1)$$

where, $p(x)$ and $q(x)$ are the probability density functions of the two Weibull distributions [44].

The Bhattacharyya distance is computed as the negative logarithm of the Bhattacharyya coefficient, indicating the degree of divergence.

$$Bhattacharyya\ distance = -\ln(BC) \quad (2)$$

The Bhattacharyya distances were calculated, see Snippet 6-4, with a custom function for Bhattacharyya distance which took the Weibull parameters of the two distributions as inputs, calculated the probability distribution for DBH values from 70mm to 1000mm, and output the Bhattacharyya distance for those two distributions. This function was used within a loop to calculate the Bhattacharyya distance for the distributions at for each plot; between the traditional inventory data and LiDAR processing solutions' data, and between the traditional inventory data and itself. The Bhattacharyya distances were then written to a data frame along with details of the corresponding plot and method assessed.

It should be noted that owing to rounding the Bhattacharyya distance calculated between a distribution and itself does not return 0 as it should. To amend this for the comparison of field data against field data would invalidate the subsequent analysis of variance between, given all the methods are subject to the same systematic error in rounding the interpretation of the subsequent analysis should remain the same.

Following the calculation of the Bhattacharyya distances an analysis of variance (ANOVA) was performed to assess whether there were any significant differences in the distributions

of the remote sensing solutions and the field data, with a null hypothesis that all four distributions were equal. The ANOVA does this by checking whether the Bhattacharyya distances for each method were statistically different from one another.

If the ANOVA indicates that Bhattacharyya distances of the methods are significantly different from one another, Tukey's Honestly Significant Difference (HSD) test will be used as a post hoc test to identify which methods differ from one another.

```r
# 5. Bhattacharyya Distances Calculation
calculate_bhatt_distance <- function(scale1, shape1, scale2, shape2) {
  x <- seq(70, 1000, by=1)
  p1 <- dweibull(x, shape1, scale1)
  p2 <- dweibull(x, shape2, scale2)
  bc <- sum(sqrt(p1 * p2))
  distance <- -log(bc)
  return(distance)
}

bhatt_distances <- data.frame()

for (i in 1:nrow(field_parameters)) {
  plot <- field_parameters$Plot[i]
  scale_field <- field_parameters$scale_field[i]
  shape_field <- field_parameters$shape_field[i]

  lidar_data_plot <- lidar_parameters %>% filter(Plot == plot)

  for (j in 1:nrow(lidar_data_plot)) {
    method <- lidar_data_plot$Method[j]
    scale_lidar <- lidar_data_plot$scale_lidar[j]
    shape_lidar <- lidar_data_plot$shape_lidar[j]

    bhatt_distance <- calculate_bhatt_distance(scale_field, shape_field,
                                               scale_lidar, shape_lidar)

    bhatt_distances <- rbind(bhatt_distances,
                             data.frame(Plot = plot,
                                        Method = method,
                                        Bhatt_Distance = bhatt_distance))
  }
  bhatt_distance <- calculate_bhatt_distance(scale_field, shape_field,
                                             scale_field, shape_field)

  bhatt_distances <- rbind(bhatt_distances,
                           data.frame(Plot = plot,
                                      Method = "Field",
                                      Bhatt_Distance = bhatt_distance))
}

# 6. Statistical Analysis of Bhattacharyya Distances
perform_anova <- function(data) {
  anova_result <- aov(Bhatt_Distance ~ Method, data = data)
  return(anova_result)
  }

anova_result <- perform_anova(bhatt_distances)
print(summary(anova_result))

# 7. Perform Tukey's HSD
tukey_result <- HSD.test(anova_result, "Method")
print(tukey_result)
```

Snippet 6-4. Example R code depicting the approach to calculating Bhattacharyya distances and performing an analysis of variance.

6.3.3.3 Welch's T-test and Cohen's d

To assess how well each remote sensing solution replicated the DBH measurements themselves, as opposed to the plot level distribution, Welch's t-test was employed. A pairwise t-test was performed for each of the remote sensing solutions, the t-test assesses whether two populations are different with a null hypothesis of no significant difference.

The t-test was performed in R with the R core stats package, a Welch's t-test was performed by setting the argument "var.equal" to "FALSE". By performing a Welch's t-test rather than a Student's t-test we account for unequal variances, and generally it should always be the preferred t-test as if variances are equal the Welch approximation to the degrees of freedom is the same as the pooled variance akin to the Student's t-test.

In addition to the t-test, Cohen's d is calculated for each of remote sensing solutions. Cohen's d is a standardised effect size measure which quantifies the differences between the means of two groups, in terms of the number of standard deviations. It's a way to express the size of the difference between groups' means in a common unit, making it easier to compare effect sizes across different studies or contexts. In this context, Cohen's d serves as a measure of the practical significance of differences between groups, if the t-test shows that there are significant differences.

Cohen's d is calculated as:

$$Cohen's\ d = \frac{\mu_1 - \mu_2}{\sigma_{pooled}} \quad (3)$$

where μ_1 represents the mean of population 1, the DBH measurements from the remote sensing method; μ_2 represents the mean of population 2, the DBH measurements from the traditional inventory; and σ_{pooled} represents the pooled standard deviation, which is a combined measure of the variability within both groups.

```r
# 8. Set up pairwise t-tests for LiDAR Methods vs. Field Data
lidar_methods <- unique(lidar_parameters$Method)
field_data <- all_diameters %>% filter(Method == "Field")

t_test_results <- list()

for (method in lidar_methods) {
  lidar_data <- all_diameters %>% filter(Method == method)

  t_test_result <- t.test(lidar_data$Diameter, field_data$Diameter,
                          var.equal = FALSE)
  t_test_results[[method]] <- t_test_result

# 9. Calculate Cohen's d as a measure of how meaningful statistical
#    differences are
  mean_diff <- mean(lidar_data$Diameter) - mean(field_data$Diameter)
  pooled_sd <- sqrt((var(lidar_data$Diameter) + var(field_data$Diameter)) / 2)
  cohen_d <- mean_diff / pooled_sd

# 10. Print result of t-test and Cohen's d
  cat("Welch's T-Test for", method, "vs. Field Data:\n")
  cat("p-value:", t_test_result$p.value, "\n")
  cat("Cohen's d:", cohen_d, "\n\n")
}

```

Snippet 6-5. Example R code depicting the approach to performing pairwise t-tests and calculating Cohen's d.

Interpretation of Cohen's d broadly follows the pattern that values between 0 and approximately 0.2 are small effects that may not be impactful. Values around 0.5 are moderate effects where the difference is expected to be meaningful, and values around 0.8 or higher are large effects where the difference is substantial.

6.4 Results

The analyses were run twice, once with the complete dataset and once with plots 3 and 4 removed owing to poor point cloud quality and reduced point density which could impact

and skew results. Owing to the poor point cloud quality not all the processing solutions were able to extract inventory data for plots 3 and 4, FORTLS failed to extract inventory data at plot 3, and 3DFin failed on plot 4. Where solutions did extract inventory data for plots 3 and 4 there were very few trees identified compared to the traditional inventory which indicated that the solutions have been unable to identify and measure many of the trees in each plot. The results were found to change significantly from this the removal of poor-quality data as outlined below.

6.4.1 Complete dataset – all plots

The results presented in this section are from analyses performed on the Weibull distributions depicted below, figure 6-1.

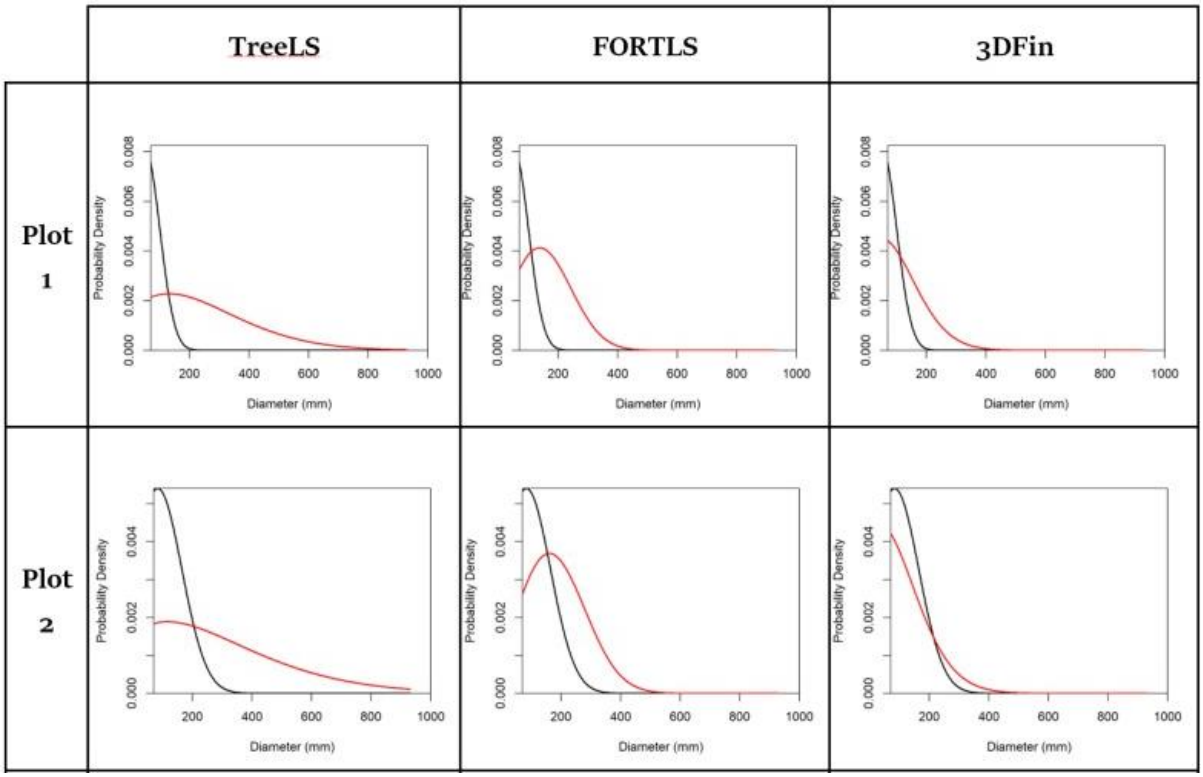

Plot 3	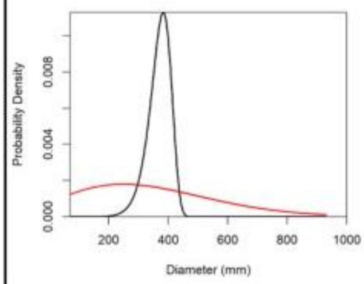		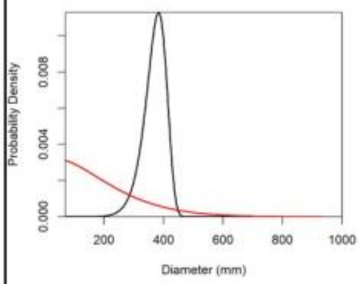
Plot 4	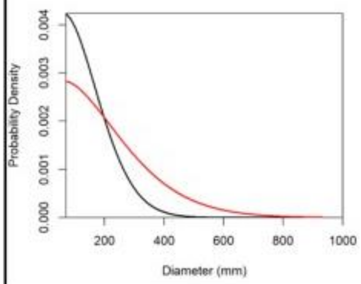	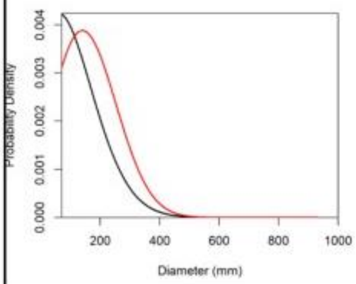	
Plot 5	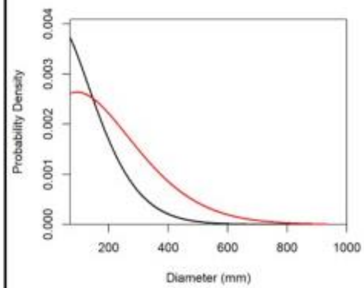	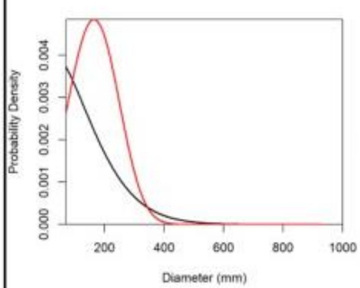	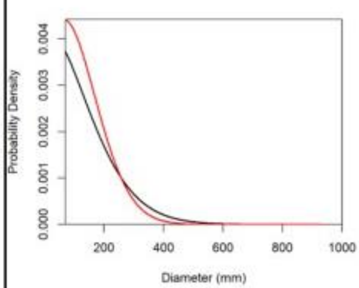
Plot 6	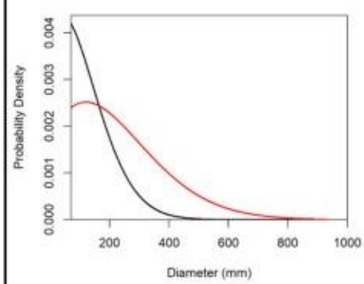	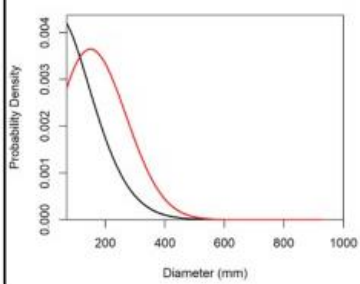	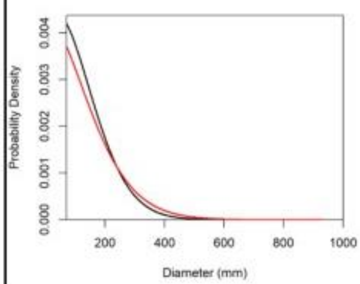
Plot 7	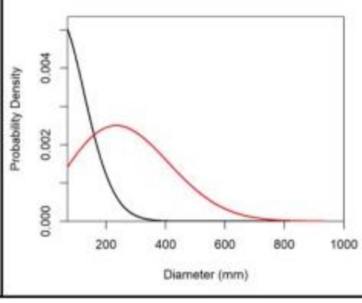	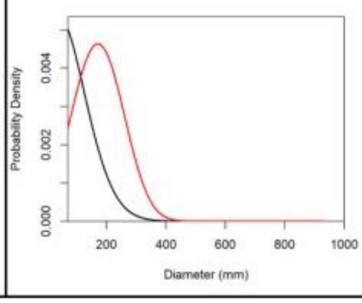	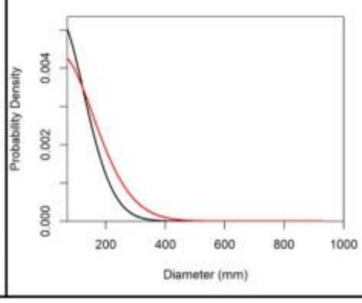

Figure 6-1 – Plots of probability density curves of diameter arranged by plot and point cloud processing solution. Each plot includes the reference curve, black, generated from traditional inventory data at that plot and the curve for the processing solution data.

6.4.1.1 Analysis of variance and Tukey's HSD

For the complete dataset, the ANOVA results indicated that there was no statistically significant difference in the probability distributions of tree diameters for the four methods ($F(3, 22) = 2.438$, $p = 0.092$). To confirm this non-significant result, post hoc testing was performed using Tukey' HSD to confirm the relationship indicated by the ANOVA. The results of the Tukey's HSD, summarised in Table 7-1, indicated that the mean Bhattacharyya distances for all methods were not significantly different ($p>0.05$) than the mean Bhattacharyya distance for the traditional inventory or from one another.

Table 6-1 Results of the Tukey's HSD post hoc testing for the complete dataset.

Method	Mean Bhattacharyya distance	SD	n	SE	Upper 95% CI	Lower 95% CI	Groups
Traditional Inventory	0.143	0.079	7	0.076	0.292	-0.006	A
TreeLS	0.391	0.176	7	0.071	0.530	0.252	A
FORTLS	0.224	0.103	6	0.076	0.373	0.075	A
3DFin	0.338	0.314	6	0.071	0.477	0.199	A

6.4.1.2 Welch's t-test and Cohen's d

The t-test results showed significant differences between the remote sensing solutions and traditional inventory data in terms of DBH measurements. For TreeLS, the t-test yielded a highly significant p-value ($p < 0.01$), coupled with a substantial effect size (Cohen's $d = 0.690$), indicating substantial overestimates in DBH estimations. Similarly, FORTLS

demonstrated a highly significant p-value ($p < 0.01$) and an intermediate effect size (Cohen's $d = 0.404$), signifying meaningful overestimations relative to traditional inventory measurements.

3DFin exhibited a highly significant p-value ($p < 0.01$), accompanied by a smaller negative, but still notable, effect size (Cohen's $d = -0.218$) compared to the other solutions. The negative value suggests that 3DFin underestimates DBH values in this setting and that the effect size is less pronounced compared to the positive values observed for TreeLS and FORTLS.

6.4.2 Partial dataset – plots 1,2,5,6,7

6.4.2.1 Analysis of variance and Tukey's HSD

For the partial dataset, the analysis of variance was repeated, and the results changed indicating the low-quality point clouds may have skewed the initial data analysis.

The ANOVA results indicated a significant difference among the diameter probability distributions for each of the methods ($F(3, 16) = 4.279$, $p < 0.05$). Owing to the highly significant result of the ANOVA, a Tukey's HSD post hoc test was again conducted to examine where there were significant differences between pairs of methods.

The Tukey's HSD test revealed significant differences in Bhattacharyya distances among the methods. Only mean Bhattacharyya distance of TreeLS was significantly different from that of the traditional inventory, no other pairs of methods had significantly different mean Bhattacharyya distances from one another. This indicates that 3DFin and FORTLS may be

statistically indistinguishable from traditional inventory however these methods also overlap with the lower confidence interval of TreeLS.

Table 6-2 Results of the Tukey's HSD post hoc testing for the partial dataset.

Method	Mean Bhattacharyya distance	SD	n	SE	Upper 95% CI	Lower 95% CI	Groups
Traditional Inventory	0.171	0.057	5	0.046	0.261	0.081	A
TreeLS	0.389	0.162	5	0.046	0.479	0.299	B
FORTLS	0.244	0.101	5	0.046	0.334	0.154	AB
3DFin	0.211	0.046	5	0.046	0.301	0.121	AB

6.4.2.2 Welch's t-test and Cohen's d

The t-test results revealed significant discrepancies between the solutions and traditional inventory data in terms of estimating DBH. For TreeLS, the t-test yielded a highly significant p-value ($p < 0.01$) along with a substantial effect size (Cohen's $d = 0.978$), indicating notable disparities in DBH estimations. Similarly, FORTLS exhibited a highly significant p-value ($p < 0.01$) and a substantial effect size (Cohen's $d = 0.987$), suggesting substantial deviations from traditional inventory measurements.

3DFin had a statistically significant p-value ($p = 0.05$), accompanied by a small effect size (Cohen's $d = 0.140$), especially compared to the other solutions. This implies a small but detectable difference in DBH estimations between 3DFin and traditional inventory data, though the effect size may not be meaningful.

6.5 Discussion

Upon entering discussion of these results, their implications, and where this work fits in in the greater context of the field, it should be noted that the chosen study areas were selected

to provide the greatest challenge to the solutions for inventory data extraction. It is only with this in mind that one can discuss these results as all the processing solutions assessed are known to perform accurately with data from more favourable, plantation forest settings [19,32,34,35].

Given the differences in results between the complete and partial datasets, it appears that the inclusion of plots 3 and 4 in the complete dataset skewed the results. For each of plots 3 and 4, one processing solution failed to extract any inventory data and the other two solutions yielded data for fewer than twenty trees. The point clouds for the clipped plots of plots 3 and 4 were found to be 6 to 8 times smaller in file size and this reflects a significantly lower number of points which is assumed to be caused by operator error or technical error during data collection. For both scans only a portion of the plot had been successfully scanned before appearing to drop dramatically in quality or cease altogether, as such it may have been user error, corruption of the data when transferred from the data logger or a transient technical issue with the scanner. It should not be understated that the potential for such poor-quality data collections could severely impact operational suitability of MLS for inventory data collections. We experienced a 28% failure rate for data collection on this occasion, though typically we find this to be much lower, but in operational use this would significantly reduce the efficiency gains for this approach and could even result in a lack of data where traditional inventory would have delivered. It is our belief, however, that this is unlikely to be a significant issue most of the time and that with widespread adoption of the methods operator error would decrease and technical reliability would improve.

For the sake of comparison, so that all solutions were tested on the same 5 plots, this discussion draws exclusively upon the results of the partial dataset when comparing the performance of the different LiDAR processing solutions.

The results of the analysis of variance for the partial dataset indicated that there were significant differences in the diameter probability distributions of the four methods, and the Tukey's HSD indicated that the primary difference was traditional inventory and TreeLS; FORTLS and TreeLS. This is consistent with the highly significant ANOVA result and suggests there were significant differences in how well the LiDAR solutions replicated the traditional inventory measurements. The Tukey's HSD also showed that there were non-significant differences in the diameter probability distributions of both traditional inventory and 3DFin and traditional inventory and FORTLS. This suggests that the inventory data produced by 3DFin and FORTLS is similarly distributed to the traditional inventory data and that the datasets could therefore be describing the same population, which is necessary if a remote sensing tool is to be used to replicate traditional inventory methods.

The results of Welch's t-test indicated that for all the LiDAR processing solutions the DBH values were statistically different from the traditional inventory values. This result is unsurprising as there are several opportunities to accumulate systematic and random errors in the LiDAR derived data. Identifying the correct point on a tree for a DBH measurement is a likely source of error as the normalisation process may not be entirely accurate and the solutions may calculate the base of the tree differently. The circle fitting algorithms used in LiDAR processing solutions select the circle that best fits the stem points, and this can be influenced by the shape of the stem and may result in different measurements to the averaged calliper measurement used. The MLS can introduce random error during data

collection and has a variable precision depending upon variables such as distance to target, changes in movement speed, and sensor temperature. Additionally, the SLAM algorithm that generates the point clouds can introduce noise and misattribute points.

Cohen's d was used as a post hoc measure of effect size for the t-test results, and the results show that for TreeLS and FORTLS the effect is significant and meaningful but for 3DFin the effect size is small and within the range that it could be considered not impactful.

Had the traditional inventory data for each tree been correlated with its digital twin it would have been possible to validate both how effectively the LiDAR processing solutions identified trees and how accurate each DBH estimate was, without the need for plot level assessments of probability distributions and diameters [15], as in the tree identification validation performed by Bienart et al. (2021). This would allow for greater confidence in the assessment of processing solution performance and is an area for improvement should this work be repeated in future. It can be seen from the counts of diameters measured at each plot by the different methods (Addendum 2) that the methods often under and over predicted the number of trees at each plot which suggests all the solutions struggled at times with the complex understory structure resulting in erroneous detections or omissions of trees. And thus, we do believe there is a need for further assessment of the capacity of such processing tools to function in complex forest types like CCF at an individual tree level going forwards.

Even without geolocated inventory data, the results of these analyses indicate that 3DFin is most capable of replicating traditional inventory measurements with a statistically significant similarity in distribution, and with a non-meaningful difference in DBH values, in the structurally complex and computationally taxing forest types chosen for testing. There

are, of course, areas for improvement, MLS cannot currently classify species and thus while it is possible to get DBH distributions for a stand it is not possible to subset these by species which may impact its adoption operationally. Tools are being developed that work in concert with MLS or may even be used in place of MLS and which may address the issues of species detection. Multiple laser scanner manufacturers now offer a camera attachment to their handheld scanners which can capture images of the forest which can then be mapped onto the point cloud and provide context information that could be assessed visually or by machine learning tools for this application currently in development by various research groups globally.

These findings underscore the critical importance of carefully testing remote sensing solutions for accuracy in diverse forest environments. There is a dearth of literature in which remote sensing tools are tested in or applied to CCF systems and this may negatively impact the uptake of CCF or impede the progression of research in CCF.

6.6 Conclusions

In summary, this work has shown that point cloud processing solutions, specifically 3DFin and FORTLS, can replicate plot-level traditional field inventory derived distributions of DBH from point clouds such that there is no statistically significant difference. Furthermore, it was shown that when comparing the populations of individual diameters returned by remote sensing processing solutions and traditional forest inventory no meaningful difference was observed for DBH measurements returned by 3DFin. Therefore, one can conclude that ground-based remote sensing can be used as a suitable substitute for traditional inventory in CCF stands and that if one wishes to use ground-based laser scanning in this way, they should use 3DFin to process their data.

CHAPTER 7

Discussion and Conclusions

7.1 Introduction

The overall aim of this thesis, as set out in the statement of intent, was to examine the use of remote sensing for describing and monitoring CCF stands. Given the extensive discussion of remote sensing and continuous cover forestry in Chapter 2, and the end of chapter discussions for the other sections of this work, this final discussion section will serve to: further justify why this work was needed, explore how the work from the previous chapters addresses needs, where this work could have been improved, implications for operational use of remote sensing in CCF, where things could be taken next, and, finally, a summary of whether hypotheses were proven and what this work has demonstrated.

7.2 Justification for work

This body of work represents just the beginning of what is needed if UK forestry is to transition successfully to sustainable silviculture and stay productive. Considering the ongoing global climate crisis [1], we must all make efforts to transition to more sustainable practices to reduce carbon emissions. The UK has committed to becoming net-zero by 2050 but currently has one of the lowest forest cover rates in Europe at just 13% [2] which is paltry compared to the European average of 46% and still less than half the global average of 31%. While forest cover is not the only path to net-zero and will by no means be the only way the UK reaches this goal it will be a significant part of the effort to sequester and offset carbon emissions where they cannot be reduced. Consequently, the UK intends address the

low forest cover through forest and woodland creation. To date Forest Research has identified a potential 2.7 million hectares in Scotland, 3.9 million hectares in Wales and 1.5 million hectares in England for woodland creation in Britain. With woodland creation comes considerations for what to plant and how to manage it. Matthews et al. (2022) showed that over 80 years the planting of any forest with any management approach was expected to result in an annualised net sequestration of CO_2 emissions of at least 5 tonnes/hectare, see Matthews et al. figure S1, and that over the first 30 years none of the options the presented data for resulted in significant net emissions [3].

From the data presented in Matthews et al. (2022) it initially appears that a fast-growing Sitka spruce monoculture with thinning is the best option for carbon mitigation, and it may well be when solely considering sequestration. However, forests provide more than simply timber and carbon sequestration; as stated in the introduction, sustainable forests are managed to provide improved community and ecosystem services without significantly sacrificing timber production. Matthews et al. (2022) show that depending upon the type of CCF practiced – such as whether species mixtures are employed, whether those mixtures are coniferous or broadleaved, and the intensity of management – the potential annualised net carbon sequestration is still more than 10 tonnes/hectare [3].

Given the benefits of CCF, as explored in section 2.2, and the current efforts to transform traditional production forests, it stands to reason that much of the new planting will be some form of CCF. This will therefore greatly increase the demand for reliable methods of inventory assessment and monitoring in CCF stands and thus creates a considerable urgency for the development of these methods. Additionally, scalable, and more efficient means of data collection are going to be necessary if the UK forestry sector is to keep up with the

increase in forest cover and so remote sensing will be essential to the success of these methods.

7.3 Addressing current needs and shortcomings

As laid out in the justification, and in section 2.2, there are growing needs for methods of remote sensing in CCF, and this work was conceptualised to address some of these demands. Applications to CCF has long been an overlooked area of remote sensing research and though doctoral research has nominally been performed in these areas previously it has primarily been either in CCF or remote sensing but rarely addressing the specific niche of the overlap of these two subject areas.

Chapter 3 of this work addressed a knowledge gap within the field regarding the availability of point cloud processing tools, this itself was not directly CCF related however it was a fundamental steppingstone that led to Chapter 6. Chapter 3 is of course an incomplete reference for all publicly available ground-based point cloud processing solutions as they continue to be updated and new solutions released. This is why the goal of the COST action working group has been to create a live database that is regularly maintained by the community that it serves and thus the work following my own contributions is already well underway.

Chapter 6 contributes to addressing perhaps the most crucial knowledge gap in the application of remote sensing to CCF – how accurately can remote sensing collect inventory data in complex stands. From chapter 6 we can see that remote sensing can replicate the distributions of datasets collected with traditional forest inventory techniques and therefore, given the known advantages of speed and efficiency and capacity for direct volume

measurement [4-6], remote sensing is a far more practical tool for monitoring CCF stand distributions than traditional inventory methods. As first discussed in section 2.3.2, the reverse-J distribution (J-curve model) for stem diameters is an easily identifiable and achievable distribution within CCF that could be used as an indicator of when to harvest and where to concentrate harvests and this can be easily monitored through remote sensing methods. Chapter 6 also highlighted both the importance of good data collection and the importance of analyses like these to assess varying performance of tools which otherwise outwardly appear broadly similar. Chapter 6 was, however, limited in scope by the lack of individual-tree level analyses of diameter estimation and assessments of the tree detection accuracy to establish the number of missed stems when fully enumerating stands and the accuracy of the DBH algorithms in these complex forest environments. Were the work to be repeated or completed with knowledge gained in hindsight some means of correlating the individual trees between MLS point clouds and the field would have been incorporated. This could have been achieved through unique high contrast, reflective patterns or potentially even numbers affixed to trees or through use of more advanced tools that have since become available. What is possible with remote sensing tools changes rapidly and so it would now be possible to use RTK equipped poles to mark individual tree locations, allowing for co-registration of their physical locations with the point clouds..

Chapter 5 of this work used ALS and took a landscape level view of the forest stands in which it was being used to monitor disturbance and growth. Such approaches will be required when scaling up plot level measurements recorded with TLS/MLS and so this chapter explored methods of modelling biomass from remotely sensed data that would be more sensitive to the structural complexity and heterogeneity of CCF stands. This work did not

show an increased accuracy in predicted biomass for the model with terms that accounted for structural complexity however this may have been due to the low number of reference plots in areas with high levels of heterogeneity in stand structure, caused by selective logging. It stands to reason that models with terms to account for the heterogeneity of structures in CCF should more accurately predict biomass than those that are solely informed by top-of-canopy height. Further testing of this approach in highly heterogeneous forest with more extensive reference data coverage in areas of heterogeneity may highlight the theorised advantages of a structurally informed model for biomass estimation.

7.4 Operational use of remote sensing in CCF

For those interested in pursuing the use of remote sensing in CCF I would direct your attention back to Chapter 2 and then recommend that they keep an ear to the ground with regards to further developments in the field. For now, it is worth remembering that remote sensing cannot yet provide all the answers and is not magic; for monitoring diameter distributions at the plot level, it is more than capable however for accurately quantifying volume of mercantile timber, while the functional capacity is there, the accuracy of results is highly variable.

The method of remote sensing you intend to use will affect how operationally useful remote sensing will be to CCF; ALS may have limited value for management and monitoring of complex forest types with significant below canopy structures but will remain valuable for upscaling ground-based data collections from plot level to forest level. Ground-based LiDAR will likely become the most valuable tool in CCF management as it can fully capture the below canopy structure and precise direct measurements, albeit with their accuracy dependent upon the quality of tree segmentation and circle or cylinder fitting algorithms.

Thus, as the field develops it is worth always approaching CCF management conscious of what remote sensing has successfully been shown to do so far to get the most value out of it. Currently, I recommend adopting the use of diameter distributions to monitor stand structure and dynamics and make decisions and MLS as the potential efficiency gains in this case appear significant.

7.5 Directions for future work

There are plenty of opportunities for further work that could fall within the scope of the thesis title, "Exploring the application of remote sensing to the monitoring of continuous cover forestry". In addition to improving upon the work that has been presented here, there are many directions for work that were simply not explored here due to the constraints of time and resources with many theses worth of questions to answer.

In section 2.5 a list of topics for further research was proposed. Of these, the first, "Development of remote sensing supplemented inventory protocols for improved CCF management" is now partially addressed through the work of Chapter 6, and the corresponding methods in section 4.4.2. The other proposed directions for work are still areas of great need. To identify areas of future research of the greatest interest to forest stakeholders I engaged in two days of discussions with forest stakeholders, approximately 80 stakeholders over 16 hours, about potential uses for remote sensing in a range of forest types, though primarily with regards to facilitating CCF. From these discussions, it became evident that of the potential directions for research already identified in section 2.5 the areas greatest interest to stakeholders were stem volume estimation and marketable timber estimation. Many cited the development of reliable methods for estimation of these two values, in addition to the development of reliable remote sensing inventory methods would

encourage them to fully embrace both CCF and remote sensing. Consequently, below are expanded outlines on how one might proceed with such research.

- *Stem volume estimation from below-canopy point clouds to improve estimates of standing stocks.*

  Assessments of point cloud processing tools for the accuracy with which direct measurement with laser scanning can be used to measure stem volumes would eliminate error introduced by allometric modelling. This work would require measurement of stands with remote sensing and traditional inventory methods before destructive sampling to collect reference volumes for validation. This work is of course applicable to more than just CCF but given the added complexity in CCF stands, where species and age mixtures are commonplace, it would provide greatest added value and facilitate the ongoing to transition of silvicultural practices.

- *Stem segmentation and marketable timber estimation from below-canopy point clouds.*

  Like with the previous point, this work would require data collections with remote sensing tools in areas marked for harvesting and then validation against post-harvest data, such as that generated at a mill. Here, merchantable timber estimation implies estimates of the number of logs of appropriate length and profile for processing into solid-wood products by lumber mills. Developments in this area would benefit managers of CCF woodland where accurately predicting the yield of timber after a prescribed partial harvest would otherwise prove extremely difficult relative to a clear felling.

7.6 Conclusions

In closing, all that remains is to address whether the aims and hypotheses goals laid out in section 1.2.1 were addressed by the body of work presented here.

Aim 1 was addressed first by Chapter 2 systematically reviewing the literature surrounding remote sensing in CCF, the knowledge gaps and the ways that other forest remote sensing work could be applied to CCF. Aim 1 was then further addressed in Chapter 3 where some of the processing solutions available for implementing remote sensing in CCF were highlighted and the groundwork was laid for further work to improve accessibility to this area of study and practice.

Chapter 5 addressed Aim 2 and subsequently confirmed Hypothesis 1 by showing that remote sensing can detect disturbances in forest structure associated with selective logging. Additionally, it showed that the most disturbance sensitive remote sensing metrics for each of the ecosystem morphological traits were found to model stand biomass with equivalent accuracy to a widely accepted and used single variable biomass model. It was also shown that remote sensing could monitor change over time in the forest structure corresponding to growth and recovery.

Finally, Aim 3 and Hypothesis 2 were addressed and confirmed by showing that through use of appropriate processing solutions one could use remotely sensed point clouds to replicate field inventory derived plot-level distributions of DBH. It is possible to find no significant difference between the distributions of the different methods, though this finding was contingent on the use of good quality data. Additionally, it was shown that the individual diameters returned by remote sensing processing solutions could be found to non-meaningfully differ from those observed with traditional inventory, and thus ground-based remote sensing is a suitable substitute for traditional inventory.

It is my hope that this work is recognised as meaningful contribution to the field of remote sensing and CCF and that the scarcity of CCF specific remote sensing knowledge will come to an end as further research is conducted.

REFERENCES

CHAPTER 1

1. Ampoorter, E., Barbaro, L., Jactel, H., Baeten, L., Boberg, J., Carnol, M., Castagneyrol, B., Charbonnier, Y., Dawud, S.M., Deconchat, M., Smedt, P.D., Wandeler, H.D., Guyot, V., Hättenschwiler, S., Joly, F.-X., Koricheva, J., Milligan, H., Muys, B., Nguyen, D., Ratcliffe, S., Raulund-Rasmussen, K., Scherer-Lorenzen, M., van der Plas, F., Keer, J.V., Verheyen, K., Vesterdal, L. and Allan, E. (2020), Tree diversity is key for promoting the diversity and abundance of forest-associated taxa in Europe. Oikos, 129: 133-146. https://doi.org/10.1111/oik.06290
2. Jönsson, A.M., Lagergren, F. & Smith, B. Forest management facing climate change - an ecosystem model analysis of adaptation strategies. Mitig Adapt Strateg Glob Change 20, 201–220 (2015). https://doi.org/10.1007/s11027-013-9487-6
3. Thompson, I., Mackey, B., McNulty, S., Mosseler, A. (2009). Forest Resilience, Biodiversity, and Climate Change. A synthesis of the biodiversity/resilience/stability relationship in forest ecosystems. Secretariat of the Convention on Biological Diversity, Montreal. Technical Series no. 43
4. Guerra, C.A., Maes, J., Geijzendorffer, I., Metzger, M.J. An assessment of soil erosion prevention by vegetation in Mediterranean Europe: Current trends of ecosystem service provision, Ecological Indicators, Volume 60, 2016, Pages 213-222,
5. Dhubháin, Á. N.and Farrelly, N. "Understanding and managing windthrow," COFORD Connects, Silviculture/Management No. 23 ed: Department of Agriculture, Food and the Marine, Dublin, 2018
6. Hahn T; Eggers J; Subramanian N; Caicoya AT; Uhl E; Snäll T (2021) Specified resilience value of alternative forest management adaptations to storms, Scandinavian Journal of Forest Research, 36:7-8, 585-597, DOI: 10.1080/02827581.2021.1988140
7. Pukkala, T., Olavi Laiho, Erkki Lähde,Continuous cover management reduces wind damage, Forest Ecology and Management, Volume 372, 2016, Pages 120-127, ISSN 0378-1127, https://doi.org/10.1016/j.foreco.2016.04.014.
8. Forestry Commission, 2017, The UK Forestry Standard. The Government's approach to sustainable forestry (Edinburgh: Forestry Commission)
9. UKWAS, 2017 The UK Woodland Assurance Standard, 4th Edition (Edinburgh: UKWAS)
10. Mason WL, Diaci J, Carvalho J, Valkonen S, Continuous cover forestry in Europe: usage and the knowledge gaps and challenges to wider adoption, *Forestry: An International Journal of Forest Research*, Volume 95, Issue 1, January 2022, Pages 1–12, https://doi.org/10.1093/forestry/cpab038
11. Brede, B., Calders, K., Lau, A., Raumonen, P., Bartholomeus, H. M., Herold, M., & Kooistra, L. (2019). Non-destructive tree volume estimation through quantitative structure modelling: Comparing UAV laser scanning with terrestrial LIDAR. Remote Sensing of Environment, 223, 111355.
12. Brede, B., Lau, A., Bartholomeus, H. M., & Kooistra, L. (2017). Comparing RIEGL RiCOPTER UAV LiDAR Derived Canopy Height and DBH with T
13. Wulder MA, White JC, Nelson RF, et al. 2012. Lidar sampling for large-area forest characterization: a review. Remote Sensing of Environment 121: 196–209.
14. Asner, G. P., Mascaro, J., Muller-Landau, H. C., Vieilledent, G., Vaudry, R., Rasamoelina, M., Hall, J. S., & van Breugel, M. (2012). A universal airborne LiDAR approach for tropical forest carbon mapping. Oecologia, 168(4), 1147–1160
15. Boucher PB, Paynter I, Orwig DA, Valencius I, Schaaf C. 2021. Sampling forests with terrestrial laser scanning. Annals of Botany. 128: 689–707.
16. Bienert A, Georgi KL, Kunz M, von Oheimb G, Maas H-G. 2021. Automatic extraction and measurement of individual trees from mobile laser scanning point clouds of forests. Annals of Botany.

17. Cabo, C., Ordóñez, C., López-Sánchez, C. A., & Armesto, J. (2018). Automatic dendrometry: Tree detection, tree height and diameter estimation using terrestrial laser scanning. International Journal of Applied Earth Observation and Geoinformation, 69, 164–174. https://doi.org/10.1016/j.jag.2018.01.011
18. Liang X, Hyyppä J. (2013). Automatic stem mapping by merging several terrestrial laser scans at the feature and decision levels. Sensors 13: 1614–1634.
19. Liang X, Hyyppä J, Kaartinen H, et al. (2018). International benchmarking of terrestrial laser scanning approaches for forest inventories. ISPRS Journal of Photogrammetry and Remote Sensing 144: 137–179.
20. Liang X, Kankare V, Hyyppä J, et al. (2016). Terrestrial laser scanning in forest inventories. ISPRS Journal of Photogrammetry and Remote Sensing 115: 63–77.
21. Kukko A, Kaartinen H, Hyyppä J, Chen Y. (2012). Multiplatform mobile laser scanning: usability and performance. Sensors 12: 11712–11733.
22. Liang X, Kukko A, Kaartinen H, et al. (2014). Possibilities of a personal laser scanning system for forest mapping and ecosystem services. Sensors 14: 1228–1248.
23. Bauwens S, Bartholomeus H, Calders K, Lejeune P. 2016. Forest inventory with terrestrial LiDAR: a comparison of static and hand-held mobile laser scanning. Forests 7: 127.
24. Wang Y, Chen Q, Zhu Q, Liu L, Li C, Zheng D. 2019a. Laser scanning applications and key techniques over urban areas. Remote Sensing 11: 1540.

CHAPTER 2

1. UN. 1992a. United Nations Convention on Biological Diversity. New York, USA. [also available at https://www.cbd.int/doc/legal/cbd-en.pdf]
2. MCPFE. *Ministerial Conference on the Protection of Forests in Europe, 16–17 June 1993 in Helsinki Documents*; Ministry of Agriculture and Forestry: Helsinki, Finland, 1993; ISBN 951-47-8283-6.
3. Helliwell, Rodney. (1997). Dauerwald. Forestry. 70. 10.1093/forestry/70.4.375
4. Pommerening A; Murphy ST 2004 A review of the history, definitions and methods of continuous cover forestry with special attention to afforestation and restocking, Forestry: An International Journal of Forest Research, Volume 77, Issue 1
5. Stiers, M., Annigh¨ofer, P., Seidel, D., Willim, K., Neudam, L., Ammer, C., 2020. Quantifying the target state of forest stands managed with the continuous cover approach – revisiting Moller's "Dauerwald" concept after 100 years. Trees For. People 1, 100004. https://doi.org/10.1016/j.tfp.2020.100004
6. Puettmann KJ, Wilson SM, Baker SC *et al.* Silvicultural alternatives to conventional even-aged forest management - what limits global adoption?. *For. Ecosyst.* 2, 8 (2015). https://doi.org/10.1186/s40663-015-0031-x
7. Mason WL, Diaci J, Carvalho J, Valkonen S, Continuous cover forestry in Europe: usage and the knowledge gaps and challenges to wider adoption, *Forestry: An International Journal of Forest Research*, Volume 95, Issue 1, January 2022, Pages 1–12, https://doi.org/10.1093/forestry/cpab038 ***** A comprehensive review of CCF; important both for highlighting challenges and illustrating the lack of remote sensing application in this area through the absence of inclusion.***
8. Pommerening A, Grabarnik P (2019) Individual-based methods in forest ecology and management. Springer Nature, Switzerland
9. Krumm F; Lachat T; Schuck A; Bütler R; Kraus D 2019 Marteloscopes as training tools for the retention and conservation of habitat trees in forests. *Schweiz. Z. Forstwes.* 170, 86–93
10. Çolak, A., Rotherham, I. and Çalikoglu, M. 2003 Combining 'naturalness concepts' with close-to-nature silviculture. *Forstwissenschaftliches Centralblatt* 122, 421–431.
11. Morgan P, **The Case for Continuous Cover Forestry**. *(2015) The Forestry & Timber News Journal*, p.19-20
12. O'Hara, K.L. 2016 What is close-to-nature silviculture in a changing world? *Forestry* 89, 1–6
13. Schütz JP; Pukkala T; Donoso PJ; von Gadow K 2012 Historical emergence and current application of CCF. In *Continuous Cover Forestry*. T., Pukkala, K., von Gadow (eds.). Springer Science, pp. 1–28.
14. Brang, P., Spathelf, P., Larsen, J.B., Bauhus, J., Boncina, A., Chauvin, C. et al. 2014 Suitability of close-to-nature silviculture for adapting temperate European forests to climate change. *Forestry* 87, 492–503
15. European Commission. 2020 *EU Biodiversity Strategy for 2030: Bringing Nature Back Into our Lives*. https://ec.europa.eu/environment/strategy/biodiversity-strategy-2030_en Accessed:03/11/2022
16. Ampoorter, E., Barbaro, L., Jactel, H., Baeten, L., Boberg, J., Carnol, M., Castagneyrol, B., Charbonnier, Y., Dawud, S.M., Deconchat, M., Smedt, P.D., Wandeler, H.D., Guyot, V., Hättenschwiler, S., Joly, F.-X., Koricheva, J., Milligan, H., Muys, B., Nguyen, D., Ratcliffe, S., Raulund-Rasmussen, K., Scherer-Lorenzen, M., van der Plas, F., Keer, J.V., Verheyen, K., Vesterdal, L. and Allan, E. (2020), Tree diversity is key for promoting the diversity and abundance of forest-associated taxa in Europe. Oikos, 129: 133-146. https://doi.org/10.1111/oik.06290
17. Jönsson, A.M., Lagergren, F. & Smith, B. Forest management facing climate change - an ecosystem model analysis of adaptation strategies. *Mitig Adapt Strateg Glob Change* 20, 201–220 (2015). https://doi.org/10.1007/s11027-013-9487-6

18. Thompson, I., Mackey, B., McNulty, S., Mosseler, A. (2009). Forest Resilience, Biodiversity, and Climate Change. A synthesis of the biodiversity/resilience/stability relationship in forest ecosystems. Secretariat of the Convention on Biological Diversity, Montreal. Technical Series no. 43, 67 pages.
19. Peura, M., Burgas, D., Eyvindson, K., Repo, A., Mönkkönen, M., 2018. Continuous cover forestry is a cost-efficient tool to increase multifunctionality of boreal production forests in Fennoscandia. Biol. Conserv. 217, 104–112. https://doi.org/10.1016/j.biocon.2017.10.018.
20. Kuuluvainen T, Tahvonen O, Aakala T. Even-aged and uneven-aged forest management in boreal Fennoscandia: a review. Ambio. 2012;41(7):720–37.
21. Calladine J; Bray J; Broome A; Fuller RJ Comparison of breeding bird assemblages in conifer plantations managed by continuous cover forestry and clearfelling, Forest Ecology and Management, Volume 344, 2015, Pages 20-29, https://doi.org/10.1016/j.foreco.2015.02.017.
22. Alder DC, Fuller RJ, Marsden SJ, Implications of transformation to irregular silviculture for woodland birds: A stand wise comparison in an English broadleaf woodland, Forest Ecology and Management, Volume 422, 2018, Pages 69-78, https://doi.org/10.1016/j.foreco.2018.04.004.
23. Alder DC, Edwards B, Poore A., Norrey J, Marsden SJ, Irregular silviculture and stand structural effects on the plant community in an ancient semi-natural woodland, Forest Ecology and Management, Volume 527, 2023, https://doi.org/10.1016/j.foreco.2022.120622.
24. Gustafsson, L., Bauhus, J., Asbeck, T. *et al.* Retention as an integrated biodiversity conservation approach for continuous-cover forestry in Europe. *Ambio* 49, 85–97 (2020). https://doi.org/10.1007/s13280-019-01190-1**sen** JB, Angelstam P, Bauhus J, Carvalho JF, Diaci J, Dobrowolska D, Gazda A, Gustafsson L, Krumm F, Knoke T, Konczal A, Kuuluvainen T, Mason B, Motta R, Pötzelsberger E, Rigling A, Schuck A, **2022**. **Closer-to-Nature Forest Management**. From Science to Policy 12. European Forest Institute.
25. Bauhus, J., K. Puettmann, and C. Kuehne. 2013. Close-to-nature forest management in Europe: Does it support complexity and adaptability of forest ecosystems? In *Managing forests as complex adaptive systems: Building resilience to the challenge of global change*, ed. K. Puettmann, C. Messier, and K.D. Coates, p187–213
26. Guerra, C.A., Maes, J., Geijzendorffer, I., Metzger, M.J. An assessment of soil erosion prevention by vegetation in Mediterranean Europe: Current trends of ecosystem service provision, Ecological Indicators, Volume 60, 2016, Pages 213-222, https://doi.org/10.1016/j.ecolind.2015.06.043
27. Dhubháin, Á. N.and Farrelly, N. "Understanding and managing windthrow," COFORD Connects, Silviculture/Management No. 23 ed: Department of Agriculture, Food and the Marine, Dublin, 2018
28. Hahn T; Eggers J; Subramanian N; Caicoya AT; Uhl E; Snäll T (2021) Specified resilience value of alternative forest management adaptations to storms, Scandinavian Journal of Forest Research, 36:7-8, 585-597, DOI: 10.1080/02827581.2021.1988140
29. Pukkala, T., Olavi Laiho, Erkki Lähde,Continuous cover management reduces wind damage, Forest Ecology and Management, Volume 372, 2016, Pages 120-127, ISSN 0378-1127, https://doi.org/10.1016/j.foreco.2016.04.014.
30. Hale, S.E. (2004). Managing Light to Enable Natural Regeneration in British Conifer Forests (PDF-100K) . Information Note 63. Forestry Commission, Edinburgh. pp. 6.
31. Knoke, T. The economics of continuous cover forestry. In Pukkala, Timo, and Klaus von Gadow, editors *Continuous Cover Forestry.* 2nd ed. Dordrecht: Springer, 2011. Print. pp. 167-193
32. Willoughby, I., Moore, R. & Nisbet, T. Interim guidance on the integrated management of Hylobius abietis in UK forestry. (2017)
33. Hanewinkel, M. (2001). Financial Results of Selection Forest Enterprises with High Proportions of Valuable Timber – Results of an Empirical Study and their Application. Schweiz. Z. Forstwes. (Swiss Forestry Journal) 152,8: 343-349.

34. Tahvonen, O. and Rämö, J. 2016 Optimality of continuous cover vs. clear-cut regimes in managing forest resources. *Can. J. For. Res.* 46, 891–901.
35. Hertog, I.M., Brogaard, S., Krause, T. (2022) Barriers to expanding continuous cover forestry in Sweden for delivering multiple ecosystem services, Ecosystem Services 53, 2022 https://doi.org/10.1016/j.ecoser.2021.101392.
36. Kerr, G., Mason, B., Boswell, R. and Pommerening, A. (2002) Monitoring the Transformation of Even-aged Stands to Continuous Cover Management. Forestry Commission Information Note 45 Forestry Commission, Edinburgh.
37. Kerr, G.; Stokes, V.; Peace, A.; Wylder, B. Prediction of conifer natural regeneration in a "data-poor" environment. *Scott. For.* **2011**, *65*, 28–36
38. Zawila-Niedzwiecki, T., Wisniewska, E. (2002). Continuous Cover Forestry: New Challenges for Remote Sensing. In: von Gadow, K., Nagel, J., Saborowski, J. (eds) Continuous Cover Forestry. Managing Forest Ecosystems, vol 4. Springer, Dordrecht. https://doi.org/10.1007/978-94-015-9886-6_3
39. Larsen, J.B., Angelstam, P., Bauhus, J., Carvalho, J.F., Diaci, J., Dobrowolska, D., Gazda, A., Gustafsson, L., Krumm, F., Knoke, T., Konczal, A., Kuuluvainen, T., Mason, B., Motta, R., Pötzelsberger, E., Rigling, A., Schuck, A., 2022. Closer-to-Nature Forest Management. From Science to Policy 12. European Forest Institute. https://doi.org/10.36333/fs12
**** A comprehensive report of the current state of CCF in Europe with a strong evaluation of the barriers to the implementation of CCF.***
40. Coops, N.C. et al., (2016) A forest structure habitat index based on airborne laser scanning data. Ecol. Ind. 67, 346–357, https://doi.org/10.1016/j.ecolind.2016.02.057
41. Schneider, F.D., Morsdorf, F., Schmid, B., Petchey, O.L., Hueni, A., Schimel, D.S., Schaepman, M.E. (2017) Mapping functional diversity from remotely sensed morphological and physiological forest traits. Nat Commun 8, 1441. https://doi.org/10.1038/s41467-017-01530-3
42. Fahey, R.T., Atkins, J.W., Gough, C.M., Hardiman, B.S., Nave, L.E., Tallant, J.M., Nadehoffer, K.J., Vogel, C., Scheuermann, C.M., Stuart-Haëntjens, E., Haber, L.T., Fotis, A.T., Ricart, R. and Curtis, P.S. (2019), Defining a spectrum of integrative trait-based vegetation canopy structural types. Ecol Lett, 22: 2049-2059. https://doi.org/10.1111/ele.13388
43. Valbuena, R., O'Connor, B., Zellweger, F., Simonson, W., Vihervaara, P., Maltamo, M., Silva, C.A., Almeida, D.R.A., Danks, F., Morsdorf, F., Chirici, G., Lucas, R., Coomes, D.A., Coops, N.C. (2020) Standardizing Ecosystem Morphological Traits from 3D Information Sources Trends in Ecology & Evolution, Volume 35, Issue 8, 656-667, https://doi.org/10.1016/j.tree.2020.03.006
**** A proposed approach to modelling ecosystems with remote sensing derived traits across a range of complex environments.***
44. Stoddart J; de Almeida DRA; Silva CA; Görgens EB; Keller M; Valbuena R 2022 A Conceptual Model for Detecting Small-Scale Forest Disturbances Based on Ecosystem Morphological Traits. Remote Sens. 2022,14, 933, https://doi.org/10.3390/rs14040933
45. Díaz, G. M. (2023). Optimizing forest canopy structure retrieval from smartphone-based hemispherical photography. Methods in Ecology and Evolution, 14, 875–884. https://doi.org/10.1111/2041-210X.14059
46. Bennett G, Hardy A, Bunting P, Morgan P, Fricker A. A Transferable and Effective Method for Monitoring Continuous Cover Forestry at the Individual Tree Level Using UAVs. Remote Sensing. 2020; 12(13):2115. https://doi.org/10.3390/rs12132115
47. Yancho, J.M.M., Coops, N.C., Tompalski, P., Goodbody, T.R.H. and Plowright, A. "Fine-Scale Spatial and Spectral Clustering of UAV-Acquired Digital Aerial Photogrammetric (DAP) Point Clouds for Individual Tree Crown Detection and Segmentation," in *IEEE Journal of Selected Topics in Applied*

Earth Observations and Remote Sensing, vol. 12, no. 10, pp. 4131-4148, Oct. 2019, doi: 10.1109/JSTARS.2019.2942811.

48. Li L, Chen J, Mu X, Li W, Yan G, Xie D, Zhang W. Quantifying Understory and Overstory Vegetation Cover Using UAV-Based RGB Imagery in Forest Plantation. *Remote Sensing*. **2020**; 12(2):298. https://doi.org/10.3390/rs12020298
49. Valbuena R, Packalén P, Mehtätalo L, García-Abril A, Maltamo M, 2013 Characterizing forest structural types and Shelterwood dynamics from Lorenzbased indicators predicted by airborne laser scanning. Can. J. Forest Res. 43 (11), 1063–1074.
50. Hamraz, H., Contreras, M.A. & Zhang, J. Forest understory trees can be segmented accurately within sufficiently dense airborne laser scanning point clouds. *Sci Rep* 7, 6770 (2017). https://doi.org/10.1038/s41598-017-07200-0
51. Kukkonen, M., Maltamo, M., Korhonen, L., Packalen, P., 2019. Comparison of multispectral airborne laser scanning and stereo matching of aerial images as a single sensor solution to forest inventories by tree species. Remote Sensing ofEnvironment 231, 111208. https://doi.org/10.1016/j.rse.2019.05.027.
52. Sačkov, I.; Sedliak, M.; Kulla, L.; Bucha, T. Inventory of Close-to-Nature Forests Based on the Combination of Airborne LiDAR Data and Aerial Multispectral Images Using a Single-Tree Approach. Forests 2017, 8, 467. https://doi.org/10.3390/f8120467
53. Donager, J.J.; Sánchez Meador, A.J.; Blackburn, R.C. Adjudicating Perspectives on Forest Structure: How Do Airborne, Terrestrial, and Mobile Lidar-Derived Estimates Compare? Remote Sens. 2021, 13, 2297. https://doi.org/10.3390/rs13122297
54. Whelan, A.W., Cannon, J.B., Bigelow, S.W., Rutledge, B.T., Sánchez Meador, A.J. Improving generalized models of forest structure in complex forest types using area- and voxel-based approaches from lidar, Remote Sensing of Environment, Volume 284, 2023, 113362,ISSN 0034-4257, https://doi.org/10.1016/j.rse.2022.113362.
**** Addresses the use of remote sensing in complex forest types which is of interest for CCF, very recent.***
55. R. Gaulton & T. J. Malthus (2010) LiDAR mapping of canopy gaps in continuous cover forests: A comparison of canopy height model and point cloud based techniques, International Journal of Remote Sensing, 31:5, 1193-1211, DOI: 10.1080/01431160903380565
56. Magnussen, Steen & Wulder, Michael & Seemann, David. (2002). Stand Canopy Closure Estimated by Line Sampling with airborne Lidar. Continuous cover forestry, Kluwer Academic Publishers, Dordrecht, Netherlands. 1-12. 10.1007/978-94-015-9886-6_1.
57. Amiri, N., Yao, W., Heurich, M., Krzystek, P., Skidmore, A.K., Estimation of regeneration coverage in a temperate forest by 3D segmentation using airborne laser scanning data, International Journal of Applied Earth Observation and Geoinformation, Volume 52, 2016, Pages 252-262, https://doi.org/10.1016/j.jag.2016.06.022.
58. Mäyrä J; Keski-Saari S; Kivinen S; Tanhuanpää T; Hurskainen P; Kullberg P; Poikolainen L; Viinikka A; Tuominen S; Kumpula T; Vihervaara P 2021 Tree species classification from airborne hyperspectral and LiDAR data using 3D convolutional neural networks, Remote Sensing of Environment, Volume 256, 112322, doi.org/10.1016/j.rse.2021.112322.
59. Liang X, Hyyppä J, Kaartinen H, Lehtomäki M, Pyörälä J, Pfeifer N, Holopainen M, Brolly G, Francesco P, Hackenberg J, Huang H (2018) International benchmarking of terrestrial laser scanning approaches for forest inventories. ISPRS J Photogramm Remote Sens 144:137–179
60. Bienert A, Georgi L, Kunz M, von Oheimb G, Maas HG. Automatic extraction and measurement of individual trees from mobile laser scanning point clouds of forests. Ann Bot. 2021 Oct 27;128(6):787-804. doi: 10.1093/aob/mcab087. PMID: 34232276; PMCID: PMC8557376.

61. Calders, K., Adams, J., Armston, J., Bartholomeus, H., Bauwens, S., Bentley, L.P., Chave, J., Danson, F.M., Demol, M., Disney, M., Gaulton, R., Krishna Moorthy, S.M., Levick, S.R., Saarinen, N., Schaaf, C., Stovall, A., Terryn, L., Wilkes, P., Verbeeck, H., 2020. Terrestrial laser scanning in forest ecology: Expanding the horizon. Remote Sens. Environ. 251, 112102. https://doi.org/10.1016/J.RSE.2020.112102.
***** A key review on the uses of TLS in forestry.***
62. Forsman, M., Börlin, N., Olofsson, K., Reese, H. and Holmgren, J. (2018). Bias of cylinder diameter estimation from ground-based laser scanners with different beam widths: A simulation study, ISPRS Journal of Photogrammetry and Remote Sensing, Volume 135, Pages 84-92.
63. Atkins, JW, Bohrer, G, Fahey, RT, et al. Quantifying vegetation and canopy structural complexity from terrestrial LiDAR data using the forestr r package. Methods Ecol Evol. 2018; 9: 2057– 2066. https://doi.org/10.1111/2041-210X.13061
64. Batchelor, J.L.; Wilson, T.M.; Olsen, M.J.; Ripple, W.J. New Structural Complexity Metrics for Forests from Single Terrestrial Lidar Scans. Remote Sens. 2023, 15, 145. https://doi.org/10.3390/rs15010145
65. Nguyen, V.T.; Fournier, R.A.; Côté, J.F.; Pimont, F. Estimation of vertical plant area density from single return terrestrial laser scanning point clouds acquired in forest environments. Remote Sens. Environ. 2022, 279, 113115.
66. Ramirez, F.A.; Armitage, R.P.; Danson, F.M. Testing the Application of Terrestrial Laser Scanning to Measure Forest Canopy Gap Fraction. Remote Sens. 2013, 5, 3037-3056. https://doi.org/10.3390/rs5063037
67. Woodgate, W., Jones, S.D., Suarez, L., et al., 2015. Understanding the variability in ground-based methods for retrieving canopy openness, gap fraction, and leaf area index in diverse forest systems. Agric. For. Meteorol. 205, 83–95
68. Calders K, Newnham G, Burt A, et al. 2015. Nondestructive estimates of above-ground biomass using terrestrial laser scanning. Methods in Ecology and Evolution 6: 198–208.
69. Chianucci, F., Puletti, N., Grotti, M., Ferrara, C., Giorcelli, A., Coaloa, D., & Tattoni, C. (2020). Nondestructive tree stem and crown volume allometry in hybrid poplar plantations derived from terrestrial laser scanning. Forest Science, 66(6), 737-746. doi:https://doi.org/10.1093/forsci/fxaa021
70. Terryn, L., Calders, K., Disney, M., Origo, N., Malhi, Y., Newnham, G., Raumonen, P., Åkerblom, M., Verbeeck, H., 2020. Tree species classification using structural features derived from terrestrial laser scanning. ISPRS J. Photogram. Rem. Sens. 168,170–181.
71. Xi, Z. Hopkinson, C. Rood, S.B. Peddle, D.R See the forest and the trees: Effective machine and deep learning algorithms for wood filtering and tree species classification from terrestrial laser scanning, ISPRS J. Photogramm. Remote Sens. 168 (2020) 1–16.
72. Qian C, Liu H, Tang J, Chen Y, Kaartinen H, Kukko A, Zhu L, Liang X, Chen L, Hyyppä J (2017) An integrated GNSS/INS/LiDAR-SLAM positioning method for highly accurate forest stem mapping. Remote Sens 9:3 https://doi.org/10.3390/rs9010003
73. Qi Y; Coops NC; Daniels LD; Butson CR 2022 Comparing tree attributes derived from quantitative structure models based on drone and mobile laser scanning point clouds across varying canopy cover conditions, ISPRS Journal of Photogrammetry and Remote Sensing, Volume 192, Pages 49-65, https://doi.org/10.1016/j.isprsjprs.2022.07.021
***** A key paper looking at comparisons between remote sensing approaches in varied canopy conditions making it ideal for application to CCF.***
74. Hartley RJL, et al. "Assessing the Potential of Backpack-Mounted Mobile Laser Scanning Systems for Tree Phenotyping." Remote Sensing 14.14 (2022): 3344.
75. Pelak JR. Evaluation of Mobile Lidar Scanning and Associated Workflows for Estimating Structural Attributes in Mixed-Conifer Forests. Diss. Northern Arizona University, 2022.

76. Forsman, M., Olofsson, K., Holmgren, J. (2016). Tree Stem Diameter Estimation from Mobile Laser Scanning Using Line-Wise Intensity-Based Clustering. Forests, 7(9), 206.
77. Neudam L, Annighöfer P, Seidel D. Exploring the Potential of Mobile Laser Scanning to Quantify Forest Structural Complexity, Frontiers in Remote Sensing, 2022, doi:10.3389/frsen.2022.861337
78. Liu, B.; Chen, S.; Huang, H.; Tian, X. Tree Species Classification of Backpack Laser Scanning Data Using the PointNet++ Point Cloud Deep Learning Method. Remote Sens. 2022, 14, 3809. https://doi.org/10.3390/rs14153809
79. Bohlin, J., Wallerman, J., Fransson, J. (2012). Forest variable estimation using photogrammetric matching of digital aerial images in combination with a high-resolution DEM. Scandinavian Journal of Forest Research. 27. 10.1080/02827581.2012.686625.
80. Bohlin, J., & Bohlin, I., Jonzén, J., Nilsson, M. (2017). Mapping forest attributes using data from stereophotogrammetry of aerial images and field data from the national forest inventory. Silva Fennica. 51. 10.14214/sf.2021.
81. Fromm M, Schubert M, Castilla G, Linke J, McDermid G. Automated Detection of Conifer Seedlings in Drone Imagery Using Convolutional Neural Networks. Remote Sensing. 2019; 11(21):2585. https://doi.org/10.3390/rs11212585
82. Bohlin J; Wallerman J; Fransson J (2021). Extraction of Spectral Information from Airborne 3D Data for Assessment of Tree Species Proportions. Remote Sensing. 13. 720. 10.3390/rs13040720.
83. Krisanski S, Taskhiri MS, Turner P. Enhancing Methods for Under-Canopy Unmanned Aircraft System Based Photogrammetry in Complex Forests for Tree Diameter Measurement. Remote Sensing. 2020; 12(10):1652. https://doi.org/10.3390/rs12101652
84. Chisholm RA, Rodríguez-Ronderos ME, Lin F. Estimating Tree Diameters from an Autonomous Below-Canopy UAV with Mounted LiDAR. Remote Sensing. 2021; 13(13):2576. https://doi.org/10.3390/rs13132576
85. Forsman, M., Börlin, N. and Holmgren, J. (2016). Estimation of Tree Stem Attributes Using Terrestrial Photogrammetry with a Camera Rig. Forests, 7(3), 61.
86. Schiefer, F., Kattenborn, T., Frick, A., Frey, J., Schall, P., Koch, B., Schmidtlein, S. Mapping forest tree species in high resolution UAV-based RGB-imagery by means of convolutional neural networks,ISPRS Journal of Photogrammetry and Remote Sensing,170,2020, Pages 205-215,https://doi.org/10.1016/j.isprsjprs.2020.10.015.
87. Natesan, S., Armenakis, C., and Vepakomma, U. (2020) Individual tree species identification using Dense Convolutional Network (DenseNet) on multitemporal RGB images from UAV. *Journal of Unmanned Vehicle Systems*. 8(4): 310-333. https://doi.org/10.1139/juvs-2020-0014
88. Ozdemir, I., Donoghue, D.N.M., Modelling tree size diversity from airborne laser scanning using canopy height models with image texture measures, Forest Ecology and Management, Volume 295, 2013, Pages 28-37, ISSN 0378-1127, https://doi.org/10.1016/j.foreco.2012.12.044.
89. Miyoshi GT, Arruda MdS, Osco LP, Marcato Junior J, Gonçalves DN, Imai NN, Tommaselli AMG, Honkavaara E, Gonçalves WN. A Novel Deep Learning Method to Identify Single Tree Species in UAV-Based Hyperspectral Images. Remote Sensing. 2020; 12(8):1294. https://doi.org/10.3390/rs12081294
90. Tao, S., Labrière, N., Calders, K. *et al.* Mapping tropical forest trees across large areas with lightweight cost-effective terrestrial laser scanning. *Annals of Forest Science* 78, 103 (2021). https://doi.org/10.1007/s13595-021-01113-9
91. Spazzi, J., O Tuama, P., Wilson, E. and Short, I. (2019) "Comparison of three inventory protocols for use in privately-owned plantations under transformation to Continuous Cover Forestry", *Irish Forestry*, 76(1&2), pp. 8-28

92. Wilkes P, Lau A, Disney M, Calders K, Burt A, de Tanago JG, Bartholomeus H, Brede B, Herold M (2017) Data acquisition considerations for terrestrial laser scanning of forest plots. Remote Sens Environ 196:140–153
93. Wang Y, Lehtomäki M, Liang X, et al. 2019b. Is field-measured tree height as reliable as believed – a comparison study of tree height estimates from field measurement, airborne laser scanning and terrestrial laser scanning in a boreal forest. ISPRS Journal of Photogrammetry and Remote Sensing 147: 132–145.
94. Kuželka K, Marušák,R. Surový, P. Inventory of close-to-nature forest stands using terrestrial mobile laser scanning, International Journal of Applied Earth Observation and Geoinformation, Volume 115, 2022,103104, doi:10.1016/j.jag.2022.103104.
95. Čerňava, J. - Tuček, J. - Koreň, M. - Mokroš, M. (2017). Estimation of diameter at breast height from mobile laser scanning data collected under a heavy forest canopy. Journal of Forest Science 63, 433–441. doi:10.17221/28/2017-JFS
96. Trochta, J., Krucek, M., Vrška, T., Král, K. (2017). 3D Forest: An application for descriptions of three-dimensional forest structures using terrestrial LiDAR. PLoS ONE. 12. 10.1371/journal.pone.0176871.
97. Terryn, L., Calders, K., Åkerblom, M., Bartholomeus, H., Disney, M., Levick, S., Origo, N., Raumonen, P., & Verbeeck, H. (2022). Analysing individual 3D tree structure using the R package ITSMe. Methods in Ecology and Evolution, 00, 1– 11. https://doi.org/10.1111/2041-210X.14026
98. de Conto T., Olofsson K., Görgens E.B., Rodriguez L.C.E., Almeida G., Performance of stem denoising and stem modelling algorithms on single tree point clouds from terrestrial laser scanning, Comput. Electron. Agric., 143 (2017), pp. 165-176 https://doi.org/10.1016/j.compag.2017.10.019.
99. Panagiotidis, d.; Abdollahnejad, a. Reliable estimates of merchantable timber volume from terrestrial laser scanning. remote sens. 2021, 13, 3610. https://doi.org/10.3390/rs13183610
100. Puletti N, Grotti M, Ferrara C, Scalercio S. Traditional and TLS-based forest inventories of beech and pine forests located in Sila National Park: A dataset. Data Brief. 2020 Dec 5;34:106617. doi: 10.1016/j.dib.2020.106617.
101. Windrim, L., & Bryson, M. (2020). Detection, segmentation, and model fitting of individual tree stems from airborne laser scanning of forests using deep learning. Remote Sensing, 12(9), 1469.
102. Asner, G.P., Mascaro, J., Mapping tropical forest carbon: Calibrating plot estimates to a simple LiDAR metric, Remote Sensing of Environment, Volume 140, 2014, https://doi.org/10.1016/j.rse.2013.09.023.
103. Bouvier, M., Durrieu, S., Fournier, R. A., & Renaud, J. P. (2015). Generalizing predictive models of forest inventory attributes using an area-based approach with airborne LiDAR data. Remote Sensing of Environment, 156, 322-334.
104. Fahey, R.T., Atkins, J.W., Gough, C.M., Hardiman, B.S., Nave, L.E., Tallant, J.M., Nadehoffer, K.J., Vogel, C., Scheuermann, C.M., Stuart-Haëntjens, E., Haber, L.T., Fotis, A.T., Ricart, R. and Curtis, P.S. (2019), Defining a spectrum of integrative trait-based vegetation canopy structural types. Ecol Lett, 22: 2049-2059. https://doi.org/10.1111/ele.13388
105. Kane, V.R., McGaughey, R.J., Bakker, J.D., Gersonde, R.F., Lutz, J.A., Franklin, J.F. (2010) Comparisons between field- and LiDAR-based measures of stand structural complexity. Can. J. For. Res. 40 (4), 761–773, lo.1139/X10-024
106. Zellweger, F., Baltensweiler, A., Ginzler, C., Roth, T., Braunisch, V., Bugmann, H. and Bollmann, K. (2016) Environmental predictors of species richness in forest landscapes: abiotic factors versus vegetation structure. J. Biogeogr., 43: 1080-1090. https://doi.org/10.1111/jbi.12696
107. di Lucca, C.M. 1999. TASS/SYLVER/TIPSY: systems for predicting the impact of silvicultural practices on yield, lumber value, economic return and other benefits. In: Stand Density Management Conference: Using the Planning Tools. November 23–24, 1998, Colin R. Bamsey [Ed.] Clear Lake Ltd., Edmonton, AB.

108. di Lucca, C.M. 2019. Using the Tree and Stand Simulator (TASS) model to predict the effect of stand management on quantity and value of carbon and biomass in British Columbia, Canada. Poster prepared for IUFRO 2019, Curitiba, Brazil. Sept. 29 – October 5, 2019
109. Suarez JC "An Analysis of the Consequences of Stand Variability in Sitka Spruce Plantations in Britain using a combination of airborne LiDAR analysis and models" Diss., University of Sheffield, 2010
110. Fortin M., Sattler D., and Schneider R. 2021. An alternative simulation framework to evaluate the sustainability of annual harvest on large forest estates. Canadian Journal of Forest Research. 52(5): 704-715. https://doi.org/10.1139/cjfr-2021-0255
111. Roussel J., Auty D., Coops N.C., Tompalski P., Goodbody T.R., Meador A.S., Bourdon J., de Boissieu F., Achim A. (2020). LidR: An R package for analysis of Airborne Laser Scanning (ALS) data. Remote Sensing of Environment, 251, 112061. ISSN 0034-4257, doi:10.1016/j.
112. Q JAG, Hernandez R, Sanchez-Azofeifa A (2021). rTLS: Tools to Process Point Clouds Derived from Terrestrial Laser Scanning. R pacakge version 0.2.5, https://CRAN.R-project.org/package=rTLS.
113. Molina-Valero, J. A., Martínez-Calvo, A., Ginzo Villamayor, M. J., Novo Pérez, M. A., Álvarez González, J. G., Montes, F., & Pérez-Cruzado, C. (2022). Operationalizing the use of tls in forest inventories: The R package fortls. Environmental Modelling & Software, 150, 105337.
114. Martin-Ducup O., & Lecigne B. (2022). R Package 'aRchi'. Quantitative Structural Model ('QSM') Treatment for Tree Architecture Version 2.1.0.
115. Cabo, C; Mokros, M; Murtiyoso, A; Singh, A; Pereira, D; Stoddart, J (2023, September 6-8) Software solutions for close-range forest point clouds: What is out there? [Conference presentation] Silvilaser Conference, London, UK https://www.conftool.org/silvilaser2023/index.php?page=browseSessions&form_session=11
116. Mokros, M; Rehush, N; Murtiyoso, A; Cabo, C; Singh, A; Cherlet, W; Beloiu, M (2023, September 6-8) A web platform for forest point cloud processing algorithms Silvilaser Conference, London, UK https://www.conftool.org/silvilaser2023/index.php?page=browseSessions&form_session=11

CHAPTER 3

1. Cabo, C; Mokros, M; Murtiyoso, A; Singh, A; Pereira, D; Stoddart, J (2023, September 6-8) Software solutions for close-range forest point clouds: What is out there? [Conference presentation] Silvilaser Conference, London, UK https://www.conftool.org/silvilaser2023/index.php?page=browseSessions&form_session=11
2. Mokros, M; Rehush, N; Murtiyoso, A; Cabo, C; Singh, A; Cherlet, W; Beloiu, M (2023, September 6-8) A web platform for forest point cloud processing algorithms Silvilaser Conference, London, UK https://www.conftool.org/silvilaser2023/index.php?page=browseSessions&form_session=11
3. Murtiyoso, A.; Cabo, C.; Singh, A.; Pereira Obaya, D.; Cherlet, W.; Stoddart, J.; et al. (2024) A review of software solutions to process ground-based point clouds in forest applications. [Manuscript submitted for publication]
4. Krisanski, S.; Taskhiri, M.S.; Gonzalez Aracil, S.; Herries, D.; Muneri, A.; Gurung, M.B.; Montgomery, J.; Turner, P. Forest Structural Complexity Tool—An Open Source, Fully-Automated Tool for Measuring Forest Point Clouds. Remote Sens. 2021, 13, 4677. https://doi.org/10.3390/rs13224677
5. Koreň, M., 2017. DendroCloud: Point Cloud Processing Software for Forestry, Version 1.45. Available online: http://gis.tuzvo.sk/dendrocloud/default.aspx
6. Trochta J, Krůček M, Vrška T, Král K (2017) 3D Forest: An application for descriptions of three-dimensional forest structures using terrestrial LiDAR. PLoS ONE 12(5): e0176871. https://doi.org/10.1371/journal.pone.0176871
7. Puletti, N; Castronuovo, R; Ferrara, C; crossing3dforest: an R package for evaluating empty space structure in forest ecosystems bioRxiv 2023.02.01.526548; doi: https://doi.org/10.1101/2023.02.01.526548
8. Yrttimaa T. (2021). Automatic Point Cloud Processing Tools to Characterize Trees (Point-Cloud-Tools: v1.0.1). Zenodo. https://doi.org/10.5281/zenodo.5779288.
9. GreenValley International (2022) LiDAR360 [Computer software], Available online: https://greenvalleyintl.com/LiDAR360/
10. Terryn, L. (2022). lmterryn/ITSMe: submission release (Version v1.0.0) [Computer software]. https://doi.org/10.5281/zenodo.6769105
11. Hackenberg, J; Calders, K; Miro, D; Pasi, R; Alexandre, P; Disney, M; SimpleForest - a comprehensive tool for 3d reconstruction of trees from forest plot point clouds bioRxiv 2021.07.29.454344; https://doi.org/10.1101/2021.07.29.454344 (Pre-print)
12. Computree Project. Version 5. Available online: http://computree.onf.fr/?lang=en
13. Montoya, O., Icasio-Hernandez, O., Salas, J., 2021. TreeTool: A tool for detecting trees and estimating their DBH using forest point clouds. [Computer software] SoftwareX 16, 100889. https://doi.org/10.1016/j.softx.2021.100889.
14. Raumonen, P., 2019. InverseTampere/TreeQSM: Version 2.3.1. [Computer software] Zenodo, http://dx.doi.org/10.5281/zenodo.3482908.
15. Conto T (2022). _TreeLS: Terrestrial Point Cloud Processing of Forest Data_. R package version 2.0.5, <https://github.com/tiagodc/TreeLS>.
16. Wang, D, Momo Takoudjou, S, Casella, E. LeWoS: A universal leaf-wood classification method to facilitate the 3D modelling of large tropical trees using terrestrial LiDAR. Methods Ecol Evol. 2020; 11: 376– 389. https://doi.org/10.1111/2041-210X.13342
17. Molina-Valero, J. A., Martínez-Calvo, A., Ginzo Villamayor, M. J., Novo Pérez, M. A., Álvarez-González, J. G., Montes, F., Pérez-Cruzado, C. (2022). Operationalizing the use of TLS in forest inventories: The R package FORTLS. Environmental Modelling & Software, 105337. doi.org/10.1016/j.envsoft.2022.105337
18. Molina-Valero, J. A.; Martínez-Calvo, A.; Seppelt, A.; Álvarez-González, J.G.; Montes, F.; Pérez-Cruzado, C.; (2023). Automatic Processing of Terrestrial-Based Technologies Point Cloud Data for Forestry Purposes. R package version 1.2.0. https://CRAN.R-project.org/package=FORTLS

19. Guzman, JA, Hernandez, R., and Sanchez-Azofeifa, A., (2021), rTLS: Tools to Process Point Clouds Derived from Terrestrial Laser Scanning. R pacakge version 0.2.5. https://CRAN.R-project.org/package=rTLS
20. Vicari, M.B.; Disney, M.I.; Wilkes, P.; Burt, A.; Calders, K.; Woodgate, W. Leaf and wood classification framework for terrestrial LiDAR point clouds. Methods Ecol. Evol. 2019, 10, 680–694

CHAPTER 4

1. Rex, FE, Silva, C.A., Dalla Corte, A.P., Klauberg, C, Mohan, M., Cardil, A., Silva, V.S., Almeida, D.R.A., Garcia, M., Broadbent, E.N., Valbuena, R., Stoddart, J., Merrick, T., Hudak, A.T (2020) Comparison of Statistical Modelling Approaches for Estimating Tropical Forest Aboveground Biomass Stock and Reporting Their Changes in Low-Intensity Logging Areas Using Multi-Temporal LiDAR Data. Remote Sensing. 12(9):1498. https://doi.org/10.3390/rs12091498
2. Costa M.A.T., Silva C.A., Broadbent E.N., Leite R.V., Mohan M., Liesenberg V., Stoddart J., Amaral C.H., Almeida D.R.A., da Silva A.L., Ré Y Goya L.R., Cordeiro V.A., Rex F., Hirsch A., Marcatti G.E., Cardil A., Mendonça B.A.F., Hamamura C., Dalla A.P., Matricardi E.A.T., Hudak A.T., Almeyda A.M., , Valbuena R., Faira B.L., Silva C.H.L., Aragao L., Ferreira M.E., Liang J., Carvalho S.P.C., & Klauberg C. (2021) Beyond Trees: Mapping Total Aboveground Biomass Density in the Brazilian Savanna Using High-Density UAV-Lidar Data. Forest Ecology and Management 491: 119155
3. Görgens E.B., Nunes M.H., Jackson T., Coomes D.A., Keller M., Reis C.R., Valbuena R., Rosette J., Almeida D.R.A., Gimenez B., Cantinho R., Motta A.Z., Assis M., Pereira F.S., Spanner G., Higuchi N., Ometto J.P. (2020a) Resource Availability and Disturbance Shape Maximum Tree Height across the Amazon. Global Change Biology 27 (1): 177-189.
4. Pinagé, E.R., Keller, M., Duffy, P., Longo, M., dos-Santos, M.N., Morton, D.C. (2019) Long-Term Impacts of Selective Logging on Amazon Forest Dynamics from Multi-Temporal Airborne LiDAR. Remote Sens. 11, 709. https://doi.org/10.3390/rs11060709
5. Longo, M., Keller, M., dos-Santos, M.N., Leitold, V., Pinagé, E.R., Baccini, A., Saatchi, S., Nogueira, E.M., Batistella, M., Morton, D.C. (2016), Aboveground biomass variability across intact and degraded forests in the Brazilian Amazon, Global Biogeochem. Cycles, 30, 1639–1660, https://doi.org/10.1002/2016GB005465
6. Silva, C.A., Hudak, A.T., Vierling, L.A., Klauberg, C., Garcia, M., Ferraz, A., Keller, M., Eitel, J., Saatchi, S. (2017) Impacts of Airborne Lidar Pulse Density on Estimating Biomass Stocks and Changes in a Selectively Logged Tropical Forest. Remote Sens. 9, 1068. https://doi.org/10.3390/rs9101068
7. Görgens, E.B., Mund, J.P., Cremer, T., de Conto, T., Krause, S., Valbuena, R. & Rodríguez, L.C. (2020b) Automated Operational Logging Plan Considering Multi-Criteria Optimization. Computers and Electronics in Agriculture 170: 105253
8. Marchesan, J., Alba, E., Schuh, M., Favarin, J., Pereira, R., (2020) Aboveground Biomass Estimation In A Tropical Forest With Selective Logging Using Random Forest And Lidar Data Floresta 50(4):1873, DOI: 10.5380/rf.v50i4.66589
9. 60. Rex, F.E., Corte, A.P.D., Machado, S.D.A., Silva, C.A., Sanquetta, C.R. (2019) Estimating Above-Ground Biomass of Araucaria angustifolia (Bertol.) Kuntze Using LiDAR Data. Floresta E Ambiente, 26
10. Chave, J., Réjou-Méchain, M., Búrquez, A., Chidumayo, E., Colgan, M.S., Delitti, W.B., Duque, A., Eid, T., Fearnside, P.M., Goodman, R.C., Henry, M., Martínez-Yrízar, A., Mugasha, W.A., Muller-Landau, H.C., Mencuccini, M., Nelson, B.W., Ngomanda, A., Nogueira, E.M., Ortiz-Malavassi, E., Pélissier, R., Ploton, P., Ryan, C.M., Saldarriaga, J.G. and Vieilledent, G. (2014), Improved allometric models to estimate the aboveground biomass of tropical trees. Glob Change Biol, 20: 3177-3190. https://doi.org/10.1111/gcb.12629
11. Forestry Commission (2017) Alice Holt Forest Forest Plan, https://www.forestryengland.uk/sites/default/files/documents/Alice%20Holt%20Forest%20Forest%20Plan.pdf accessed: 01/06/2023
12. Forestry Commission (2014) Great Pen Wood Forest Plan, https://www.forestryengland.uk/sites/default/files/documents/Great%20Pen%20Wood%20Forest%20Plan_0.pdf accessed: 01/06/2023
13. Forestry Commission (2013) South Downs II Forest Design Plan, https://www.forestryengland.uk/sites/default/files/documents/South%20Downs%202%20Forest%20Plan%20Introduction.pdf accessed: 01/06/2023
14. Matthews, R. W. and Mackie, E. D. (2006). Forest Mensuration. A Handbook for practitioners. Forestry Commission Publications. Edinburgh.

15. Geoslam ZEB Horizon Specification Website: https://geoslam.com/wp-content/uploads/2021/03/Horizon_Spec_Sheet.pdf accessed: 07/03/2023
16. Fahle, L., Holley, E.A., Walton, G. *et al.* Analysis of SLAM-Based Lidar Data Quality Metrics for Geotechnical Underground Monitoring. *Mining, Metallurgy & Exploration* **39**, 1939–1960 (2022). https://doi.org/10.1007/s42461-022-00664-3
17. Roussel, J.R., Auty, D., Coops, N.C., Tompalski, P., Goodbody, T.R.H., Sánchez Meador, A., Bourdon, J.F., De Boissieu, F., Achim, A. (2020). lidR : An R package for analysis of Airborne Laser Scanning (ALS) data. Remote Sensing of Environment, 251 (August), 112061. <doi:10.1016/j.rse.2020.112061>.
18. Roussel, J.R. and Auty, D (2023). Airborne LiDAR Data Manipulation and Visualization for Forestry Applications. R package version 4.0.3. https://cran.r-project.org/package=lidR
19. CloudCompare (version 2.1) [GPL software]. (2023). Retrieved from http://www.cloudcompare.org/
20. Zhang, W. Qi, J. Wan, P Wang, H,. Xie, D. Wang, X., and Yan, G., "An Easy-to-Use Airborne LiDAR Data Filtering Method Based on Cloth Simulation," Remote Sens., vol. 8, no. 6, p. 501, 2016. (http://www.mdpi.com/2072-4292/8/6/501/htm)

CHAPTER 5

1. Brienen, R., Phillips, O., Feldpausch, T. et al. (2015) Long-term decline of the Amazon carbon sink. Nature 519, 344–348. https://doi.org/10.1038/nature14283
2. Phillips, O.L., Brienen, R.J.W. & the RAINFOR collaboration. (2017) Carbon uptake by mature Amazon forests has mitigated Amazon nations' carbon emissions. Carbon Balance Manage 12, 1. https://doi.org/10.1186/s13021-016-0069-2
3. Reboredo, F. (2013) Socio-economic, environmental, and governance impacts of illegal logging. Environ Syst Decis 33, 295–304 https://doi.org/10.1007/s10669-013-9444-7
4. Condé, M., Higuchi, N., Adriano J. N. (2019) "Illegal Selective Logging and Forest Fires in the Northern Brazilian Amazon" Forests 10, no. 1: 61. https://doi.org/10.3390/f10010061
5. Hansen, M.C., Potapov, P.V., Moore, R., Hancher, M., Turubanova, S.A., Tyukavina, A., Thau, D., Stehman, S.V., Goetz, S.J., Loveland, T.R., Kommareddy, A., Egorov, A., Chini, L., Justice, C.O., Townshend J.R.G. (2013) High-Resolution Global Maps of 21st-Century Forest Cover Change, Science, DOI: 10.1126/science.1244693
6. Assunção, J., Gandour, C., Rocha, R. (2017) DETERing deforestation in the Amazon: Environmental monitoring and law enforcement. Climate Policy Initiative, Núcleo de Avaliação de Políticas Climáticas, Pontifica Universidade Católica (PUC), Rio de Janeiro, pp. 36 http://climatepolicyinitiative.org/wp-content/uploads/2013/05/DETERring-Deforestation-in-the-Brazilian-Amazon-Environmental-Monitoring-and-Law-Enforcement-Technical-Paper.pdf. (Accessed June 2021)
7. Coops, N.C. et al., (2016) A forest structure habitat index based on airborne laser scanning data. Ecol. Ind. 67, 346–357, https://doi.org/10.1016/j.ecolind.2016.02.057
8. Schneider, F.D., Morsdorf, F., Schmid, B., Petchey, O.L., Hueni, A., Schimel, D.S., Schaepman, M.E. (2017) Mapping functional diversity from remotely sensed morphological and physiological forest traits. Nat Commun 8, 1441. https://doi.org/10.1038/s41467-017-01530-3
9. Fahey, R.T., Atkins, J.W., Gough, C.M., Hardiman, B.S., Nave, L.E., Tallant, J.M., Nadehoffer, K.J., Vogel, C., Scheuermann, C.M., Stuart-Haëntjens, E., Haber, L.T., Fotis, A.T., Ricart, R. and Curtis, P.S. (2019), Defining a spectrum of integrative trait-based vegetation canopy structural types. Ecol Lett, 22: 2049-2059. https://doi.org/10.1111/ele.13388
10. Valbuena, R., O'Connor, B., Zellweger, F., Simonson, W., Vihervaara, P., Maltamo, M., Silva, C.A., Almeida, D.R.A., Danks, F., Morsdorf, F., Chirici, G., Lucas, R., Coomes, D.A., Coops, N.C. (2020) Standardizing Ecosystem Morphological Traits from 3D Information Sources Trends in Ecology & Evolution, Volume 35, Issue 8, 656-667, https://doi.org/10.1016/j.tree.2020.03.006
11. Lefsky, M.A., Hudak, A.T., Cohen, W.B., Acker, S.A. (2005) Patterns of covariance between forest stand and canopy structure in the Pacific Northwest Remote Sens. Environ., 95 (4), pp. 517-531, 10.1016/j.rse.2005.01.004
12. Asner, G.P., Mascaro, J., Muller-Landau, H.C. et al., A universal airborne LiDAR approach for tropical forest carbon mapping. Oecologia 168, 1147–1160 (2012). https://doi.org/10.1007/s00442-011-2165-z
13. Locks, C.J. and Matricardi, E.A.T. (2019) Estimation of impacts of selective logging in the Amazon using LIDAR data. Forest Science [online]. v. 29, no. 2 [Accessed 9 July 2021], pp. 481-495. Available at: https://doi.org/10.5902/1980509826007
14. Lefsky, M.A., Cohen, W.B., Parker, G.G., Harding, D.J. (2002) Lidar Remote Sensing for Ecosystem Studies: Lidar, an emerging remote sensing technology that directly measures the three-dimensional distribution of plant canopies, can accurately estimate vegetation structural attributes and should be of particular interest to forest, landscape, and global ecologists, BioScience, Volume 52, Issue 1, Pages 19–30, https://doi.org/10.1641/0006-3568

15. Naesset, E. (2002) Predicting forest stand characteristics with airborne scanning laser using a practical two-stage procedure and field data. Remote Sens. Environ. 80(1): 88–99. https://doi.org/10.1016/S0034-4257(01)00290-5
16. Asner, G.P., Rudel, T.K., Aide, T.M., Defries, R. And Emerson, R. (2009), A Contemporary Assessment of Change in Humid Tropical Forests. Conservation Biology, https://doi.org/10.1111/j.1523-1739.2009.01333.x
17. Zolkos, S., Goetz, S.J., Dubayah, R. (2013) A meta-analysis of terrestrial aboveground biomass estimation using lidar remote sensing Remote Sensing of Environment 128:289–298, https://doi.org/10.1016/j.rse.2012.10.017
18. Valbuena R., Hernando A., Manzanera J.A., Görgens E.B., Almeida D.R.A., Mauro F., García-Abril A., Coomes D.A. (2017) Enhancing of Accuracy Assessment for Forest Above-Ground Biomass Estimates Obtained from Remote Sensing via Hypothesis Testing and Overfitting Evaluation. Ecological Modelling 366: 15-26
19. Houghton, R.A. (2005), Aboveground Forest Biomass and the Global Carbon Balance. Global Change Biology, 11: 945-958. https://doi.org/10.1111/j.1365-2486.2005.00955.x
20. Görgens E.B., Nunes M.H., Jackson T., Coomes D.A., Keller M., Reis C.R., Valbuena R., Rosette J., Almeida D.R.A., Gimenez B., Cantinho R., Motta A.Z., Assis M., Pereira F.S., Spanner G., Higuchi N., Ometto J.P. (2020a) Resource Availability and Disturbance Shape Maximum Tree Height across the Amazon. Global Change Biology 27 (1): 177-189.
21. Clark, M.L., Roberts, D.A., Ewel, J.J., Clark, D.B. (2011) Estimation of tropical rain forest aboveground biomass with small-footprint lidar and hyperspectral sensors Remote Sensing of Environment, 115 (11), pp. 2931-2942
22. Asner, G.P., Mascaro, J., Mapping tropical forest carbon: calibrating plot estimates to a simple LiDAR metric Remote Sens. Environ., 140 (2014), pp. 614-624, 10.1016/j.rse.2013.09.023
23. Latifi, H., Heurich, M., Hartig, F., Müller, J., Krzystek, P., Jehl, H., Dech, S. (2015a) Estimating over and understorey canopy density of temperate mixed stands by airborne LiDAR data. Forestry 89 (1): 69-81
24. Latifi, H., Fassnacht, F.E., Muller, J., Tharani, A., Dech, S., Heurich, M. (2015b) Forest inventories by LiDAR data: A comparison of single tree segmentation and metric-based methods for inventories of a heterogeneous temperate forest. International Journal of Applied Earth Observation and Geoinformation 42, 162-174
25. Longo, M., Keller, M., dos-Santos, M.N., Leitold, V., Pinagé, E.R., Baccini, A., Saatchi, S., Nogueira, E.M., Batistella, M., Morton, D.C. (2016), Aboveground biomass variability across intact and degraded forests in the Brazilian Amazon, Global Biogeochem. Cycles, 30, 1639–1660, https://doi.org/10.1002/2016GB005465
26. Jucker, T., Asner, G. P., Dalponte, M., Brodrick, P. G., Philipson, C. D., Vaughn, N. R., Teh, Y. A., Brelsford, C., Burslem, D. F. R. P., Deere, N. J., Ewers, R. M., Kvasnica, J., Lewis, S. L., Malhi, Y., Milne, S., Nilus, R., Pfeifer, M., Phillips, O. L., Qie, L., Renneboog, N. et al. (2018) Estimating aboveground carbon density and its uncertainty in Borneo's structurally complex tropical forests using airborne laser scanning, Biogeosciences, 15, 3811–3830, https://doi.org/10.5194/bg-15-3811-2018
27. Almeida, D.R.A., Stark, S.C., Schietti, J., Camargo, J.L.C., Amazonas, N.T., Görgens, E.B., Rosa, D.M., Smith, M.N., Valbuena, R., Saleska, S., Nelson, B.W., Andrade, A., Mesquita, R., Laurance, S.G., Laurance, W.F., Lovejoy, T.E., Broadbent, E.N., Shimabukuro, Y.E., Parker, G., Lefsky, M., Silva, C.A., Brancalion, P.H.S (2019) Persistent Effects of Fragmentation on Tropical Rainforest Canopy Structure after 20 Years of Isolation. Ecological Applications 29 (6): e01952.
28. Almeida, D.R.A., Broadbent, E., Wendt, A., Wilkinson, B., Papa, D.A., Chazdon, R., Meli, P., Görgens, E.B., Silva, C.A., Stark, S.C., Valbuena, R., Almeyda, A., Fagan, M., Foster, P. & Brancalion, P.H.S. (2020) Detecting Successional Changes In Tropical Forest Structure Using Gatoreye Drone-Borne Lidar. Biotropica 52: 1155-1167.

29. Beland, M., Parker G., Sparrow, B., Harding, D., Chasmer, L., Phinn, S., Antonarakis, A., Strahler, A. (2019) On promoting the use of lidar systems in forest ecosystem research. Forest Ecology and Management, https://doi.org/10.1016/j.foreco.2019.117484
30. Hernando A., Puerto L., Mola-Yudego B., Manzanera J.A., García-Abril A., Maltamo M. & Valbuena R. (2019) Estimation of Forest Biomass Components through Airborne LiDAR and Multispectral Sensors. iForests - Biogeosciences and Forestry 12: 207-213
31. Adnan, S., Maltamo, M., Mehtätalo, L., Ammaturo, R.N., Packalen, P. & Valbuena, R. (2021) Determining Maximum Entropy in 3D Remote Sensing Height Distributions and Using it to Improve Aboveground Biomass Modelling via Stratification. Remote Sensing of Environment 260: 112464.
32. Costa M.A.T., Silva C.A., Broadbent E.N., Leite R.V., Mohan M., Liesenberg V., Stoddart J., Amaral C.H., Almeida D.R.A., da Silva A.L., Ré Y Goya L.R., Cordeiro V.A., Rex F., Hirsch A., Marcatti G.E., Cardil A., Mendonça B.A.F., Hamamura C., Dalla A.P., Matricardi E.A.T., Hudak A.T., Almeyda A.M., , Valbuena R., Faira B.L., Silva C.H.L., Aragao L., Ferreira M.E., Liang J., Carvalho S.P.C., & Klauberg C. (2021) Beyond Trees: Mapping Total Aboveground Biomass Density in the Brazilian Savanna Using High-Density UAV-Lidar Data. Forest Ecology and Management 491: 119155
33. Rex, FE, Silva, C.A., Dalla Corte, A.P., Klauberg, C, Mohan, M., Cardil, A., Silva, V.S., Almeida, D.R.A., Garcia, M., Broadbent, E.N., Valbuena, R., Stoddart, J., Merrick, T., Hudak, A.T (2020) Comparison of Statistical Modelling Approaches for Estimating Tropical Forest Aboveground Biomass Stock and Reporting Their Changes in Low-Intensity Logging Areas Using Multi-Temporal LiDAR Data. Remote Sensing. 12(9):1498. https://doi.org/10.3390/rs12091498
34. Nunes, M.H., Jucker, T., Riutta, T., Svátek, M., Kvasnica J., Rejžek, M., Matula, R., Majalap, N., Ewers, R.M., Swinfield, T., Valbuena, R., Vaughn, N.R., Asner, G.P., Coomes, D.A. (2021) Recovery of logged forest fragments in a human-modified tropical landscape during the 2015-16 El Niño. Nat Commun 12, 1526 https://doi.org/10.1038/s41467-020-20811-y
35. d'Oliveira, M.V., Reutebuch, S.E., McGaughey, R., & Andersen, H. (2012). Estimating forest biomass and identifying low-intensity logging areas using airborne scanning lidar in Antimary State Forest, Acre State, Western Brazilian Amazon. Remote Sensing of Environment, 124, 479-491.
36. Meyer, V., Saatchi, S.S., Chave, J., Dalling, J.W., Bohlman, S., Fricker, G.A., Robinson, C., Neumann, M., Hubbell, S. (2013) Detecting tropical forest biomass dynamics from repeated airborne lidar measurements, Biogeosciences, 10, 5421–5438, https://doi.org/10.5194/bg-10-5421-2013
37. Kankare, V., Vastaranta, M., Holopainen, M., Räty, M., Yu, X., Hyyppä, J., Hyyppä, H., Alho, P., Viitala, R. (2013) Retrieval of Forest Aboveground Biomass and Stem Volume with Airborne Scanning LiDAR. Remote Sens. 5, 2257-2274. https://doi.org/10.3390/rs5052257
38. Marchesan, J., Alba, E., Schuh, M., Favarin, J., Pereira, R., (2020) Aboveground Biomass Estimation In A Tropical Forest With Selective Logging Using Random Forest And Lidar Data Floresta 50(4):1873, DOI: 10.5380/rf.v50i4.66589
39. Valbuena R., Maltamo M., Mehtätalo L. & Packalen P. (2017b) Key Structural Features of Boreal Forests May Be Detected Directly Using L-Moments from Airborne Lidar Data. Remote Sensing of Environment 194: 437-446.
40. Garcia, M., Saatchi, S., Ustin, S., Balzter, H. (2018) Modelling forest canopy height by integrating airborne LiDAR samples with satellite Radar and multispectral imagery, International Journal of Applied Earth Observation and Geoinformation, 66, 159-173, https://doi.org/10.1016/j.jag.2017.11.017
41. Bouvier, M., Durrieu, S., Fournier, R.A., Renaud, J.P. (2015) Generalizing predictive models of forest inventory attributes using an area-based approach with airborne LiDAR data, Remote Sensing of Environment, 156, 322-334
42. Wang, Y., Lehtomäki, M., Liang, X., Pyörälä, J., Kukko A., Jaakkola A., Liu, J., Feng, Z., Chen, R., Hyyppä, J. (2019) Is field-measured tree height as reliable as believed–a comparison study of tree height estimates

from field measurement, airborne laser scanning and terrestrial laser scanning in a boreal forest ISPRS J. Photogramm. Remote Sens., 147, pp. 132-145

43. Lefsky, M.A., Harding, D., Cohen, W.B., Parker, G., Shugart, H.H. (1999) Surface lidar remote sensing of basal area and biomass in deciduous forests of eastern Maryland, USA. Remote Sensing of Environment 67, 83–98.
44. Hinsley, S.A., Hill, R.A., Fuller, R.J., Bellamy, P.E., Rothery, P. (2009) Bird species distributions cross woodland canopy structure gradients. Commun Ecol 10:99–110
45. Kane, V.R., McGaughey, R.J., Bakker, J.D., Gersonde, R.F., Lutz, J.A., Franklin, J.F. (2010) Comparisons between field- and LiDAR-based measures of stand structural complexity. Can. J. For. Res. 40 (4), 761–773, lo.1139/X10-024
46. Zellweger, F., Baltensweiler, A., Ginzler, C., Roth, T., Braunisch, V., Bugmann, H. and Bollmann, K. (2016) Environmental predictors of species richness in forest landscapes: abiotic factors versus vegetation structure. J. Biogeogr., 43: 1080-1090. https://doi.org/10.1111/jbi.12696
47. Bater, C., Wulder, M.A., Coops, N.C., Nelson, R., Hilker, T. (2011) Stability of sample-based scanning-LiDAR-derived vegetation metrics for forest monitoring, IEEE Transactions of Geoscience and Remote Sensing, vol. 49, no. 6, pp. 2385–2392
48. Nelson, R., Krabill, W., Tonelli, J., (1988) Estimating Forest Biomass and Volume Using Airborne Laser Data. Remote Sensing of Environment 24, 247–267, https://doi.org/10.1016/0034-4257(88)90028-4
49. Morsdorf, F., Kötz, B., Meier, E., Itten, K.I., Allgöwer, B. (2006) Estimation of LAI and fractional cover from small footprint airborne laser scanning data based on gap fraction. Remote Sens Environ 104:50–61
50. Solberg, S. (2010) Mapping gap fraction, LAI and defoliation using various ALS penetration variables. Int. J. Remote Sens. 31:1227–1244.
51. Korhonen, L., Korpela, I., Heiskanen, J., Maltamo, M. (2011) Airborne discrete-return LiDAR data in the estimation of vertical canopy cover, angular canopy closure and leaf area index. Remote Sens Environ 115:1065–1080
52. Wedeux, B. M. M., Coomes, D. A. (2015) Landscape-scale changes in forest canopy structure across a partially logged tropical peat swamp, Biogeosciences, 12, 6707-6719, https://doi.org/10.5194/bg-12-6707-2015
53. Clawges, R., Vierling, K., Vierling, L., Rowell, E. (2008) The use of airborne lidar to assess avian species diversity, density, and occurrence in a pine/aspen forest, Remote Sensing of Environment, Volume 112, Issue 5, Pages 2064-2073, ISSN 0034-4257, https://doi.org/10.1016/j.rse.2007.08.023.
54. Bergen, K. M., Goetz, S. J., Dubayah, R. O., Henebry, G. M., Hunsaker, C. T., Imhoff, M. L., Nelson, R. F., Parker, G. G., and Radeloff, V. C. (2009), Remote sensing of vegetation 3-D structure for biodiversity and habitat: Review and implications for lidar and radar spaceborne missions, *J. Geophys. Res.*, 114, G00E06, doi:10.1029/2008JG000883.
55. Valbuena R., Packalen P., Martín-Fernández S., Maltamo M. (2012) Diversity and equitability ordering profiles applied to the study of forest structure. Forest Ecology and Management 276: 185–195. http://dx.doi.org/10.1016/j.foreco.2012.03.036
56. Valbuena, R., Maltamo, M., Martín-Fernández, S., Packalen, P., Pascual, C., Nabuurs G.J. (2013) Patterns of covariance between airborne laser scanning metrics and Lorenz curve descriptors of tree size inequality Can. J. Remote Sens. https://doi.org/10.5589/m13-012
57. Pinagé, E.R., Keller, M., Duffy, P., Longo, M., dos-Santos, M.N., Morton, D.C. (2019) Long-Term Impacts of Selective Logging on Amazon Forest Dynamics from Multi-Temporal Airborne LiDAR. Remote Sens. 11, 709. https://doi.org/10.3390/rs11060709
58. Silva, C.A., Hudak, A.T., Vierling, L.A., Klauberg, C., Garcia, M., Ferraz, A., Keller, M., Eitel, J., Saatchi, S. (2017) Impacts of Airborne Lidar Pulse Density on Estimating Biomass Stocks and Changes in a Selectively Logged Tropical Forest. Remote Sens. 9, 1068. https://doi.org/10.3390/rs9101068

59. Görgens, E.B., Mund, J.P., Cremer, T., de Conto, T., Krause, S., Valbuena, R. & Rodríguez, L.C. (2020b) Automated Operational Logging Plan Considering Multi-Criteria Optimization. Computers and Electronics in Agriculture 170: 105253
60. Rex, F.E., Corte, A.P.D., Machado, S.D.A., Silva, C.A., Sanquetta, C.R. (2019) Estimating Above-Ground Biomass of Araucaria angustifolia (Bertol.) Kuntze Using LiDAR Data. Floresta E Ambiente, 26.
61. Chave, J., Réjou-Méchain, M., Búrquez, A., Chidumayo, E., Colgan, M.S., Delitti, W.B., Duque, A., Eid, T., Fearnside, P.M., Goodman, R.C., Henry, M., Martínez-Yrízar, A., Mugasha, W.A., Muller-Landau, H.C., Mencuccini, M., Nelson, B.W., Ngomanda, A., Nogueira, E.M., Ortiz-Malavassi, E., Pélissier, R., Ploton, P., Ryan, C.M., Saldarriaga, J.G. and Vieilledent, G. (2014), Improved allometric models to estimate the aboveground biomass of tropical trees. Glob Change Biol, 20: 3177-3190. https://doi.org/10.1111/gcb.12629
62. McGaughey (2019) R.J. FUSION/LDV: Software for LiDAR Data Analysis and Visualization; Version 3.80; U.S. Department of Agriculture Forest Service, Pacific Northwest Research Station, University of Washington
63. Isenburg M. (2019) "LAStools - efficient LiDAR processing software" (version 191018, unlicensed)
64. Roussel, J.R., Auty, D., Coops, N. C., Tompalski, P., Goodbody, T. R. H., Sánchez Meador, A., Bourdon, J.F., De Boissieu, F., Achim, A. (2020) lidR: An R package for analysis of Airborne Laser Scanning (ALS) data. Remote Sensing of Environment, 251 (August), 112061. doi: 10.1016/j.rse.2020.112061
65. McArthur, R.H., McArthur, J.W. (1961). On bird species diversity. Ecology 42: 594–598. https://doi.org/10.2307/1932254
66. R Core Team (2021). R: A language and environment for statistical computing. R Foundation for Statistical Computing, Vienna, Austria. URL https://www.R-project.org/
67. QGIS.org, (2021) QGIS Geographic Information System. QGIS Association http://www.qgis.org
68. Wickham, H. (2016) ggplot2: Elegant Graphics for Data Analysis. Springer-Verlag New York.
69. Baskerville, G. L. (1972). Use of Logarithmic Regression in the Estimation of Plant Biomass. Canadian Journal of Forest Research, 2(1), 49–53.
70. Enquist, B.J., Brown, J.H. & West, G.B. (1998). Allometric scaling of plant energetics and population density. Nature, 395, 163–165.
71. Chave, J., Andalo, C., Brown, S., Cairns, M.A., Chamber, J.Q., Eamus, D., Folster, H., Fromard, F., Higuchi, N., Kira, T., Lescure, J.-P., Nelson, B.W., Ogawa, H., Puig, H., Riera, B., Yamakura, T. (2005) Tree allometry and improved estimation of carbon stocks and balance in tropical forests. *Oecologia* **145,** 87–99. https://doi.org/10.1007/s00442-005-0100-x
72. Niklas, K.J. (2006) A phyletic perspective on the allometry of plant biomass-partitioning patterns and functionally equivalent organ categories, New Phytol 171:27–40
73. Lipovetsky, S., (2013) How good is best? Multivariate case of Ehrenberg-Weisberg analysis of residual errors in competing regressions. J. Mod. Appl. Stat.Methods 12 (2), 14.
74. Pineiro, G., Perelman, S., Guerschman, J.P., Paruelo, J.M. (2008) How to evaluate models: Observed vs. predicted or predicted vs. observed? Ecological Modelling, 216, https://doi.org/10.1016/j.ecolmodel.2008.05.006
75. Taylor, K.E. (2001). "Summarizing multiple aspects of model performance in a single diagram". J. Geophys. Res. 106: 7183–7192
76. Lemon, J. (2006). "Plotrix: a package in the red light district of R." *R-News*, **6**(4), 8-12.
77. Freedman, D., Pisani, R., & Purves, R. (2007). Statistics (international student edition). Pisani, R. Purves, 4th Edn. WW Norton & Company, New York.
78. Hethcoat, M.G., Edwards, D.P., Carreiras, J.M.B., Bryant, R.G., França, F.M., Quegan, S. (2018) A Machine Learning Approach to Map Tropical Selective Logging 451856; https://doi.org/10.1101/451856

79. Su, H., Shen, W., Wang, J. et al., Machine learning and geostatistical approaches for estimating aboveground biomass in Chinese subtropical forests. For. Ecosyst. 7, 64 (2020). https://doi.org/10.1186/s40663-020-00276-7
80. St-Onge, B., Vega, C., Fournier, R.A., Hu, Y. (2008) Mapping canopy height using a combination of digital stereo-photogrammetry and lidar, International Journal of Remote Sensing, 29:11, 3343-3364, https://doi.org/10.1080/01431160701469040
81. Kent, R., Lindsell, J., Laurin, G., Valentini, R., & Coomes, D. (2015). Airborne LiDAR detects selectively logged tropical forest even in an advanced stage of recovery. Remote Sensing, 7 8348-8367. https://doi.org/10.3390/rs70708348
82. Valbuena, R., Vauhkonen, J., Packalen, P., Pitkänen, J., Maltamo, M. (2014) Comparison of airborne laser scanning methods for estimating forest structure indicators based on Lorenz curves, ISPRS Journal of Photogrammetry and Remote Sensing, https://doi.org/10.1016/j.isprsjprs.2014.06.002
83. Valbuena, R.; Hernando, A.; Manzanera, J.A.; Görgens, E.B.; Almeida, D.R.A.; Silva, C.A.; García-Abril, A. (2019) Evaluating observed versus predicted forest biomass: R-squared, index of agreement or maximal information coefficient?, European Journal of Remote Sensing, 52:1, 345-358, DOI: 10.1080/22797254.2019.1605624
84. Lau A, Calders K, Bartholomeus H, Martius C, Raumonen P, Herold M, Vicari M, Sukhdeo H, Singh J, Goodman RC. Tree Biomass Equations from Terrestrial LiDAR: A Case Study in Guyana. Forests. 2019; 10(6):527. https://doi.org/10.3390/f10060527

CHAPTER 6

1. Schreuder, H.T., Gregoire, T.G., Wood, G.B., 1993. Sampling Methods for Multiresource Forest Inventory. John Wiley & Sons 978-0-471-55245-1.
2. Hunter, M.O., Keller, M., Vitoria, D., Morton, D.C., 2013. Tree height and tropical forest biomass estimation. Biogeosciences 108385–8399. https://doi.org/10.5194/bg-10-8385-2013.
3. Wang Y, Lehtomäki M, Liang X, et al. 2019b. Is field-measured tree height as reliable as believed – a comparison study of tree height estimates from field measurement, airborne laser scanning and terrestrial laser scanning in a boreal forest. ISPRS Journal of Photogrammetry and Remote Sensing 147: 132–145.
4. Shao, J., Zhang, W., Luo, L., Cai, S., and Jiang, H.: SLAM-BASED BACKPACK LASER SCANNING FOR FOREST PLOT MAPPING, ISPRS Ann. Photogramm. Remote Sens. Spatial Inf. Sci., V-2-2020, 267–271, https://doi.org/10.5194/isprs-annals-V-2-2020-267-2020, 2020.
5. Duncanson, L., Armston, J., Disney, M., Avitabile, V., Barbier, N., Calders, K., Carter, S., Chave, J., Herold, M., MacBean, N., McRoberts, R., Minor, D., Paul, K., Réjou-Méchain, M., Roxburgh, S., Williams, M., Albinet, C., Baker, T., Bartholomeus, H., Bastin, J.F., Coomes, D. et al. (2021). Aboveground Woody Biomass Product Validation Good Practices Protocol. Version 1.0. In L. Duncanson, M. Disney, J. Armston, J. Nickeson, D. Minor, and F. Camacho (Eds.), Good Practices for Satellite Derived Land Product Validation, (p. 236): Land Product Validation Subgroup (WGCV/CEOS), doi:10.5067/doc/ceoswgcv/lpv/agb.001
6. Huxley, J. S., and G. Teissier. 1936. Terminology of relative growth. Nature, 137780-781.
7. Calder, W.A. III. (1984) Size, function, and life history. Harvards Univ. Press. Cambridge Mass.
8. Niklas, K. J. (1994). Plant Allometry: The Scaling of Form and Process. University of Chicago Press
9. Shinozaki, K., Yoda, K., K., Hozumi, & Kira, T. (1964). A quantitative analysis of plant form-the pipe model theory: II. Further evidence of the theory and its application in forest ecology. Japanese Journal of Ecology, 14(4), 133−139.
10. Enquist, B. J., & Niklas, K. J. (2002). Global allocation rules for patterns of biomass partitioning in seed plants. Science, 295(5559), 1517–1520
11. Brown, S. (1997). Estimating Biomass and Biomass Change of Tropical Forests: A Primer (Food and Agriculture Organization of the United Nations (ed.)). Food & Agriculture Org.
12. Clark, D. B., & Kellner, J. R. (2012). Tropical forest biomass estimation and the fallacy of misplaced concreteness. In Journal of Vegetation Science (Vol. 23, Issue 6, pp. 1191–1196). https://doi.org/10.1111/j.1654-1103.2012.01471.x
13. Bienert, A., Georgi, L., Kunz, M., Maas, H.-G., & Von Oheimb, G. (2018). Comparison and Combination of Mobile and Terrestrial Laser Scanning for Natural Forest Inventories. Forests, 9(7), 395.
14. ČERŇAVA J, TUČEK J, KOREŇ M, MOKROŠ M. Estimation of diameter at breast height from mobile laser scanning data collected under a heavy forest canopy. J. For. Sci.. 2017;63(9):433-441. doi: 10.17221/28/2017-JFS.
15. Ryding J, Williams E, Smith MJ, Eichhorn MP. Assessing Handheld Mobile Laser Scanners for Forest Surveys. Remote Sensing. 2015; 7(1):1095-1111. https://doi.org/10.3390/rs70101095
16. Chen S, Liu H, Feng Z, Shen C, Chen P (2019) Applicability of personal laser scanning in forestry inventory. PLOS ONE 14(2): e0211392. https://doi.org/10.1371/journal.pone.0211392
17. Oveland I, Hauglin M, Giannetti F, Schipper Kjørsvik N, Gobakken T. Comparing Three Different Ground Based Laser Scanning Methods for Tree Stem Detection. Remote Sensing. 2018; 10(4):538. https://doi.org/10.3390/rs10040538
18. Bauwens S, Bartholomeus H, Calders K, Lejeune P. Forest Inventory with Terrestrial LiDAR: A Comparison of Static and Hand-Held Mobile Laser Scanning. Forests. 2016; 7(6):127. https://doi.org/10.3390/f7060127

19. Cabo, C., Ordóñez, C., López-Sánchez, C. A., & Armesto, J. (2018). Automatic dendrometry: Tree detection, tree height and diameter estimation using terrestrial laser scanning. International Journal of Applied Earth Observation and Geoinformation, 69, 164–174. https://doi.org/10.1016/j.jag.2018.01.011
20. Bienert A, Georgi KL, Kunz M, von Oheimb G, Maas H-G. 2021. Automatic extraction and measurement of individual trees from mobile laser scanning point clouds of forests. Annals of Botany.
21. Krisanski, S.; Taskhiri, M.S.; Gonzalez Aracil, S.; Herries, D.; Muneri, A.; Gurung, M.B.; Montgomery, J.; Turner, P. Forest Structural Complexity Tool—An Open Source, Fully-Automated Tool for Measuring Forest Point Clouds. Remote Sens. 2021, 13, 4677. https://doi.org/10.3390/rs13224677
22. Koreň, M., 2017. DendroCloud: Point Cloud Processing Software for Forestry, Version 1.45. Available online: http://gis.tuzvo.sk/dendrocloud/default.aspx
23. Trochta J, Krůček M, Vrška T, Král K (2017) 3D Forest: An application for descriptions of three-dimensional forest structures using terrestrial LiDAR. PLoS ONE 12(5): e0176871. https://doi.org/10.1371/journal.pone.0176871
24. Puletti, N; Castronuovo, R; Ferrara, C; crossing3dforest: an R package for evaluating empty space structure in forest ecosystems bioRxiv 2023.02.01.526548; doi: https://doi.org/10.1101/2023.02.01.526548
25. Yrttimaa T. (2021). Automatic Point Cloud Processing Tools to Characterize Trees (Point-Cloud-Tools: v1.0.1). Zenodo. https://doi.org/10.5281/zenodo.5779288.
26. GreenValley International (2022) LiDAR360 [Computer software], Available online: https://greenvalleyintl.com/LiDAR360/
27. Terryn, L. (2022). lmterryn/ITSMe: submission release (Version v1.0.0) [Computer software]. https://doi.org/10.5281/zenodo.6769105
28. Hackenberg, J; Calders, K; Miro, D; Pasi, R; Alexandre, P; Disney, M; SimpleForest - a comprehensive tool for 3d reconstruction of trees from forest plot point clouds bioRxiv 2021.07.29.454344; https://doi.org/10.1101/2021.07.29.454344 (Pre-print)
29. Computree Project. Version 5. Available online: http://computree.onf.fr/?lang=en
30. Montoya, O., Icasio-Hernandez, O., Salas, J., 2021. TreeTool: A tool for detecting trees and estimating their DBH using forest point clouds. [Computer software] SoftwareX 16, 100889. https://doi.org/10.1016/j.softx.2021.100889.
31. Raumonen, P., 2019. InverseTampere/TreeQSM: Version 2.3.1. [Computer software] Zenodo, http://dx.doi.org/10.5281/zenodo.3482908.
32. Conto T (2022). _TreeLS: Terrestrial Point Cloud Processing of Forest Data_. R package version 2.0.5, <https://github.com/tiagodc/TreeLS>.
33. Wang, D, Momo Takoudjou, S, Casella, E. LeWoS: A universal leaf-wood classification method to facilitate the 3D modelling of large tropical trees using terrestrial LiDAR. Methods Ecol Evol. 2020; 11: 376– 389. https://doi.org/10.1111/2041-210X.13342
34. Molina-Valero, J. A., Martínez-Calvo, A., Ginzo Villamayor, M. J., Novo Pérez, M. A., Álvarez-González, J. G., Montes, F., Pérez-Cruzado, C. (2022). Operationalizing the use of TLS in forest inventories: The R package FORTLS. Environmental Modelling & Software, 105337. doi.org/10.1016/j.envsoft.2022.105337
35. Molina-Valero, J. A.; Martínez-Calvo, A.; Seppelt, A.; Álvarez-González, J.G.; Montes, F.; Pérez-Cruzado, C.; (2023). Automatic Processing of Terrestrial-Based Technologies Point Cloud Data for Forestry Purposes. R package version 1.2.0. https://CRAN.R-project.org/package=FORTLS
36. Guzman, JA, Hernandez, R., and Sanchez-Azofeifa, A., (2021), rTLS: Tools to Process Point Clouds Derived from Terrestrial Laser Scanning. R pacakge version 0.2.5. https://CRAN.R-project.org/package=rTLS
37. Vicari, M.B.; Disney, M.I.; Wilkes, P.; Burt, A.; Calders, K.; Woodgate, W. Leaf and wood classification framework for terrestrial LiDAR point clouds. Methods Ecol. Evol. 2019, 10, 680–694
38. Burt, A., Disney, M., Calders, K. (2019). Extracting individual trees from lidar point clouds using *treeseg*. *Methods Ecol Evol* 10(3), 438–445. doi: 10.1111/2041-210X.13121
39. Conto, T. et al., 2017. Performance of stem denoising and stem modelling algorithms on single tree point clouds from terrestrial laser scanning. Computers and Electronics in Agriculture, v. 143, p. 165-176.

40. Liang, X. et al., 2012. Automatic stem mapping using single-scan terrestrial laser scanning. IEEE Transactions on Geoscience and Remote Sensing, 50(2), pp.661–670.
41. Wickham H, François R, Henry L, Müller K (2022). dplyr: A Grammar of Data Manipulation_. R package version 1.0.10, <https://CRAN.R-project.org/package=dplyr>.
42. Marie Laure Delignette-Muller, Christophe Dutang (2015). fitdistrplus: An R Package for Fitting Distributions. Journal of Statistical Software, 64(4), 1-34. DOI 10.18637/jss.v064.i04.
43. R Core Team (2022). R: A language and environment for statistical computing. R Foundation for Statistical Computing, Vienna, Austria. URL https://www.R-project.org/.
44. Bhattacharyya, A. (1946). On a Measure of Divergence between Two Multinomial Populations. Sankhyā: The Indian Journal of Statistics (1933-1960), 7(4), 401–406. http://www.jstor.org/stable/25047882

CHAPTER 7

1. IPCC, 2021: Climate Change 2021: The Physical Science Basis. Contribution of Working Group I to the Sixth Assessment Report of the Intergovernmental Panel on Climate Change[Masson-Delmotte, V., P. Zhai, A. Pirani, S.L. Connors, C. Péan, S. Berger, N. Caud, Y. Chen, L. Goldfarb, M.I. Gomis, M. Huang, K. Leitzell, E. Lonnoy, J.B.R. Matthews, T.K. Maycock, T. Waterfield, O. Yelekçi, R. Yu, and B. Zhou (eds.)]. Cambridge University Press, Cambridge, United Kingdom and New York, NY, USA, In press, doi:10.1017/9781009157896.
2. FAO, 2015. Global Forest Resources Assessment. FAO. Rome
3. Matthews, R.W., Henshall, P.A., Beauchamp, K., Gruffudd, H., Hogan, G.P., Mackie, E.D., Sayce, M. and Morison, J.I.L. (2022) Quantifying the sustainable forestry carbon cycle: Summary Report. Forest Research: Farnham.
4. Liang X, Hyyppä J, Kaartinen H, Lehtomäki M, Pyörälä J, Pfeifer N, Holopainen M, Brolly G, Francesco P, Hackenberg J, Huang H (2018) International benchmarking of terrestrial laser scanning approaches for forest inventories. ISPRS J Photogramm Remote Sens 144:137–179
5. Duncanson, L., Armston, J., Disney, M., Avitabile, V., Barbier, N., Calders, K., Carter, S., Chave, J., Herold, M., MacBean, N., McRoberts, R., Minor, D., Paul, K., Réjou-Méchain, M., Roxburgh, S., Williams, M., Albinet, C., Baker, T., Bartholomeus, H., Bastin, J.F., Coomes, D. et al. (2021). Aboveground Woody Biomass Product Validation Good Practices Protocol. Version 1.0. In L. Duncanson, M. Disney, J. Armston, J. Nickeson, D. Minor, and F. Camacho (Eds.), Good Practices for Satellite Derived Land Product Validation, (p. 236): Land Product Validation Subgroup (WGCV/CEOS), doi:10.5067/doc/ceoswgcv/lpv/agb.001
6. Chianucci, F., Puletti, N., Grotti, M., Ferrara, C., Giorcelli, A., Coaloa, D., & Tattoni, C. (2020). Nondestructive tree stem and crown volume allometry in hybrid poplar plantations derived from terrestrial laser scanning. Forest Science, 66(6), 737-746.

ADDENDA

ADDENDUM 1

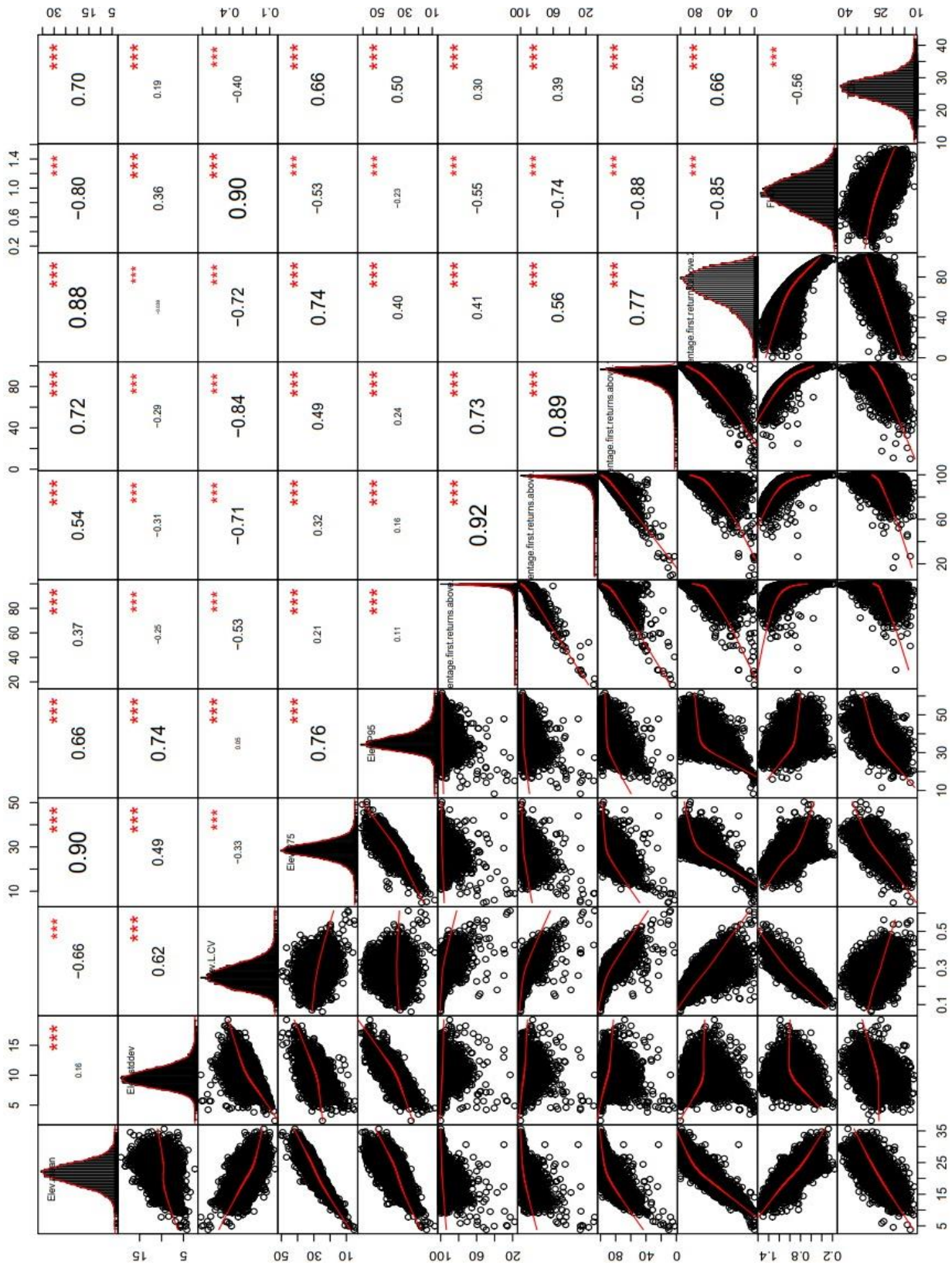

Addendum 1 consists of a correlation matrix showing the correlations between each of the tested LiDAR derived metrics used in the modelling of Chapter 5. This was done to rule out significant levels of collinearity between metrics used for different ecosystem morphological traits.

ADDENDUM 2

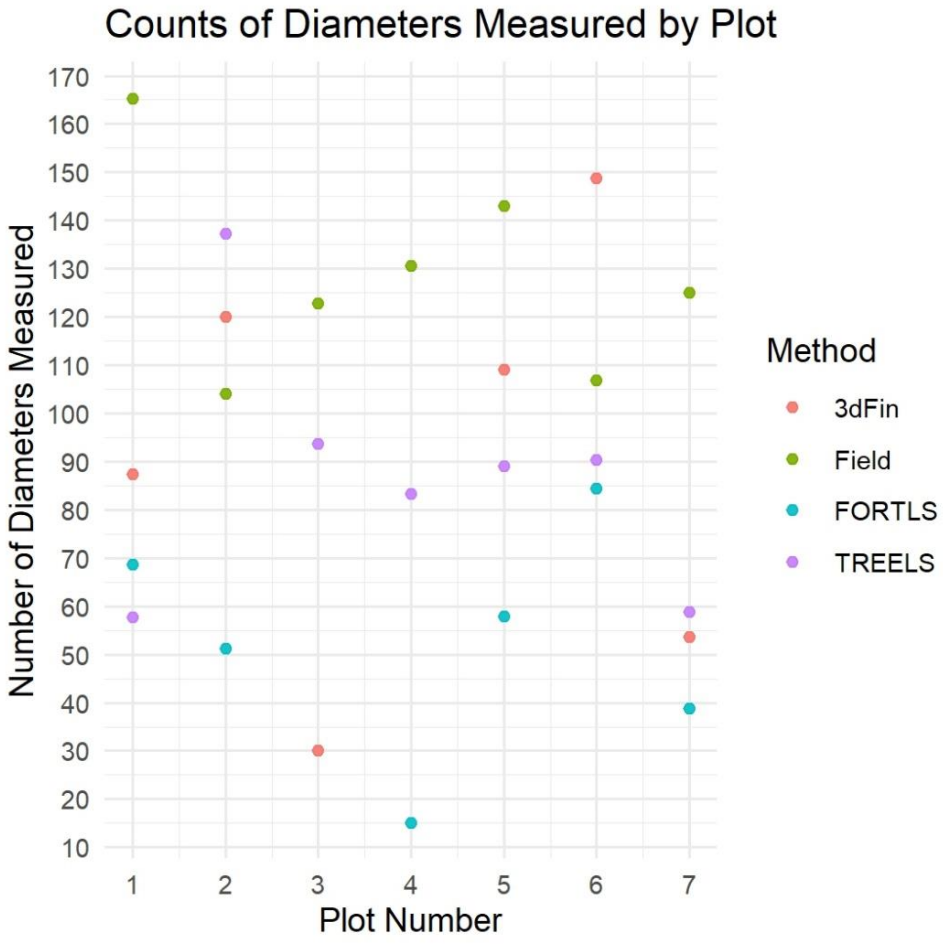

Addendum 2 consists of a plot of counts of diameters measured at each plot by each method used in Chapter 6.